Approved for public release; distribution is unlimited.

Combatting Inherent Vulnerabilites of CFAR Algorithms and a New Robust CFAR Design

by

Patrick J. Bowman
Lieutenant, United States Navy
B.S., University of Scranton, 1985

Submitted in partial fulfillment of the
requirements for the degree of

MASTER OF SCIENCE IN SYSTEMS ENGINEERING

from the

NAVAL POSTGRADUATE SCHOOL
September 1993

Unclassified

security classification of this page

REPORT DOCUMENTATION PAGE

1a Report Security Classification Unclassified		1b Restrictive Markings	
2a Security Classification Authority		3 Distribution/Availability of Report	
2b Declassification Downgrading Schedule		Approved for public release; distribution is unlimited.	
4 Performing Organization Report Number(s)		5 Monitoring Organization Report Number(s)	
6a Name of Performing Organization Naval Postgraduate School	6b Office Symbol *(if applicable)* 3A	7a Name of Monitoring Organization Naval Postgraduate School	
6c Address *(city, state, and ZIP code)* Monterey, CA 93943-5000		7b Address *(city, state, and ZIP code)* Monterey, CA 93943-5000	
8a Name of Funding/Sponsoring Organization	8b Office Symbol *(if applicable)*	9 Procurement Instrument Identification Number	
8c Address *(city, state, and ZIP code)*		10 Source of Funding Numbers	
		Program Element No / Project No / Task No / Work Unit Accession No	

11 Title *(include security classification)* COMBATTING INHERENT VULNERABILITES OF CFAR ALGORITHMS AND A NEW ROBUST CFAR DESIGN

12 Personal Author(s) Patrick J. Bowman

13a Type of Report	13b Time Covered	14 Date of Report *(year, month, day)*	15 Page Count
Master's Thesis	From To	September 1993	158

16 Supplementary Notation The views expressed in this thesis are those of the author and do not reflect the official policy or position of the Department of Defense or the U.S. Government.

17 Cosati Codes			18 Subject Terms *(continue on reverse if necessary and identify by block number)*
Field	Group	Subgroup	signal processing, Cfar.

19 Abstract *(continue on reverse if necessary and identify by block number)*

A current trend in radar technology is automatic detection and tracking systems. An integral part of these automatic systems is the CFAR (Constant False Alarm Rate) detector. A CFAR detector is the signal processing algorithm that controls the rate at which target detections are falsely declared. Given the current state of radar technology, CFAR algorithms are necessary elements of any automatic radar system. Unfortunately, CFAR systems are inherently vulnerable to degradation caused by large clutter edges, multiple targets and jamming environments.

This thesis presents eight popular and studied CFAR architectures. A comprehensive review of each system's structure, analysis and performance is detailed. Also the performance of each CFAR processor for two differenct inphase (I) and quadrature (Q) detectors: envelope approximation detector and the square law detector are compared numerically. In addition, each system is comprehensively compared to one another in the troublesome environments mention above.

This thesis continues with the development of an original CFAR architecture, the excision greatest-of (EXGO). Although more complex, this processor is shown to be more robust than the other established techniques particularly in the prescence of clutter edges, multiple targets, and electronic countermeasures (ECM) environments.

20 Distribution/Availability of Abstract	21 Abstract Security Classification	
☒ unclassified unlimited ☐ same as report ☐ DTIC users	Unclassified	
22a Name of Responsible Individual P.E. Pace	22b Telephone *(include Area code)* (408) 646-3286	22c Office Symbol EC/Pc

DD FORM 1473,84 MAR 83 APR edition may be used until exhausted
All other editions are obsolete

security classification of this page

Unclassified

ABSTRACT

A current trend in radar technology is automatic detection and tracking systems. An integral part of these automatic systems is the CFAR (Constant False Alarm Rate) detector. A CFAR detector is the signal processing algorithm that controls the rate at which target detections are falsely declared. Given the current state of radar technology, CFAR algorithms are necessary elements of any automatic radar system. Unfortunately, CFAR systems are inherently vulnerable to degradation caused by large clutter edges, multiple targets and jamming environments.

This thesis presents eight popular and studied CFAR architectures. A comprehensive review of each system's structure, analysis and performance is detailed. Also the performance of each CFAR processor for two differenct inphase (I) and quadrature (Q) detectors: envelope approximation detector and the square law detector are compared numerically. In addition, each system is comprehensively compared to one another in the troublesome environments mention above.

This thesis continues with the development of an original CFAR architecture, the excision greatest-of (EXGO). Although more complex, this processor is shown to be more robust than the other established techniques particularly in the prescence of clutter edges, multiple targets, and electronic countermeasures (ECM) environments.

THESIS DISCLAIMER

The reader is cautioned that computer programs developed in this research may not have been exercised for all cases of interest. While every effort has been made, within the time available, to ensure that the programs are free of computational and logic errors, they cannot be considered validated. Any application of these programs without additional verification is at the risk of the user.

TABLE OF CONTENTS

LIST OF TABLES

LIST OF FIGURES

TABLE OF SYMBOLS

A	Signal Amplitude
A_0^2	Average RCS
B	Distribution Scaling Parameter
C	Distribution Slope Parameter
H_0	Null Hypothesis (Noise Only)
H_1	Target Plus Noise
I	Inphase Channel
I_0	Modified Bessel Function
J	Number of Interfering Targets
K	Representative Cell (OS CFAR) or Number of Cells to Censor (CMLD CFAR)
$K_{1,2}$	Representative Cells (OSSO OSGO CFAR) or Upper and Lower Number of Cells to Censor (TM CFAR)
M	Number of Reference Cells
Q	Quadrature Channel
R	Estimate of the Envelope Magnitude
SNR	Signal to Noise Ratio
T	Threshold Multiplier
$T_{1,2}$	Threshold Multipliers (EXGO CFAR)
V_t	Adaptive Threshold Level
$V_{t1,2}$	Adaptive Threshold Levels (EXGO CFAR)
Y	Represents the Cell Under Test
$Y_{1,2}$	Noise Estimate of Leading (1) or Lagging (2) Reference Neighborhoods
Z	Estimate of the Noise Power Level
β	Standard Deviation of Noise
Γ	Gamma Function
μ	Total Background Noise Power
Φ	Error Function
Ψ	Moment Generating Function (CMLD CFAR)

ACKNOWLEDGEMENTS

The author wishes to express grateful appreciation to all the individuals who offered assistance toward the completion of this study; especially,

Dr. P.E. Pace of the Naval Postgraduate School for his support, guidance and patience, making this thesis a most valuable educational experience.

I would also like to thank Dr. M.I. Skolnik, Superintendent of the Radar Division at the Naval Research Laboratory for his support in the completion of this thesis. I also wish to express my gratitude to Dr. Skolnik for his role in preparing a six week experience tour at NRL that was both educational and enjoyable.

Finally I would like to dedicate this thesis to my wife Veronica for all her patience, unending support and understanding.

I. INTRODUCTION

A. CFAR BACKGROUND

The primary task of any radar system is to detect all objects in some area of observation and to estimate their position. One current trend in carrying out this task is automatic detection and tracking systems. This trend is driven by the demands of users who place a premium on data acquisition systems which provide rapid, highly accurate information. The basic precept of an automatic detection radar is the elimination of the human operator who was solely responsible for target detection. Early radar systems were designed to route all incoming information directly to the users video display. Clutter, noise and target amplitude variations were all displayed simultaneously. Target detection was therefore delegated to a highly trained operator who usually distinguished targets from interfering background noise, clutter and possibly electronic jamming. The requirement to replace the human operator involved factors such as operator fatigue, saturation and reaction time. Studies have shown that an operator can simultaneously track only a few targets accurately for any extended period of time. As the weakest link in the target detection and tracking problem, the human operator has been replaced by advanced digital signal processing technologies that satisfy the intense requirements of todays radar users.

Automatic target detection and tracking would be a simple task if the echoing object was always located in the clear. In this case, the signal received could simply be compared with some fixed threshold and targets declared whenever the signal exceeds this threshold. In actual application however, the target generally appears before a background filled with complicated clutter types and various sources of noise interference including jamming energies. It is clear that an automatic radar must have some means of false target rejection that was previously delegated to the skilled operator. The signal processing system that completes this task is known as the Constant False Alarm Rate (CFAR) processor. Simply put, the CFAR processor is an algorithm used by automatic detection radars to control the rate at which target detections are falsely declared. The ideal CFAR detector would be one which maximizes the probability of detection of a target when it does appear and minimizes the probability of false alarm caused by noise and clutter when no target is present. Unfortunately both problems cannot be optimized simultaneously. The best the CFAR algorithm can do is keep the false alarm rate at

some tolerable level as the background clutter changes while accepting the resulting change in signal detection probability.

As necessary as CFAR algorithms are in todays multi-function radars, a price must be paid for the control of the false alarm rate. CFAR algorithms reduce the radars probability of detection by increasing signal-to-noise ratio (SNR) requirements, and can also severely degrade a systems range resolution capabilities. One of the more serious drawbacks of CFAR processing is its inherent susceptibility to various types of Electronic Countermeasures (ECM).

B. PRINCIPAL CONTRIBUTIONS

The principal contributions of this thesis lie in the area of CFAR signal processing. The first contribution is a presentation of the weaknesses and vulnerabilities of the most popular CFAR architectures on a common ground (including jamming). The probability of false alarm and probability of detection performance for each CFAR is compared using both an envelope approximation detector and a square law detector. In this manner, the implications of using a less complex detector can be evaluated. The comprehensive knowledge derived from this investigation is then applied as a stepping stone toward the design of an original CFAR system suggested by the author. This new CFAR architecture called excision greatest-of (EXGO) is shown to be robust in all operating scenarios including ECM.

C. THESIS OUTLINE

The intended breadth of this thesis is from a clear explanation of the most basic CFAR function to the creation of an original and complex CFAR detector. Chapter II begins with a comprehensive glossary of many CFAR related terms used in the subsequent chapters. A description of a generic CFAR device is then presented. This description covers the various subfunctions found in almost all CFAR systems. The second chapter concludes with a discussion of the statistical techniques used to describe the capabilities and performance of CFAR systems. Chapter III introduces the inherent vulnerability of CFAR algorithms. By covering this material early in the thesis, the reader can better appreciate the complex tradeoffs required in CFAR design. Chapter IV comprehensively covers the eight popular CFAR detectors. The capabilities of each detector will be carefully described. Stressed here are the adaptive threshold approach to managing the false alarm problem. Other approaches such as clutter mapping and non-parametric detectors are also introduced in less detail. The performance of these eight CFAR algorithms are compared using both square law and an envelope approxi-

mation detectors. Chapter V then compares the major CFAR families with the intent of finding the best CFAR algorithm for some particular application. The systems are compared under three operating conditions. These conditions are homogeneous noise, clutter edges and multiple target environments. Chapter VI presents new results relating to the creation of an original and robust CFAR system. In this chapter the envelope approximation detector system is studied to determine the best coefficients for the approximation for the new CFAR system developed. In Chapter VII the new CFAR system operation and performance is discussed. Also, the new detector is compared to other CFAR architectures showing relative capabilities.

II. GENERAL CFAR CONCEPTS

A. INTRODUCTION

This chapter is designed so that a reader can easily discern the important elements and theory of CFAR algorithms. A comprehensive set of applicable CFAR related terminology is included. These definitions will serve as a basis of understanding for the entire thesis. The chapter will also introduce general approaches that radar engineers use when deciding on which CFAR processor best suits their particular need. A simple, generic Adaptive Threshold CFAR processor will then be covered. All the important elements that adaptive threshold CFAR algorithms employ will be described in detail. A clear understanding of these subelements will be critical in determining a CFAR systems operating characteristics and capabilities. This chapter will end with a discussion of CFAR system performance criteria and design criteria that will be followed when analyzing the many CFAR architectures discussed in this thesis.

B. DEFINITIONS.

The following definitions form a basic glossary of detection and data processing terms. The knowledge of these terms is required for an easy understanding of this thesis. This glossary was taken in part from Schlehers work [Ref. 1].

1. **Adaptive Threshold CFAR**

   A processor which provides a constant false alarm rate (CFAR) in a varying nonhomogeneous clutter and noise interference environments by adaptively adjusting the detection threshold. The procedure assumes that the general form of the interference's probability distribution is known except for a small number of unknown parameters. The unknown parameters are estimated on a cell-to-cell basis by examining the reference cells surrounding the cell under test. The resulting estimated interference probability distribution function is then used in each test cell to obtain a threshold setting that provides the desired false alarm rate.

2. **Automatic Detection Radar**

   In an automatic detection radar, the target reports are formed in the radar's signal processor before interaction with a human operator or further data processing. The function of the automatic detector is to process the high bandwidth raw radar return, which is usually contaminated with many forms of interference, and to extract the low bandwidth target reports with a minimal number of false reports. The automatic detection process places stringent requirements on the design of radars incorporating this feature with particular emphasis on the signal processing function.

3. Clutter

Clutter is defined as a conglomeration of unwanted radar echoes. Surface or area clutter consists of reflections from distributed surfaces intercepted by the radar antenna's mainbeam and sidelobes. Discrete clutter is returned from stationary objects such as water towers, buildings and other unwanted fixed targets, and can be very large. Volumetric clutter is reflected from weather, chaff, and other atmospheric disturbances. Angel clutter is primarily reflected from birds and insects, and can be very disturbing. Clutter is characterized by its mean or median equivalent backscattering cross-section, amplitude probability density function and its power spectral density or equivalent autocorrelation function.

4. CFAR Loss

CFAR loss is defined as the loss of detection sensitivity caused by the effect of the CFAR processor on the signal or the detection threshold. In general, the CFAR loss is a function of the number of reference cells used to estimate the unknown parameters, the design probabilities of detection and false alarm, the number of integrated pulses and the probability density function of the interference. Figure 1 [Ref. 2] illustrates the relative decrease in CFAR loss in dB (for a Cell Averaging system) as the number of reference cells used in the noise estimation process increase at various false alarm rates. [Ref. 3] is the impact CFAR loss has on SNR requirements.

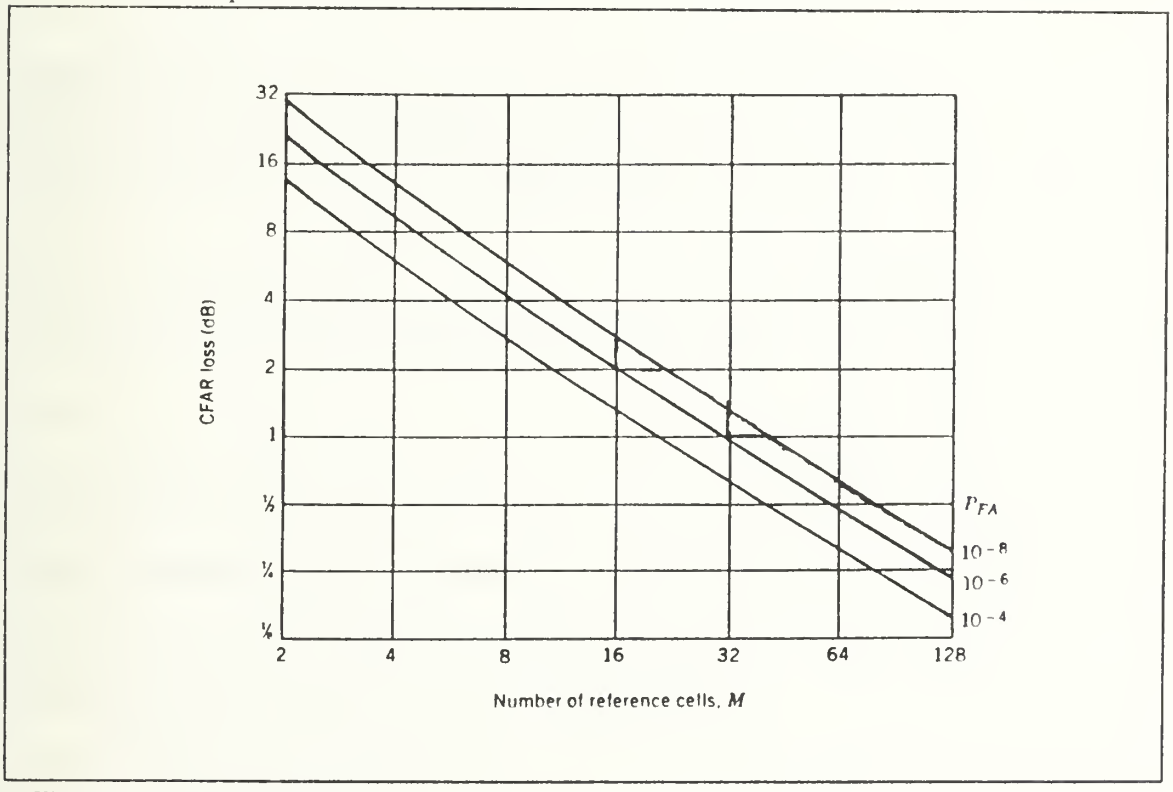

Figure 1. CFAR Loss

A nonlinear device followed by a low-pass filter which extracts the envelope of the high-frequency carrier. The envelope detector ignores any phase information contained in the carrier and hence provides only amplitude video information.

6. **False Alarm**
   An erroneous radar target detection decision caused by noise or other interfering signals exceeding the detection threshold. In radar statistical theory, the decision domain is divided into a decision between the hypothesis of noise or that of signal-plus-noise. The decision boundary is formed by the threshold level determined by the desired false alarm probability. A type I error or false alarm occurs when the threshold level is exceeded and the noise-only hypothesis is in effect.

7. **Monte Carlo Simulation**
   The technique of selecting numbers randomly from one or more probability distributions for use in a particular trial or run in a simulation study. The system or process to be studied is represented by a model which defines over time its essential characteristics. The model may be manipulated in ways impossible or impractical to perform on the system being represented. The dynamics of the behavior of the system under study may be inferred by the operation of the model.

8. **Moving Window Detector**
   A scanning radar detector which accumulates the last n radar return pulses within each range resolution cell. This is accomplished computationally through formation of the running sum of n radar pulses by adding the latest pulse to the accumulator while subtracting the pulse which occurred n PRI periods in the past.

9. **Target Fluctuation**
   Variation in the amplitude of the target signal, caused by the changes in target aspect angle, rotation, or vibration of target scattering sources, or changes in radar wavelength.

C. CFAR APPROACHES

The overall CFAR process consists of a series of techniques used by automatic detection radar systems to control the rate at which target declarations are falsely declared. It is the statistical nature of the radar background that makes a number of false alarms inevitable. These background interferers arise from receiver noise, clutter (land, sea, and rain), ECM (chaff and jamming), and interference from neighboring radars. When automatic detection is performed in homogeneous and nonhomogeneous clutter and noise environments a combination of actions are taken in the radar to lessen the false alarm effect. The hardware subsystems that reduce false alarms include [Ref. 4]:

- Transmitter:
  Waveform selection and frequency agility.
- Antenna:
  Control of sidelobe patterns.
- Receiver:
  Rejection of wideband interference, matched filters, and Sensitivity Time Control (STC)
- Signal Processor:
  Moving Target Indicator (MTI), clutter sensors, and doppler filters.
- Detection and Data Extraction:
  Adaptive Thresholding, Nonparametric and Clutter Map CFAR.

This thesis will focus on the detection and data extraction systems of the radar. In relation to CFAR, these are the most direct methods of controlling the false alarm rate. There are three main approaches to handle the detection and data extraction portion of the CFAR problem. They include Adaptive Threshold, Non-parametric Thresholding, and Clutter Mapping CFAR. Adaptive Thresholding and Non-parametric detectors are based on the assumption that homogeneity exists in range around the cell under test. These are therefore spatially significant techniques. The **Adaptive Threshold** technique assumes that the noise background/density is known except for a few unknown parameters. The neighboring reference cells are then used to estimate the unknown parameters. A variety of CFAR designs are addressed in this category. They differ in principal according to the assumptions which are made regarding the characteristics of the background noise and the parameters chosen to satisfy the requirements of implementation. These different architectures estimate the mean level of the noise differently since the target, clutter and noise can take on various temporal and spatial distributions. **Non-Parametric** detectors obtain a regulated false alarm rate by ranking the reference cells. Under the hypothesis that all the reference cell samples are independent samples from some unknown density function, the test sample has some uniform density function and consequently some threshold level which yields CFAR. **Clutter Maps**, which are temporal CFAR systems store average background levels in numerous range-azimuth cells. If new updated levels exceed the average background by some specified amount, a target is declared in that range-azimuth cell. Each of these three major CFAR approaches will be further described later in the thesis with the emphasis on the Adaptive Thresholding detectors.

D. A GENERIC ADAPTIVE THRESHOLD PROCESSOR

Adaptive Thresholding CFAR detectors share common processor subelements. In Figure 2, many of these important parts are shown operating together as part of a generic CFAR Adaptive Threshold system. The major subelements include the input envelope detector (such as linear-law, square-law or envelope approximation) , a sliding reference window that covers the leading and lagging sets of reference cells (called neighborhood 1 and 2), the threshold multiplier (T), and finally a comparator that compares the cell under test (identified as Y) with the system estimate of the noise power level. A discussion of these major subelements follow.

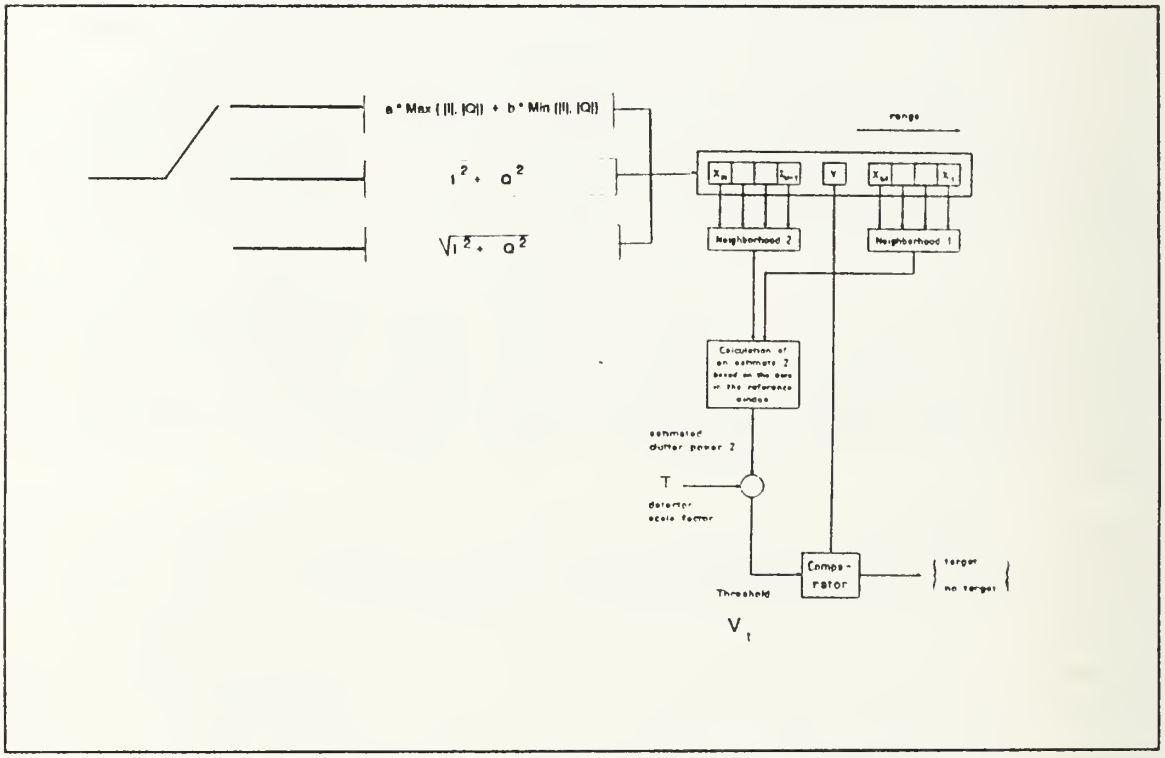

Figure 2. Generic CFAR Detector

1. System Input

A basic problem that CFAR systems overcome is graphically depicted in Figure 3. Here a sequence of one dimensional samples representing radar pulse return energy levels from various ranges or azimuths is shown. The peaks in the data samples indicate the possible presence of targets dispersed with background clutter and noise. Information of this type forms a steady stream of data into the CFAR processing unit which must determine which peaks are actual targets and which peaks are false alarms.

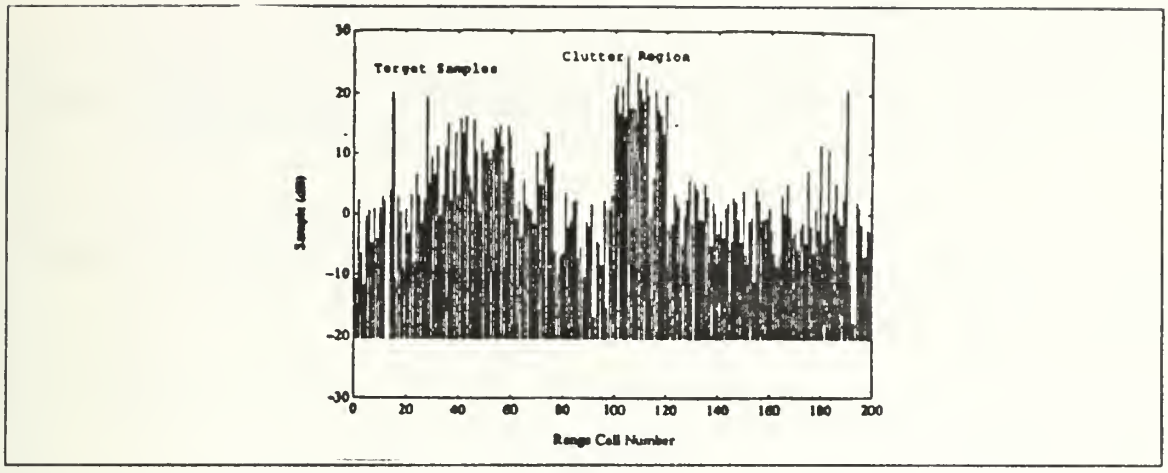

Figure 3. CFAR Data Stream

2. Input Detectors

The operation that frequently occurs in radar signal processing is the computation of the magnitude of the input complex sample stream. The processing of both the in-phase (I) and quadrature (Q) channels generally allows for an exact representation of the signal with no loss of sensitivity. Various choices of magnitude detection schemes are available to the radar engineer to best manipulate the I and Q information. Figure 2 depicts three common envelope detector choices. The square-law envelope detector estimates the magnitude as:

$$R = I^2 + Q^2. \tag{1}$$

The linear-law envelope detector estimates the magnitude as :

$$R = \sqrt{I^2 + Q^2}\,. \tag{2}$$

Since the digital computation of the square root of the sum of squares of the quadrature components is a complex task, many approximations to the envelope detector have evolved which are linear combinations of the quadrature components. Filip [Ref. 5] has shown there are 13 useful approximations which have been devised to satisfy various criteria. The envelope approximation detector estimates the magnitude as :

$$R = a \times Max[|I|,|Q|] + b \times Min[|I|,|Q|] \tag{3}$$

where a and b are scaling values. Tables 1 thru 3 describe the output Probability Density Functions of noise and signal plus noise for each of the detectors assuming that the input noise is normally distributed N(0,1). More information concerning input detectors will be covered in Chapter VI.

Table 1. PDFS FOR A TEST AND REFERENCE CELL FOR A SQUARE LAW DETECTOR

Detector Output	$I^2 + Q^2$
Noise Only PDF	$P_n(r) = \exp^{-x} \qquad x \geq 0$
Signal Plus Noise PDF	$P_{sn}(r) = \left[\frac{1}{(1+SNR)} \exp\left[\frac{-x}{(1+SNR)} \right] \right]$

Table 2. PDFS FOR A TEST AND REFERENCE CELL FOR AN ENVELOPE DETECTOR

Detector Output	$\sqrt{I^2 + Q^2}$
Noise Only PDF	$p_n(r) = \frac{r^2}{\beta^2} \exp \frac{-r^2}{2\beta^2}$
Signal Plus Noise PDF	$p_{sn}(r) = \frac{r}{\beta^2} \exp \frac{-(r^2 + A^2)}{2\beta^2} I_0\left(\frac{rA}{\beta^2}\right)$ A = *amplitude* I_0 = *Modified Bessel function of order* 0 β = *standard deviation of noise*

Table 3. PDFS FOR A TEST AND REFERENCE CELL FOR AN ENVELOPE APPROXIMATION DETECTOR

Detector Output	$a \times \max[\|I\|, \|Q\|] + b \times \min[\|I\|, \|Q\|]$
Noise Only PDF	$p_n(c) = Ce^{D(x)}[\Phi(f_1(x)) + \Phi(f_2(x))]u(x)$ $C = \dfrac{\sqrt{\frac{2}{\pi}}}{\sqrt{a^2 + b^2}}$ $D(x) = -\dfrac{x^2}{2b^2} + \dfrac{a^2x^2}{2b^2(a^2 + b^2)}$ $f_1(x) = \dfrac{a}{b}\dfrac{x}{\sqrt{2}\sqrt{a^2 + b^2}}$ $f_2(x) = \dfrac{b}{a}\dfrac{x}{\sqrt{2}\sqrt{a^2 + b^2}}$ $\Phi(y) = \dfrac{2}{\sqrt{\pi}}\displaystyle\int_0^y e^{-t^2}dt$
Signal Plus Noise PDF	$p_{sn}(c) = C_1\{e^{D(x)}[\Phi(f_1) - \Phi(f_2)] + e^{E(x)}[\Phi(f_3) - \Phi(f_4)]$ $+ e^{F(x)}[\Phi f(_5) - \Phi(f_6)]\} + C_2\{e^{G(x)}[\Phi(f_7) + \Phi(f_8)]\}$ $C_1 = \dfrac{1}{\sqrt{4\pi}\sqrt{a^2 + b^2}}$

(Table Continued)

Signal Plus Noise PDF (Cont.)	$$C_2 = \frac{1}{\sqrt{4\pi ab}\sqrt{\frac{1}{a^2}+\frac{1}{b^2}}}$$ $$D(x) = \frac{-(a\mu_1 + b\mu_2 - z)^2}{a^2+b^2}$$ $$E(x) = \frac{-(a\mu_1 - b\mu_2 + z)^2}{a^2+b^2}$$ $$F(x) = -\mu_1^2 - \mu_2^2 - \frac{2\mu_2{}^2}{b} - \frac{z^2}{b^2} + \frac{(b^2\mu_1 + ab\mu_2 + az)^2}{a^2b^2+b^4}$$ $$G(x) = -\mu_1^2 - \mu_2^2 - \frac{2\mu_2^2}{b} - \frac{z^2}{b^2} + \frac{(-b^2\mu_1 + ab\mu_2 + az)^2}{a^2b^2+b^4}$$ $$f_1 = \frac{-ab\mu_1 + a^2\mu_2 + bz}{a\sqrt{a^2+b^2}}$$ $$f_2 = \frac{-b^2\mu_1 + ab\mu_2 - az}{b\sqrt{a^2+b^2}}$$ $$f_3 = \frac{ab\mu_1 + a^2\mu_2 + bz}{a\sqrt{a^2+b^2}}$$ $$f_4 = \frac{b^2\mu_1 + ab\mu_2 - az}{b\sqrt{a^2+b^2}}$$ $$f_5 = \frac{b^2\mu_1 + ab\mu_2 + az}{b\sqrt{a^2+b^2}}$$ (Table Continued)

Signal Plus Noise PDF (Cont.)	$$f_6 = \frac{ab\mu_1 + a^2\mu_2 - bz}{a\sqrt{a^2 + b^2}}$$ $$f_7 = \frac{\frac{-2\mu_1}{a} + \frac{2\mu_2}{b} + \frac{2z}{b^2}}{2\sqrt{\frac{1}{a^2} + \frac{1}{b^2}}}$$ $$f_8 = \frac{\sqrt{\frac{1}{a^2} + \frac{1}{b^2}} \times b(ab\mu_1 - a^2\mu_2 + bz)}{a^2 + b^2}$$ $$\mu_1 = \sqrt{SNR} \times \cos(\theta)$$ $$\mu_2 = \sqrt{SNR} \times \sin(\theta)$$

3. Reference Cells

In our generic CFAR system, the sampled signals in range are the input to the reference cells. These neighboring cells yield an estimate of the true noise level in the cell under test (identified as Y). By estimating the nearby noise levels, one can determine the amplitude difference between the test cell and its neighboring cells and thereby determine if a target is present.

Often the two reference cells that are immediately adjacent to the cell under test are considered guard cells. A closer look at the guard cells is shown in Figure 4. These cells are often used to ensure that signal energy of the test cell does not spill into the adjacent cells and affect the noise power estimate. Guard cell values are therefore ignored in many Adaptive Threshold processors. Another question that often arises is whether or not the test cell itself should be included in the noise estimation. Physically speaking, the implementation of the system is often simpler if the cell under test is included in the estimate. Unfortunately, the statistical representation and theoretical analysis of a CFAR processor is much easier when the test cell is excluded. Studies however, have shown that the exclusion of the test cell from the reference cell summation can be used to accurately predict the performance of a system that physically in-

cludes the test cell. A slight modification to the system threshold value and proper choice of the number of reference cells to average are sufficient for accurate predictions.

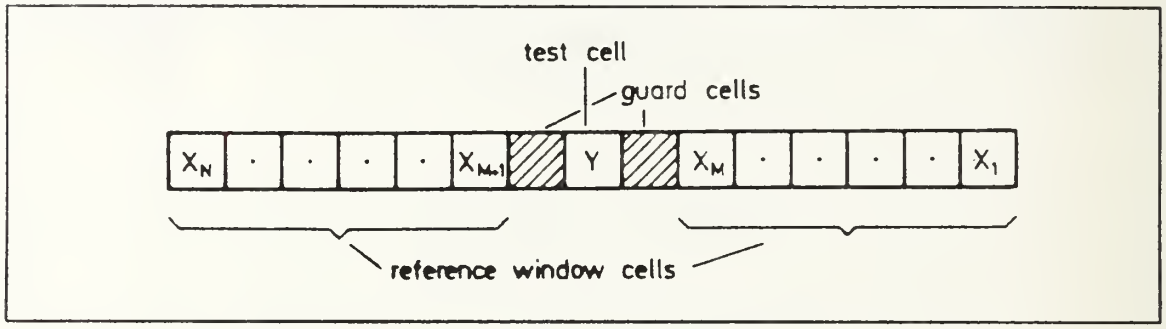

Figure 4. Reference Guard Cells

One of the more important considerations in Adaptive Threshold CFAR architectures is the appropriate choice of the number of reference cells to use. It is easily shown that as the number of cells utilized in the estimate of the mean clutter level increases, the probability of target detection approaches that of the optimum detector where the mean level of the clutter plus noise is known *a priori* [Ref. 6]. A tradeoff however must be considered since too many reference cells results in greater signal processing time as well as an increase in the probability of entering or crossing a clutter edge region. This is a result of an increased physical size of the reference cell region. Also of concern is that the likelihood that an interfering target or a large clutter return entering the reference window increases with a larger choice for M (total number of cells). Another important consideration is that a high number of reference cell samples will result in the inevitable violation of the assumption that the noise samples are identically distributed over the entire reference window. A desirable goal is to use enough reference cells so that the CFAR loss is less than 1 dB, and at the same time not let the reference cells spatially extend beyond one nautical mile on either side of the cell under test [Ref. 7].

4. Noise Estimate Calculation

The calculation of an estimate of the mean noise power (Z) can be accomplished by a great variety of techniques. It is the estimation process itself that differentiates the various CFAR processors. The type of processing done here is highly dependent of the specific clutter and interference models assumed, particularly in a non-homogeneous environment. Chapter IV deals specifically with the varieties of clutter and noise estimation techniques.

5. Thresholding

A desirable CFAR scheme is one whose probability of false alarm is insensitive to changes in the noise power within the reference cells. In this case, the optimum detector sets a fixed threshold to determine the presence of a target under the assumption that the total homogeneous noise power mean is known *a priori* . In reality, the calculation of the threshold must not only make an allowance for the specified probability of false alarm but also for the varying clutter power in the reference window. In the presence of clutter, a fixed threshold results in an enormous number of detections and will possibly saturate the data processing capability of an automatic tracking system. In fact, any small increase in total noise power can result in a corresponding increase of several orders of magnitude in the false alarm probability [Ref. 8]. Figure 5 shows the probability of false alarm as a function of the increase in noise power density for a fixed threshold. As shown, the false alarm rate increases by a factor 10,000 for only a 3 dB increase in the noise power density when a fixed threshold is set. A solution to this problem is to use adaptive thresholding techniques (CFAR) that adjust the threshold value in the presence of interference to maintain some specified false alarm rate. This adjustment is accomplished by multiplying the reference cell noise estimate by some scaling factor. The value of the scaling factor is carefully chosen by the system engineer to manipulate the noise level estimate so that a constant false alarm rate is maintained.

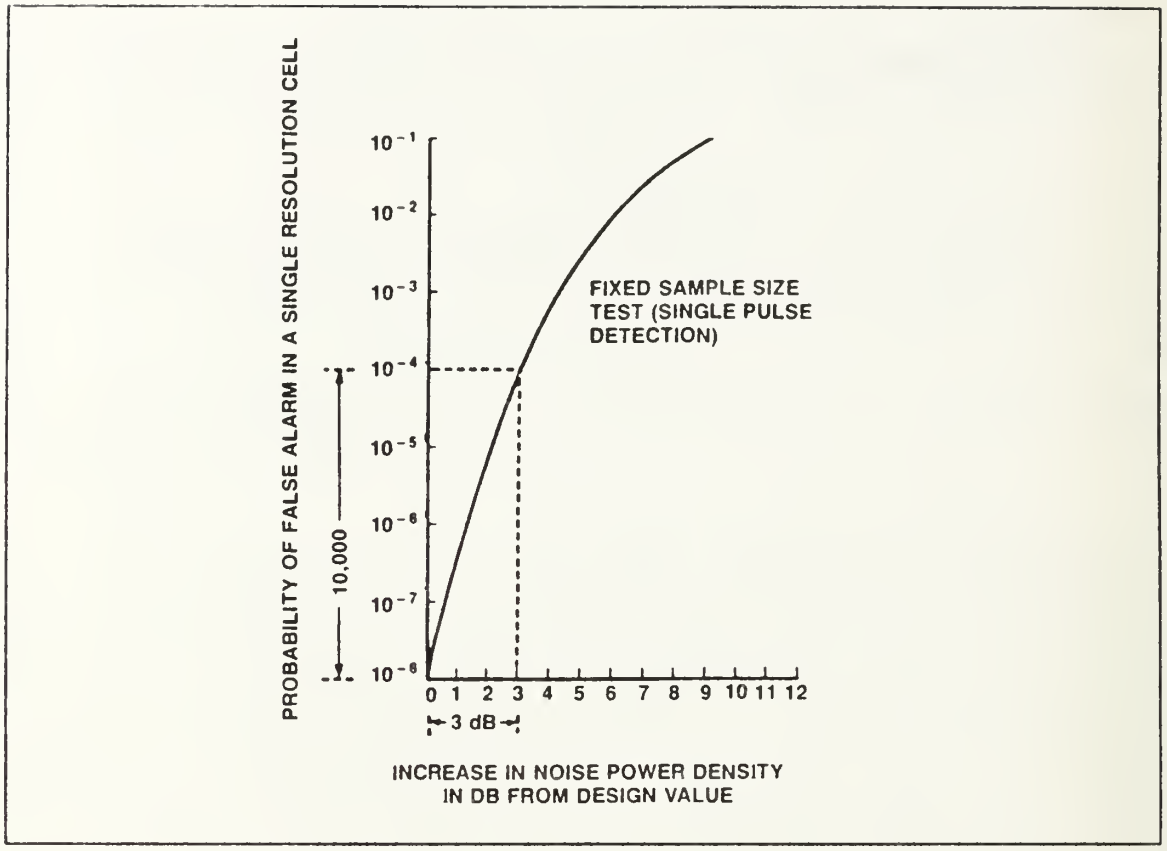

Figure 5. Fixed Threshold Loss

Source: Levanon, N. *Radar Principals* , pp. 226, John Wiley and Sons, N.Y., 1988

A graphical display of the thresholding concept is shown in Figures 6a and 6b. In 6a, the threshold value is set at a level above all but the two highest receiver output peaks so that any signals that exceed the threshold are assumed to be targets. In this scenario we have one missed target and one false alarm. Clearly, a decrease in the threshold level will increase the probability of detection but also result in an increase in the false alarm rate. In Figure 6b, it is shown that the lowered threshold results in one false alarm, yet also yields a 100% detection rate.

a. Signal-to-Noise Ratio (SNR)

SNR is the ratio of average signal power to noise variance or noise power [Ref. 9]. Although the SNR is not directly manipulated or controlled by a CFAR system, it plays a very important role in CFAR system performance. Referring again to Figure 6a, it can readily be seen that if the SNR of the input were higher, (implying

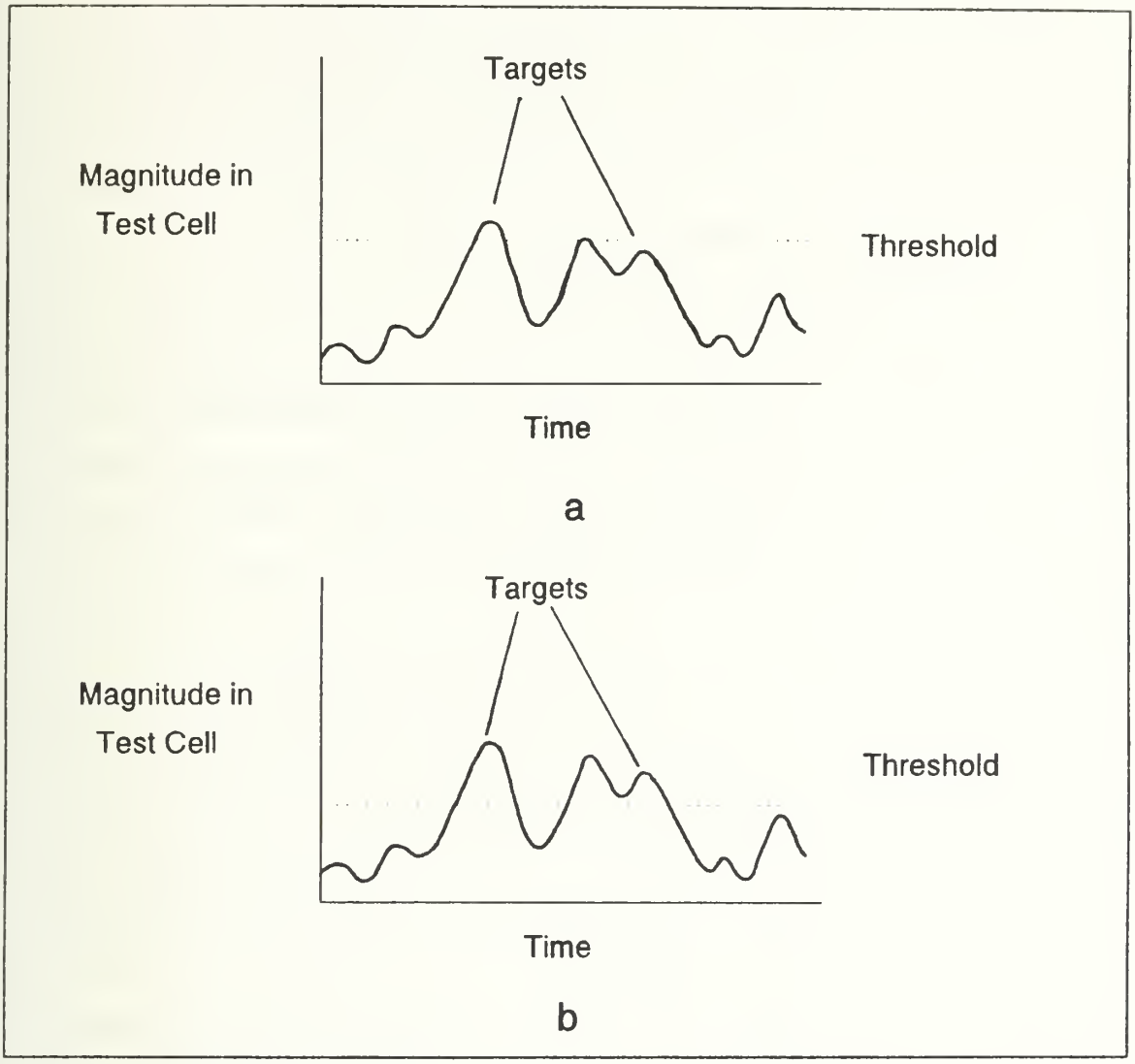

Figure 6. Adaptive Threshold

larger signal peaks) then the smaller target return would cross the original threshold value and result in a higher probability of detection. This fact shows the three way dependence between SNR, threshold values and detection probability. Mathematically, SNR is the ratio of average signal power ($\frac{A^2}{2}$), to the noise variance or noise power (β^2).

$$SNR = \frac{A^2}{2\beta^2} \qquad 4$$

6. Comparator

This is the final subelement of our Generic CFAR detector. The role of the comparator is simply to determine the relationship between the adaptive threshold level and the cell under test (Y) in determining the existence of a target. In expression form we have

$$Y \underset{H_0}{\overset{H_1}{\gtrless}} TZ. \qquad 5$$

The comparator compares the cell under test with the threshold value (TZ) where T is a selected threshold multiplier that ensures that design false alarm rates are achieved, and Z is the noise estimate derived from the neighboring reference cells. The notation H_1 denotes the presence of a target in the test cell while H_0 is the null hypothesis (noise only).

E. DETECTION STRATEGY AND PERFORMANCE CRITERIA

Early in the design of a radar system an appropriate performance criteria must be created for the systems-unique detection problem. This will serve the radar engineer in three ways. First, it sets a focus toward the desired properties of the system, it forces the design engineer to set up quantitative measures on which to base the design, and finally gives rise to specific detector structures that can be implemented or with which other suboptimum schemes can be compared.

The design of CFAR processor for use in radars that operate in clutter, interference, and jamming environments require careful consideration of many factors which will affect the systems performance. CFAR processor designs are always a compromise between hardware complexity, CFAR loss and CFAR performance. Some of the factors or limitations used in the development of a detection strategy are :

- least average CFAR loss
- small SNR ratios for detections at long ranges
- hardware and software constraints
- processing speeds
- information storage capacities
- ability to contain the false alarm rate in the presence of jamming

A simple truth of CFAR is that in high clutter and jamming environments, the fundamental purpose of the detection strategy must be the control of the false alarm rate over a wide range of variations; even at the expense of detections.

Many computation methods and models have been used to obtain performance characteristics of CFAR techniques. Usually each method was developed for a specified type of fluctuating target. Methods include direct numerical integration, Edgeworth series, recursive methods, Monte Carlo techniques, and interpolation based on curve fittings. When using models to estimate CFAR detector capabilities two main concepts must be remembered. First, that the model chosen in designing CFAR detectors will significantly affect detector performance, particularly when statistical uncertainty exists. Secondly, that it is impossible to describe all radar working conditions into a simple model which will inevitably lead to system estimation errors.

For the purpose of this thesis and the examination of the many CFAR algorithms available today, three scenarios will be analyzed. The Gaussian noise scenario, the clutter edge scenario and the multiple target situation. These scenarios will be used to evaluate the performance of the most popular CFAR algorithms on a common ground. These conditions represent the three most important environments for the CFAR processor and can either occur naturally or be artificially generated by a jammer (ECM). The Gaussian noise model describes the situation where the radar is thermally noise limited. In such a model there are two interesting cases. The first is when the target is in the clear but the reference cells have background noise, and the second is when there is uniform background noise over the entire reference window (including the test cell). In both situations the assumption is made that the cells of the reference window are independent and contain the same statistics. The clutter edge model is used to describe and study transition areas between regions with very different noise characteristics. These transitions occur naturally and can be found throughout the reference window. Various distributions including log normal, Weibull, and the K distribution can be used to represent clutter edging. Lastly, the multiple target situation occurs occasionally in radar signal processing when two or more targets are at a similar range. The consequent masking of one target by the other is called suppression.

F. CFAR STATISTICS - PROBABILITY OF DETECTION AND FALSE ALARM

The radar target detection process is inherently probabilistic or statistical in nature. This is due to actual targets being intermixed with randomly fluctuating noise levels. Often it impossible to ascertain if an increase in receiver output is the result of a target

appearance or the result of noise activity. It is possible however, to declare probabilities for this detection process and establish some quantitative values. As defined earlier, the probability of detection (P_d) is the probability that the signal when present is detected. The probability that some noise fluctuation will be mistaken for a target is called the probability of false alarm (P_{fa}). These two values form the foundation for CFAR statistics and analysis.

As shown previously in Figure 6(a), the threshold value is characterized by a voltage V_t (from Figure 2 $V_t = T \times Z$), which when exceeded results in target declaration. There is always a probability that this threshold voltage will be exceeded when no real target is present. The probability of false alarm can be found from the equation

$$P_{fa} = \int_{V_t}^{\infty} p_n(v)\, dv, \tag{6}$$

where $p_n(v)$ is the probability density function (PDF) of the noise. The probability of detection is given by the similar expression as the PDF is that of the signal and noise combined

$$P_d = \int_{V_t}^{\infty} p_{sn}(v)\, dv. \tag{7}$$

Figure 7 details an example of these two PDFs that overlap each other. From this plot we can easily see the P_{fa} region where the noise statistics are greater than the threshold level. Also it is clear that some actual targets are below the threshold level and are not detected giving a P_d less than 1.0. The signal plus noise PDF (p_{sn}) depends on the SNR as well as the signal and noise statistics. Thus, the single pulse detection probability can be also expressed as a function of the signal to noise ratio. For example, with envelope detected input the single pulse probability of detection can be described as :

$$P_d = \frac{1}{2}\left[1 - \Phi\left(\frac{V_t}{\sigma\sqrt{2}} - (SNR)^{\frac{1}{2}}\right)\right]. \tag{8}$$

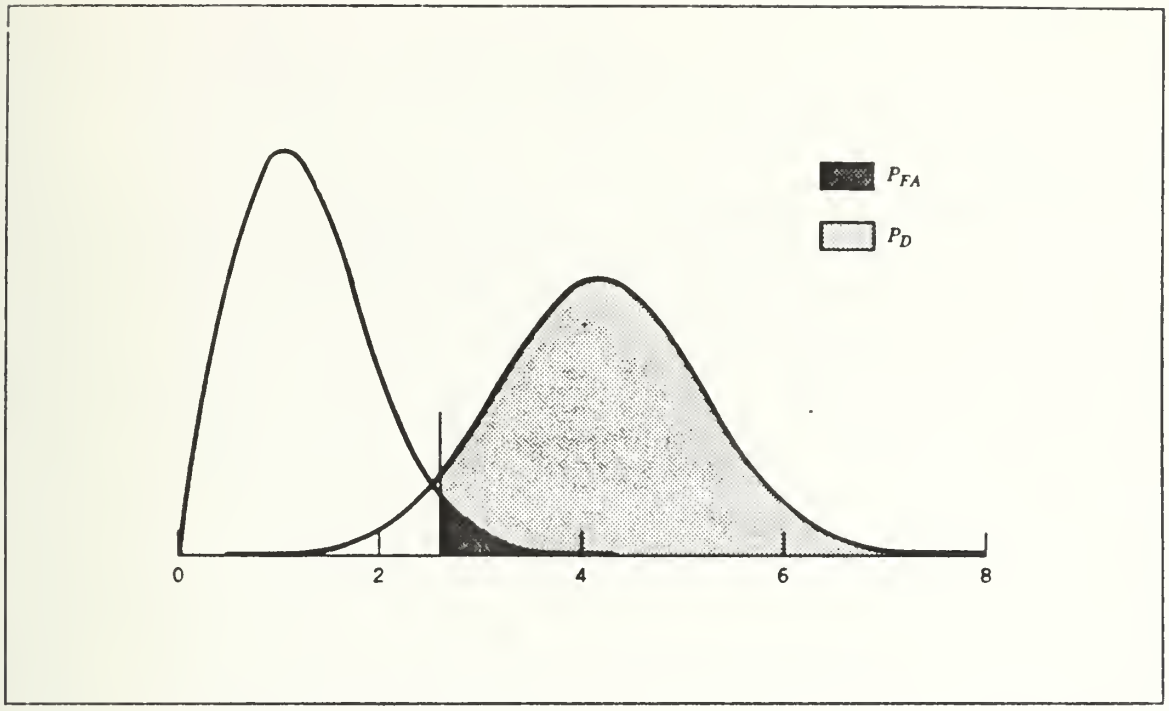

Figure 7. Two Superimposed PDFs

Source: Levanon, N. *Radar Principles* , p. 42, John Wiley and Sons, N.Y., 1988

III. CFAR ARCHITECTURE VULNERABILITY

A. INTRODUCTION

As necessary as CFAR algorithms are in automatic detection and tracking radar systems, a loss is incurred with their use. A price is be paid for the elimination of the human operator. CFAR algorithms are not the quick fix a casual reader of the literature may assume. There are real costs incurred at various levels among the numerous CFAR algorithms available today. The causes of CFAR limitations will be discussed in detail in this chapter and will form a knowledge base to be referenced when comparing CFAR systems. The major problem areas include errant operational environment assumptions made by the radar engineer, clutter sources and edges, and the multiple target situation. Also, the powerful effect ECM has on CFAR will be covered. Electronic jamming has the unique capability to replicate at will, those conditions that naturally plague CFAR algorithms. The loss effects incurred by CFAR detectors include decreased SNR resulting in a loss in system P_d. In sum, one can claim that the CFAR action may 'suppress' many real targets in its quest for false alarm control.

B. VULNERABILITIES

1. Operational Assumptions

The design of the detector for a CFAR system significantly affects CFAR performance. The general operational assumptions made in most CFAR algorithms is that noise and clutter energies found in the reference windows fall into one of two categories. First is that the noise is homogeneous, where the statistical parameters of each cell are identical [Ref. 10]. Second, that the interference fields are heterogeneous (fields having widely dissimilar elements); yet the functions controlling these parameters are known *a priori* [Ref. 11]. Clearly, in actual operation these conditions are violated; that is, the interference environment is mismatched yielding interference statistics that differ from the assumed model. In this case it can be shown that system performance significantly degrades, the false alarm rate is no longer maintained and serious target masking may be introduced. Another general assumption is that no other signals except receiver noise are present in the neighboring reference cells. Clearly this assumption is often violated as well in any dense operating environment. Also many types of clutter, particularly clutter with high specular reflectors or only a few dominant scatters have been known to cause significant deviation from model values. The presence of these strong signals

in the reference cells has a serious affect on system performance particularly if the interferers are stronger than the desired signal.

2. Clutter and Edging

Background reflectors, undesirable as they are from the standpoint of detection and tracking, are generally denoted by the term clutter. Clutter, which tends to occur in contiguous patches forms the basis for non-homogeneity in the system background. Continuously distributed in the form of a rain cloud, or manifested as spikes in individual cells. Non-uniform, strong clutter is one of the most severe problems for CFAR algorithms [Ref. 12]. Clutter is generally comprised of a continuum of scatterers, from discrete quasi-specular to distributed and diffuse [Ref. 13]. Discrete sources are water towers, buildings, sea waves and small hills. Distributed sources are sea echo and rain. Table 4 gives four popular density functions for characterizing clutter. Figure 8 displays these clutter areas and highlights the differing statistical distribution each contains. The figure displays the space -time characterization of clutter data which can be seen as either a succession of spatial snapshots or a bundle of temporal sequences. It is worth noting that temporal distribution and correlation are relevant for the temporal CFAR approach (Clutter Maps) and that the corresponding spatial characteristics apply to the spatial thresholding approaches (Mean Level Detector CFAR).

The clutter edging concept is the effect where within a very small range interval clutter levels vary drastically. As shown by Nathanson [Ref. 14] rain, a common clutter source, can change intensity from approximately 4 cm/hour to over 16 cm/hour and back to 4 cm/hour within a one mile range interval. This rate of change of results in a clutter return power as high as 60 dB/mile making for a very large clutter edge.

Table 4. FOUR POPULAR CLUTTER DISTRIBUTIONS

Distribution	Expression
Rayleigh	$p(A) = \frac{A}{A_0^2} \exp \frac{-A^2}{2A_0^2} \qquad A \geq 0$ A = *amplitude* A_0^2 = *average RCS*
Weibull	$p(A) = \frac{C}{B} \left(\frac{A}{B} \right)^{C-1} \exp \left(\frac{-A}{B} \right)^C$ A = *signal amplitude* B = *scaling parameter* C = *slope parameter*
Log Normal	$p(A) = \frac{1}{\beta A \sqrt{2\pi}} \exp \frac{-(\ln A - \alpha)^2}{2\beta^2}$ α = *mean* β = *standard deviation* A = *amplitude*
K-Distribution	$p(A) = \frac{2B}{\Gamma(C)} \times \left(\left\{ \frac{}{2} \right)^C K_{C-1}(BA) \right.$ A = *signal amplitude* K_{C-1} = *a modified Bessel function* B = *scaling parameter* C = *slope parameter*

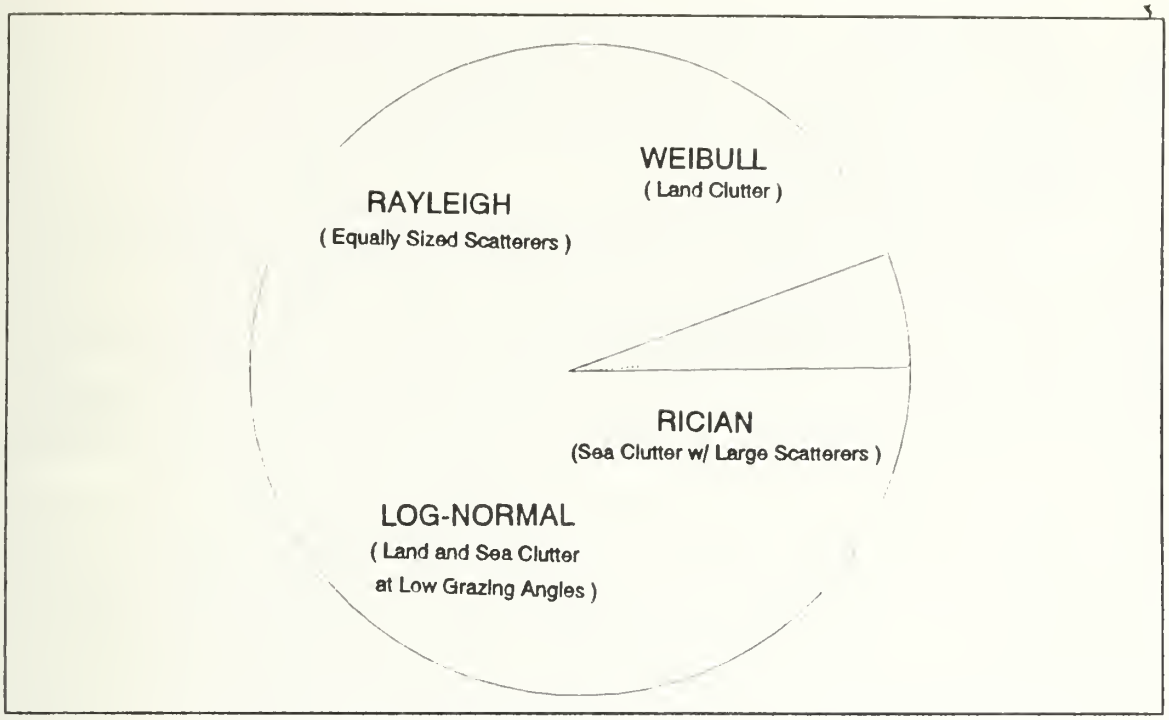

Figure 8. Clutter Types

Two clear effects of clutter and edging on CFAR systems are apparent. First, if the cell under test is in the clear while the reference cells are immersed in clutter, a masking effect results. That is, the adaptive threshold level is increased unnecessarily and therefore the P_d along with the P_{fa} are reduced significantly. This will occur even though there may be a high SNR in the cell of interest. The second case occurs when the reference cells are in the clear but the test cell is immersed in the clutter. In this condition, the P_{fa} will increase. [Ref. 15]

In terms of Naval radar operation, one must recognize that sea clutter is inherently different from land clutter in two basic ways. First, the temporal variations of the clutter tend to be larger in magnitude, and second the spatial variations tend to be smaller. A smooth sea forward-scatters incident energy so that little is reflected back to the radar, However, the likelihood of having a glassy sea at any given time is quite small, so backscattered energy is normally received. Levels of backscattered energy are directly linked to wave action and is a function of surface roughness. Radar backscatter can occur from the sides of waves as well as the small facets superimposed on the waves. These are a function of wind.

Numerous models detailing rain, land and sea clutter levels have been devised. These models can serve the radar engineer in determining optimal CFAR system characteristics based on anticipated geographical environmental conditions. [Ref. 9]

3. Multiple Target Situations

Closely separated targets are probable in military operating environments. A dense target situation occurs whenever two targets come close in range and azimuth even when clearly separated by elevation. In this common scenario, both the target returns will be contained in one reference window and possibly even in a single reference cell [Ref. 16]. If two targets are in the same cell, they are unresolved and act like one target. This situation may lead to two undesirable effects. First, if both returns are co-located in the same reference cell, some CFAR algorithms would reject that cell as a large clutter return and effectively reject both targets. A second and more common effect of interfering targets in the reference cells is the erroneous behavior of the adaptive threshold level. This is due to the interfering target increasing the systems adaptive threshold since the interferences are assumed to a legitimate noise samples. In many CFAR applications the presence of a strong return among the reference cells can cause a drastic reduction in system P_d [Ref. 17].

4. Jamming

a. Basics

The basic purpose of Electronic Countermeasures is to introduce signals into an enemies electronic systems which degrade the performance of the system so that it is unable to carry out its intended mission. Certain forms of ECM or jamming techniques are uniquely devastating to some CFAR signal processing algorithms and clearly abuse their weaknesses to unanticipated noise and multiple target situations.

There are two fundamental ways to introduce jamming energy into a radar system. First the receiver noise level can be raised through the injection of external noise through the radars antenna. This jamming can be entered into either the radar's antenna mainlobe or sidelobe. This jamming effects Adaptive Threshold CFAR systems by increasing the voltage threshold. Noise jamming has the effect of obscuring the radar target by effectively immersing it in noise. The second and more complex jamming technique forces spurious signals into the radars mainlobe or sidelobes to confuse or deceive the system. This has the effect of introducing false targets into the reference cells simulating one or more interferers. In both cases, the previously discussed vulnerabilities to clutter and multiple targets are the clear aim of the jammers. [Ref. 18]

b. Noise Jammers

Basic noise jammers can be broken down into different categories such as spot, obscuration or broadband jammers. Spot jamming occurs when only a small bandwidth is covered by the jammer, whereas the broadband jammer dilutes the power density over a large bandwidth. This enables a greater portion of the electromagnetic spectrum to be jammed at the expense of effective radiated power (ERP).

The effect of noise jamming on radars that use CFAR adaptive thresholding is the reduction of the detection probability while the system maintains the preset false alarm rate. This effect on the P_d is the result of a grossly inflated adaptive threshold level influenced by the jammer noise energies. This degrades the radar system performance.

c. False Target Jamming

A comprehensive coverage of various False Target Generating (FTG) techniques will not be covered here. The many differences among the FTG systems makes it difficult to describe them beyond some simple generalizations. In a generic sense, the use of FTGs creates transitory false targets that quickly appear and disappear at seemingly random ranges and angles of arrival. With the advent of sophisticated *smart* jamming systems (those with Electronic Support Measurement (ESM) systems integrated with the ECM units) the FTGs are capable of repeating ideal waveforms at exact radar pulse repetition intervals (PRI). In this scenario, not only are the false targets more realistic but the jamming may be more effective to an unprepared radar since it uses the non-coherent integration gain of the radar to increase the jamming effectiveness [Ref. 19].

5. Discussion

Improvement in target detection brought about through clutter suppression and Electronic Counter-Countermeasures (ECCM) can be effected through technical advances or the removal of errant assumptions by the radar engineer. As Figure 8 shows, the probabilistic models of clutter amplitudes change with environmental conditions. The characterization and understanding of radar clutter and its effect on performance is absolutely essential if the radar designer is able to accurately predict expected system performance. Therefore, in order to make proper model assumptions it will be necessary to identify differing clutter types and to be able to describe then properly such as type, size, borders, power and spectral features [Ref. 16]. The attempt must be to understand the operating environment of a particular system instead of simply trying to suppress undesirable energy returns. Unfortunately, the evolution of CFAR algorithms has not taken this approach. Rather new algorithms take advantage of more efficient technol-

taken this approach. Rather new algorithms take advantage of more efficient technologies and techniques to incrementally improve CFAR performance. These improvements, which are sometimes quite effective have the cost of additional system complexity, processing time, and cost.

IV. CFAR ARCHITECTURES

A. INTRODUCTION

As indicated earlier, each CFAR system has its own characteristic method for estimating the noise as well as its own method for determining the adaptive threshold level based on that estimate. This chapter describes eight of the most popular CFAR architectures. Information on how the systems operate, how they determine their threshold levels, their performance plots and a discussion of their inherent weaknesses and strengths will be detailed. The adaptive threshold systems will be broken down into two major categories: Mean Level Detectors and Ranked Order Detectors. Also included in this chapter will be a discussion of Non-Parametric and Clutter Mapping CFAR techniques. These are non-adaptive threshold systems that have merit and deserve attention.

B. MEAN LEVEL CFAR PROCESSORS

In this section three mean level algorithms are discussed. They are the Cell-Averaged (CA), the Greatest-Of (GO), and Smallest-Of (SO) CFAR systems The derivation of the probability of false alarm and probability of detection using square-law detection are given for each processor. Probability of false alarm and detection plots however, have created via Monte Carlo simulations for these CFAR architectures. Both square-law and envelope approximation (with a = 1 and b = 1) detector results are computed for comparison.

1. Cell Averaging CFAR

a. Background

The CA CFAR method as first introduced by Finn and Johnson [Ref. 20] in 1968 is the most basic adaptive threshold CFAR algorithm. This system can be viewed as the first step in a long evolutionary chain of CFAR systems. The CA CFAR method uses the maximum likelihood estimate of the noise power to set the adaptive threshold under the assumption that the output of the reference cells are statistically independent and identically distributed (IID) random variables. When the operating conditions of the radar meet this criteria, the CA CFAR detector is optimal in the sense that the P_d approaches that of the ideal Neyman-Pearson detector as the number of reference cells becomes large [Ref. 21].

b. System Description

The schematic diagram shown in Figure 9 outlines the CA system, which is similar to the generic CFAR depiction previously shown in Figure 2. This description shows the CA summations of the left (leading) and right (lagging) reference cells. This summing and normalizing action is what makes this detector a member of the mean level family of estimators. The summation and averaging is this systems unique way to measure the mean noise level. In operation, the returns from a given pulse are detected and a sample is taken from each range resolution cell. The cell under test is the central cell. In the CA CFAR, the inputs of the M number of cells are summed resulting in an estimate of the background noise. The adaptive threshold level is obtained by multiplying the summed value by a scaling factor (threshold multiplier) depicted as α. This value is then normalized by M yielding the overall adaptive threshold level. The magnitude of the test cell will then be compared to this adaptive threshold in order to determine the presence a target.

c. Statistics and Performance

As CFAR systems evolve technically, their characteristic statistical representations often increase in complexity and length. The statistical representation of the CA CFAR is one of the more simpler descriptions and therefore most easily understood. With this in mind a comprehensive examination of CA CFAR statistics will aid in the understanding of how other systems are statistically represented. The following equations are taken from Levanon's CA CFAR discussion [Ref. 2].

Beginning with the assumption that the M samples from the reference cells are independent and Gaussian, the envelope r of Gaussian noise will have the PDF given as

$$p(r \mid A = 0) = \frac{r}{\beta^2} e^{-\frac{r^2}{2\beta^2}}, \qquad 9$$

where β is the noise RMS value and A is the target amplitude. By normalizing the envelope with respect to β and accounting for the square law detector by making the transformation

$$z = \frac{r^2}{2\beta^2}, \qquad 10$$

the k_{th} sample of the normalized detected noise thus has the PDF of

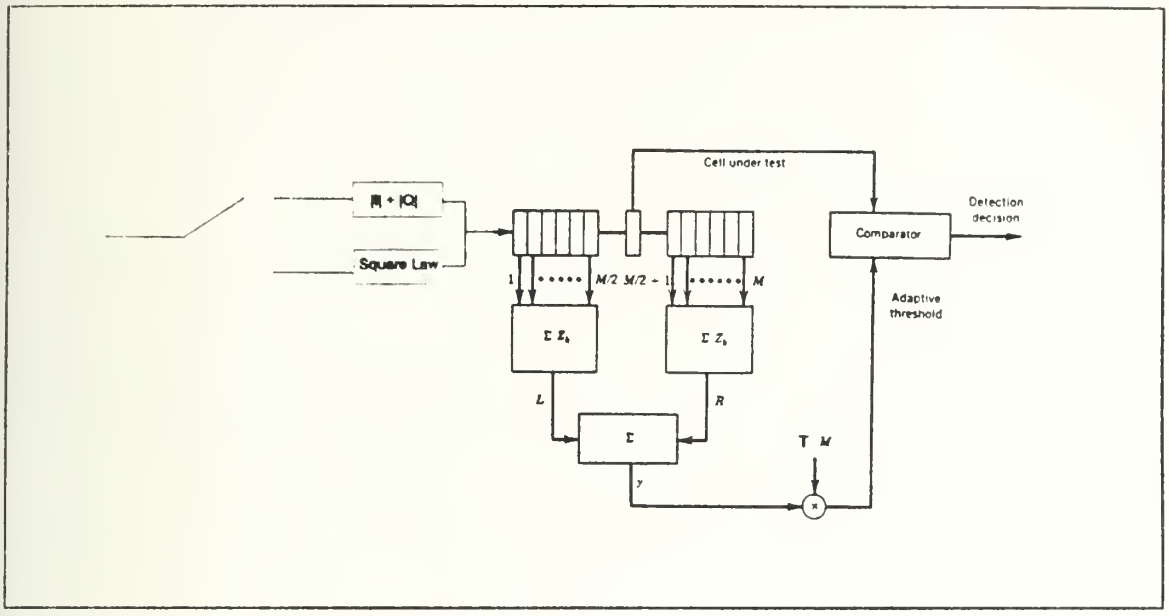

Figure 9. CA CFAR Schematic

$$p(z_k) = \exp^{(-z_k)}. \tag{11}$$

Using y for the output of the summation of leading and lagging cells

$$y = \sum_{k=1}^{M} z_k, \tag{12}$$

the PDF of y is given as

$$p(y) = \frac{y^{(M-1)}}{(M-1)!}\ exp^{-y}. \tag{13}$$

The threshold is then set at

$$V_t = y\frac{T}{M}, \tag{14}$$

where T is the threshold multiplier that determines the probability of false alarm.

To find system P_d, (the probability that the magnitude of the test cell with a target will surpass V_t) the Rayleigh PDF of the target amplitude is given as

$$p(A) = \frac{A}{A_0^2} \exp^{\frac{-A^2}{2A_0^2}}, \tag{15}$$

where A_0 is the most probable amplitude relative to the average signal power. The PDF of the signal plus noise is given as

$$p(z) = \frac{1}{1 + (\frac{A_0^2}{\beta^2})} \quad \exp^{\frac{-z}{1+(\frac{A_0^2}{\beta^2})}}, \tag{16}$$

where $\frac{A_0^2}{\beta^2}$ is the average SNR. Using (16) and the threshold fixed at V_t the probability of detection will be obtained as

$$P_d(SNR \mid V_t) = \int_{V_t}^{\infty} p(z)\, dz = \exp^{(\frac{-V_t}{1+SNR})}. \tag{17}$$

However, in the CFAR system the threshold is a function of the random variable y given in (14). Thus (17) is only a conditional probability of detection and the overall P_d will be obtained by averaging (17) over all y, that is

$$P_d(SNR) = \int_{y=0}^{\infty} P_d(SNR \mid V_t = T\frac{y}{M})\, p(y)\, dy. \tag{18}$$

Using (13), (17), and (18) we get

$$P_d(SNR) = \int_{y=0}^{\infty} \exp^{(\frac{(-T\frac{y}{m})}{1+SNR})} \frac{y^{M-1}}{(M-1)!} \exp^{(-y)}\, dy. \tag{19}$$

Finally, this known integral can be represented as

$$P_d(SNR, T, M) = (1 + \frac{T}{M(1+SNR)})^{-M}. \tag{20}$$

The P_{fa} can be easily obtained from (20) by setting the average SNR to zero. That is

$$P_{fa}(T, M) = (1 + \frac{T}{M})^{-M}. \tag{21}$$

The respective Monte Carlo CA CFAR P_{fa} and P_d plots are shown in Figures 10 and 11 for both the square law and envelope approximation detectors. As shown, the P_{fa} for the envelope approximation CA CFAR systems has a false alarm rate 10^{-2} at a threshold multiplier value of approximately 2.6, and a 10^{-4} rate at approximately 3.9 . The square law detector has much higher threshold multipliers. To maintain the false alarm rates of 10^{-2} and 10^{-4} the threshold multipliers of approximately 5.0 and 10.8 are required. Using these threshold multiplier values the P_d curves for a M = 32 cell system are generated. As expected, the superior false alarm rate threshold values require significantly higher SNRs to maintain constant detection rates. In the envelope approximation system for example, with a false alarm rate of 10^{-2} a P_d of 0.6 requires approximately 7 dB SNR whereas a 10^{-4} system requires almost 11 dB. The square law system shows slightly better performance requiring approximately 0.5 to 1.0 dB less SNR to achieve comparable detection rates.

d. Strengths and Limitations

When noise or clutter is stationary in the reference cells, CA CFAR detectors maintain effective CFAR action. Under these conditions CA CFAR is the preferred detector in that it optimizes the tradeoffs between the P_{fa} and the P_d. When these conditions are not met the performance of the system decreases as the input interference departs from the assumed Rayleigh distribution.

The two basic limitations of the system stem from interference found inside the test cell or among the reference cells. As previously mentioned, when the test cell is immersed in strong clutter regions, and the reference cells are in the clear, a natural reduction in the threshold will occur resulting in an increase in the P_{fa}. This common situation lead to the creation of the Greatest-Of (GO) CFAR algorithm, introduced in 1972 by Hansen [Ref. 22]. For the second case, when the test cell is in the clear and the reference cells have interferers, the threshold will be unnecessarily increased reducing the system P_d. This led to the introduction of the Smallest-Of (SO) CFAR algorithm introduced by Trunk [Ref. 23].

2. Greatest-Of CFAR

a. Background

As stated, the GO CFAR was developed to overcome a decreased adaptive threshold level in response to clutter regions. The GO CFAR attempts to correct this weakness by independently measuring background noise levels from the leading and lagging reference cells and then selecting the larger of these two values for use in the

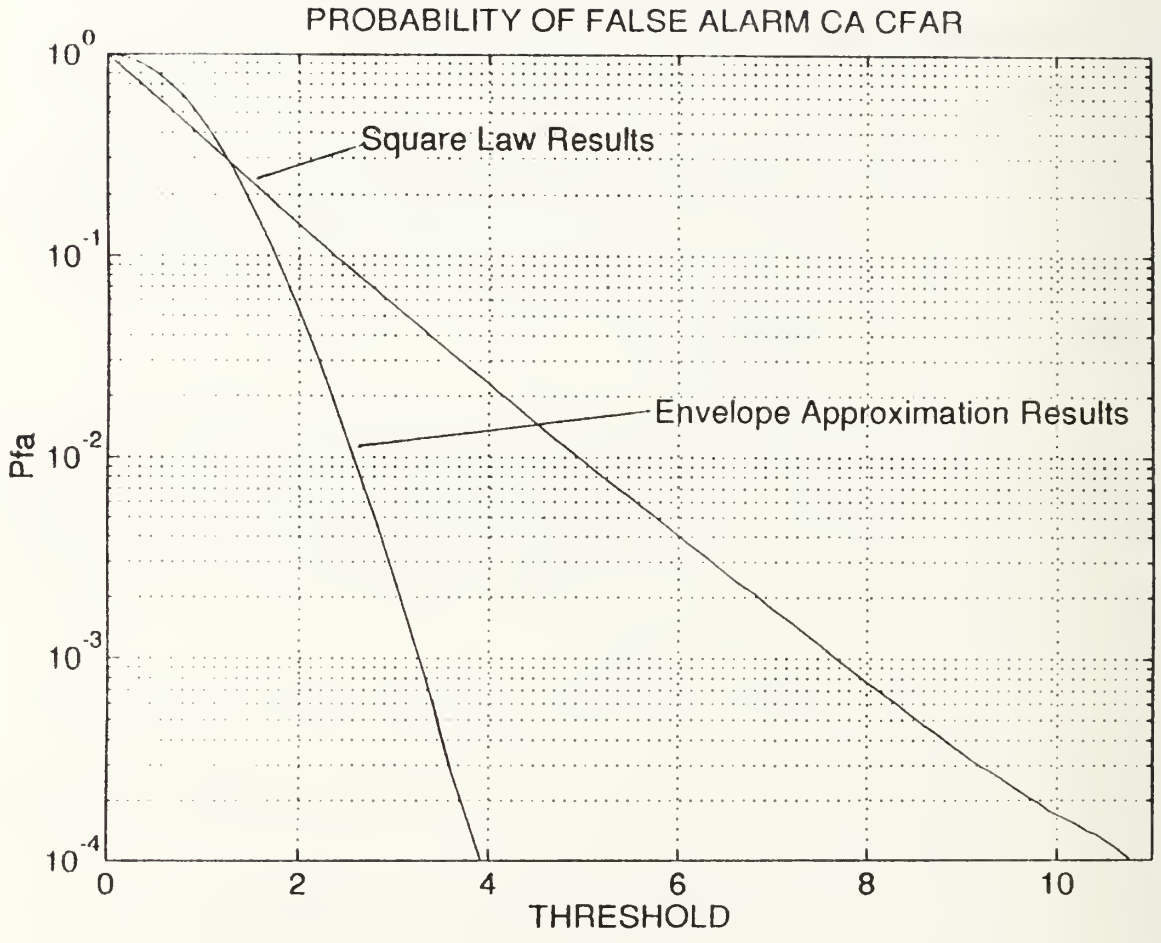

Figure 10. CA CFAR Probability of False Alarm

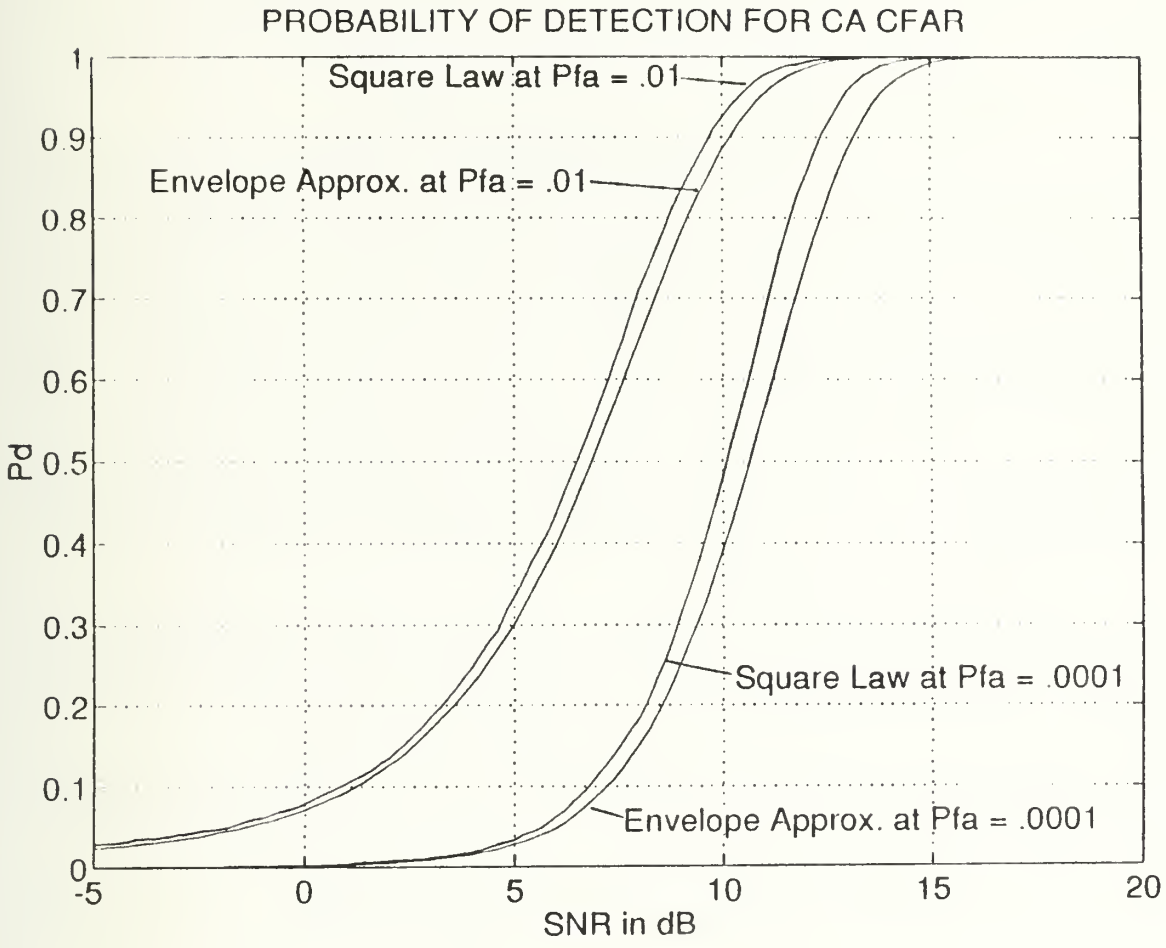

Figure 11. CA CFAR Probability of Detection

Adaptive Threshold process. This process results in a selection of the reference window that covers the clutter region thus resulting in a closer estimate of the true clutter environment.

Of note, GO CFAR has also been termed Max Mean Level Detector (MX-MLD) CFAR by Ritcey [Ref. 24]. This naming denotes both the type of local estimator (MLD) as well as the combining operation (Max vs. GO). Both terms are accepted.

b. System Description

A conventional GO processor is depicted in Figure 12. As shown, the square law or envelope approximation detector output is fed into the reference windows. The leading and lagging window summations are denoted by Y_1 and Y_2 respectfully. Both reference cell neighborhoods contain M/2 total cells. The detector threshold voltage level (V_t) is obtained by selecting the greater of Y_1 or Y_2 (normalized by M/2) and then multiplied by the threshold multiplier T. A target is declared when the cell under test exceeds V_t. In GO CFAR, the background noise is assumed to be Gaussian, the target in the test cell and any interfering targets are assumed to be fluctuating independently, each according to Rayleigh PDFs [Ref. 17].

c. Statistics and Performance

The following Square Law statistical description of the GO CFAR has been analyzed by Hansen [Ref. 25]. The detection performance of this process is derived as follows :

For a SNR at the input to the Square Law detector, the normalized pdf of the signal-plus-noise is

$$p_x(x) = \left(\frac{1}{(1+SNR)}\right) \exp\left(\frac{-x}{(1+SNR)}\right) \quad x \geq 0. \tag{22}$$

The noise level estimates Y_1 and Y_2 are IID with pdfs

$$p_y(y) = y^{\frac{M}{2}-1} \frac{\exp^{-y}}{\Gamma(\frac{M}{2})} \quad y \geq 0, \tag{23}$$

and the cumulative distribution function (cdf) of Z is then given by

$$F_z(z) = F_y(z)F_y(z), \tag{24}$$

where $F_y(z)$ is the cdf corresponding to $p_y(y)$. Thus

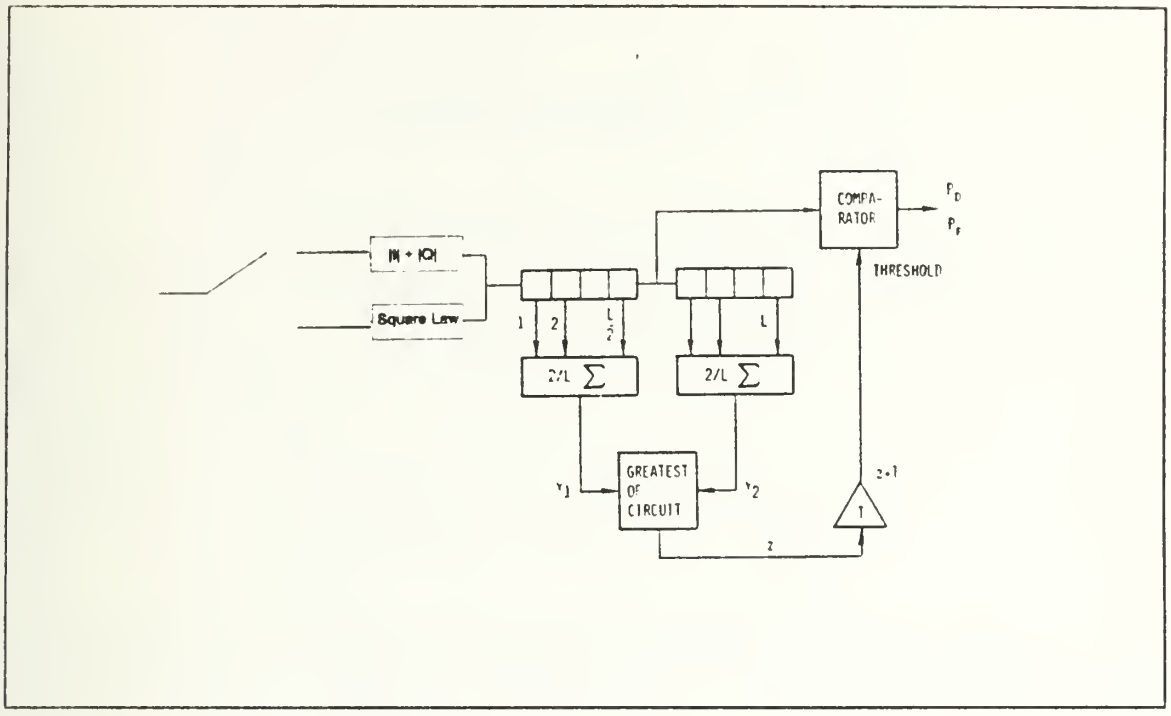

Figure 12. GO CFAR Schematic

$$p_z(z) = 2z^{\frac{M}{2}-1}\frac{\exp^{-z}}{\Gamma(\frac{M}{2})} \times \int_0^z y^{\frac{M}{2}-1}\frac{\exp^{-y}}{\Gamma(\frac{M}{2})}\,dy. \tag{25}$$

The probability of detection is then

$$P_d = \int_0^\infty p_z(z) \times \int_{2Tz/M}^\infty p_x(x)dxdz. \tag{26}$$

By direct evaluation of the inner integral and termwise integration the following numerical result is obtained.

$$P_d = 2 \times \left[\left(1 + \frac{2T}{M(1+SNR)}\right)^{\frac{-M}{2}} - \left(2 + \frac{2T}{M(1+SNR)}\right)^{\frac{-M}{2}}\right.$$

$$\times \sum_{k=0}^{\frac{M}{2}-1} \binom{\frac{M}{2}-1+k}{k} \left(2+\frac{2T}{M(1+SNR)}\right)^{-k} \Bigg] \qquad 27$$

When the SNR is set to zero, this expression yields the system P_{fa} as

$$P_{fa} = 2 \times \Bigg[\left(1+\frac{2T}{M}\right)^{\frac{-M}{2}} - \left(2+\frac{2T}{M}\right)^{\frac{-M}{2}}$$

$$\times \sum_{k=0}^{\frac{M}{2}-1} \binom{\frac{M}{2}-1+k}{k} \left(2+\frac{2T}{M}\right)^{-k} \Bigg] \qquad 28$$

The P_{fa} and P_d curves for the GO CFAR is shown in Figures 13 and 14 for the square-law and envelope approximation detectors. As with the CA CFAR, these plots were generated via Monte Carlo simulation. As Figure 13 shows, the P_{fa} values of 10^{-2} and 10^{-4} yield threshold multipliers of approximately 2.4 and 3.65 for the envelope approximation detector and 4.5 and 9.8 for the square law system. These multipliers in turn generate the P_d plots shown in Figure 14. As always, the superior false alarm rate systems require higher SNR to achieve comparable detection rates. For example, a 0.6 detection probability requires approximately 7.5 dB SNR at 10^{-2} (P_{fa}), and approximately 11.0 dB at 10^{-4} for the envelope approximation system. The square law results again show an approximate 0.5 to 1.0 dB improvement over the envelope approximation detectors. In the following chapter these values will be compared with other CFAR architectures.

d. Strengths and Limitations

A key advantage of using the MAX/GO family of detectors is that near the edge of clutter regions the 'greatest of' reference cells capture the desired clutter samples and maintains the false alarm rate. Also when a GO detector operates in a benign environment suitable for (CA CFAR), only a small CFAR loss of 0.1 to 0.3 dB is noted. This loss is due to the reduction of the total number of reference cells (by half) available for noise estimation.

Unfortunately, GO CFAR maintains the false alarm rate in clutter regions at the expense of the multiple target scenario. In the analysis by Weiss [Ref. 15] a GO

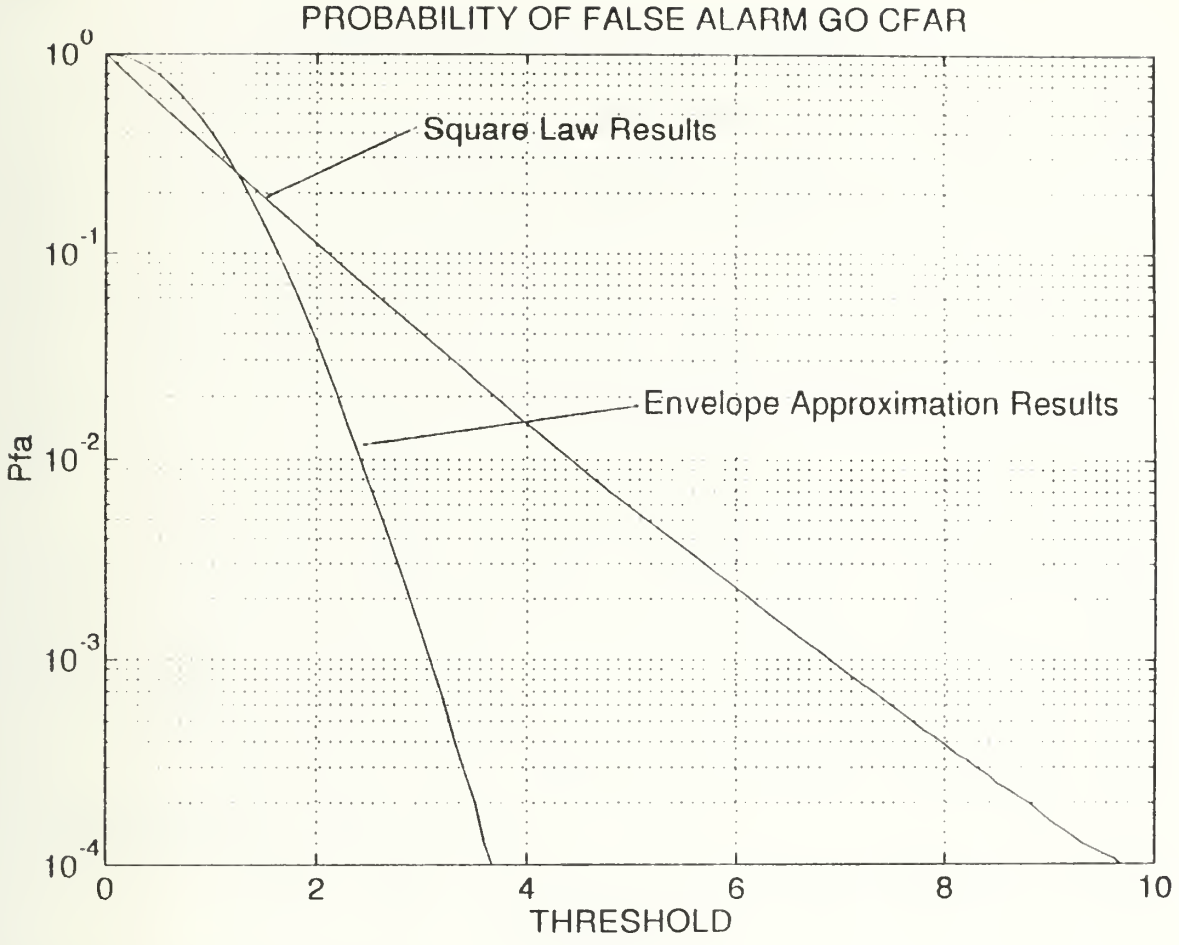

Figure 13. GO CFAR Probability of False Alarm

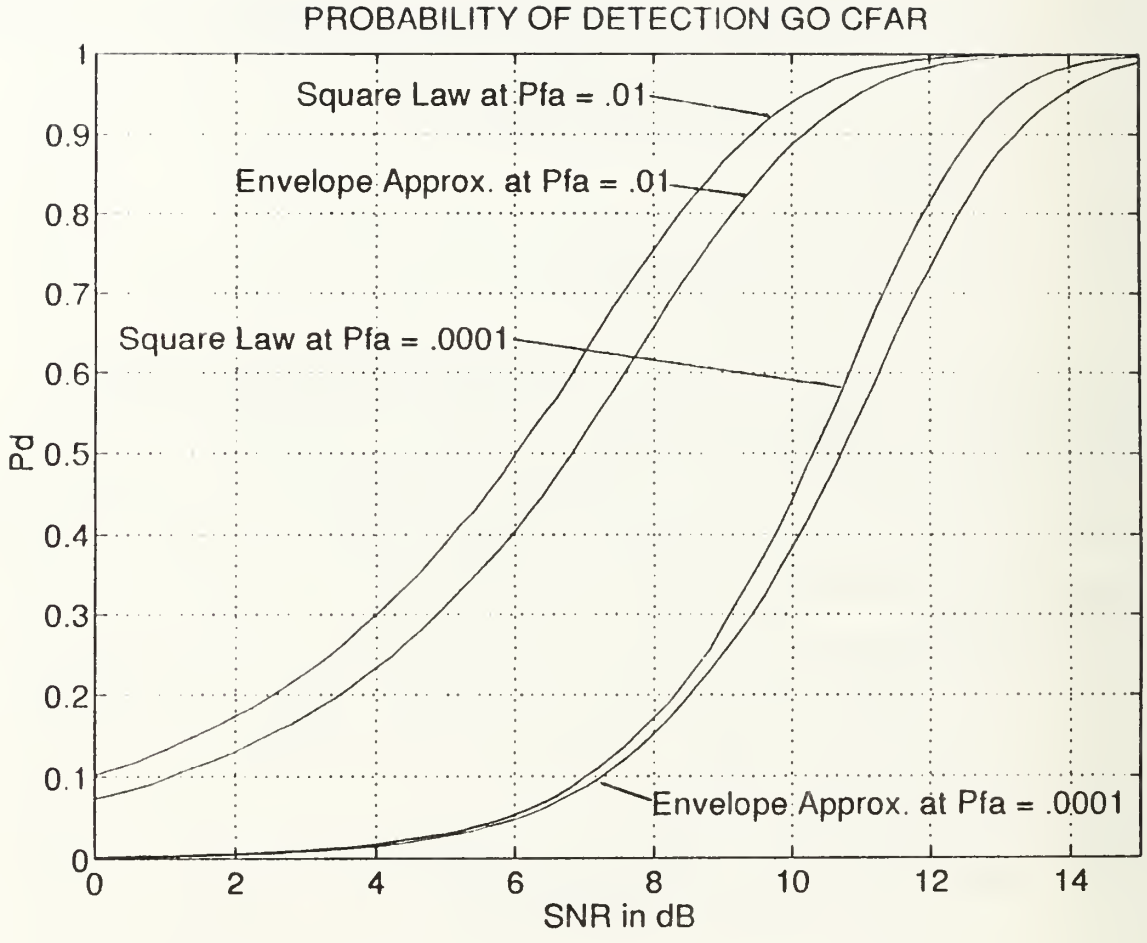

Figure 14. GO CFAR Probability of Detection

system in the presence of an interfering target shows that target detection is nearly inhibited. This problem can be grasped intuitively since when the interfering target is large, the half portion of the reference cells containing this extraneous target is almost always selected in the GO process, hence the threshold is further increased making for greater detectability loss.

3. Smallest Of CFAR

a. Background

The Smallest Of (SO) CFAR system introduced by Trunk [Ref. 23] is designed to handle closely separated target situations. Generally, if the targets are close together, the detection from both targets are merged and a single target is reported. The problem of resolving merged targets is not only a function of the target separation but also a function of the signal strength. Usually it is assumed that if targets are large enough to be detected, then they can be resolved if they are separated by at least one pulse width (PW) or equivalently, lie within different range cells [Ref. 23].

b. System Description

The operation of the SO system is exactly the same as the GO except that the smaller of the normalized leading and lagging reference window summations are used as the noise power estimate. Figure 15 shows the SO processor architecture with the sole change being the selection logic.

c. Statistics and Performance

In the SO CFAR scheme, the noise estimate uses the smaller of the sums Y_1 and Y_2. That is

$$Z = \min(Y_1, Y_2) \tag{29}$$

Where Y_1 and Y_2 are defined as

$$Y_1 = \sum_{i=1}^{n} X_i \qquad Y_2 = \sum_{i=n+1}^{N} X_i. \tag{30}$$

Gandhi [Ref. 26] completes this analysis stating that the pdf of Z is given by

$$f_Z(z) = f_1(z) + f_2(z) - [f_1(z)F_2(z) + f_2(z)F_1(z)]. \tag{31}$$

Where f_i and F_i are the pdf and cdf of the random variable Y_i. This yields the false alarm

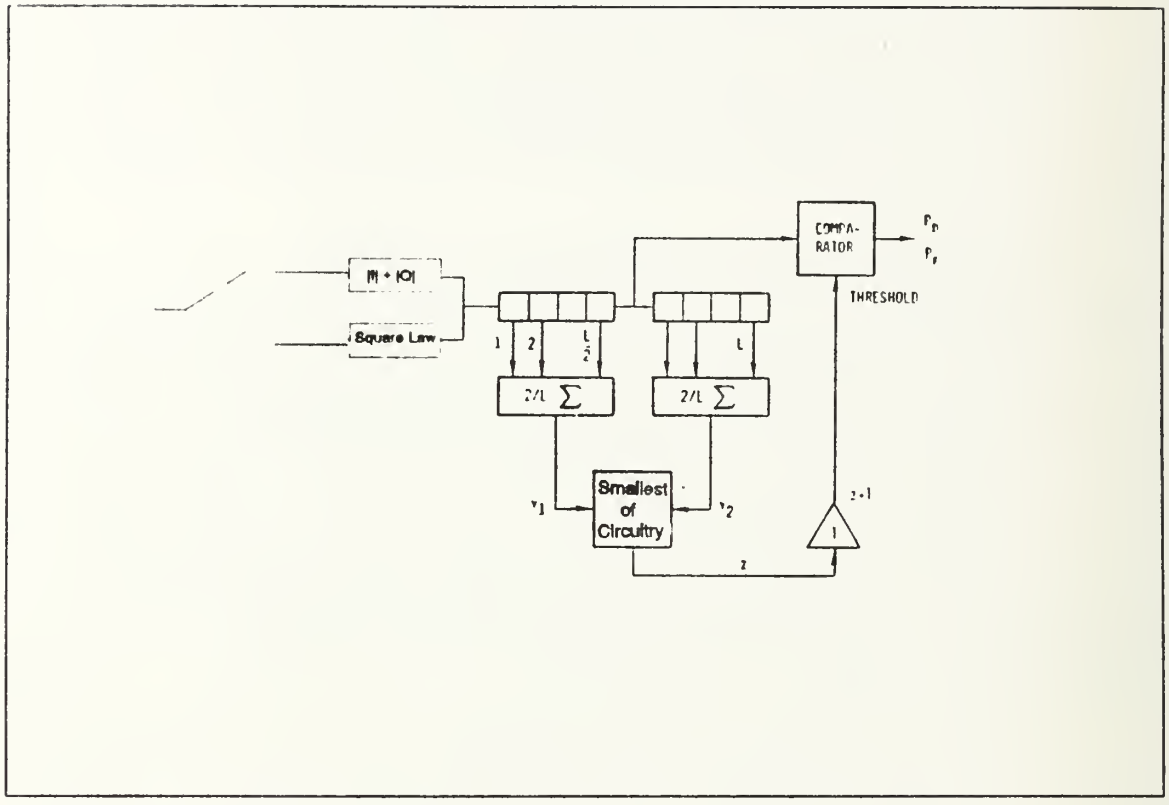

Figure 15. SO CFAR Schematic

probability :

$$P_{fa} = \Psi_{Y1}(\frac{T}{2\mu}) + \Psi_{Y2}(\frac{T}{2\mu}) - 2(1+T)^{-n}$$

$$-2 \times \sum_{i=0}^{n-1} \binom{n+i-1}{i} (2+T)^{-(n+i)} \qquad 32$$

Where $\Psi_{Y1}(T)$ and $\Psi_{Y2}(T)$ are the moment generating functions (mgf) of the random variables Y_1 and Y_2 , T is the threshold multiplier, and μ is the background total noise power. The detection probability is then obtained by replacing T with T(1+SNR) yielding :

$$P_d = \Psi_{Y1}\left(\frac{T}{(1+SNR)2\mu}\right) + \Psi_{Y2}\left(\frac{T}{(1+SNR)2\mu}\right) - 2\left(1+\frac{T}{1+SNR}\right)^{-n}$$

$$-2\times\sum_{i=0}^{n-1}\left(\frac{n+i-1}{i}\right)\left(2+\frac{T}{1+SNR}\right)^{-(n+i)} \qquad 33$$

The SO system performance plots created via Monte Carlo simulation are shown in Figures 16 and 17. Figure 16 shows the probability of false alarm using the square law detector. As shown, the envelope approximation false alarm rate of 10^{-2} results in a threshold multiplier of approximately 2.75, whereas a 10^{-4} false alarm rate results in a multiplier of approximately 4.4. The square law system results in multiplier values of approximately 2.85 and 13.8 for the 10^{-2} and 10^{-4} false alarm rates. Figure 16 displays the P_d curves at the false alarm rates of 10^{-2} , and 10^{-4}. As always, a higher SNR is required to maintain the superior false alarm rates. In Figure 17 it is shown that a 0.6 detection probability (envelope approximation) requires approximately 6 dB SNR at a 10^{-2} P_{fa} , approximately 11.5 dB at 10^{-4}. The square law results again show a 0.5 to 1.0 dB improvement over the envelope approximation system. These values will be compared against the other MLD systems in the following chapter.

d. Strengths and Limitations

The strength of the SO technique is its excellent performance in resolving closely spaced targets. The detector performance degrades significantly however if interfering targets are located in both the leading and lagging windows simultaneously. This clearly results in at least one of the interferers influencing the voltage threshold value and therefore possibly masking the primary target. Furthermore, the SO processor fails to maintain a CFAR at clutter edges. Gandhi [Ref. 26], has shown that a 15 dB clutter edge leads to an increase greater than five orders of magnitude in the false alarm rate at N = 24 and design P_{fa} of 10^{-6}. Finally, even in a relatively benign environment the SO architecture results in an excessive number of false alarms since the SO selection yields a very low Adaptive Threshold level. This level is generally lower than many clutter spikes, all of which yield false alarms.

More so than the other Mean Level Detectors, the SO processor is highly dependent on the number of reference cells chosen. For a small N, the CFAR loss is quite large but decreases considerably for increased N. For example Weiss [Ref. 15] has

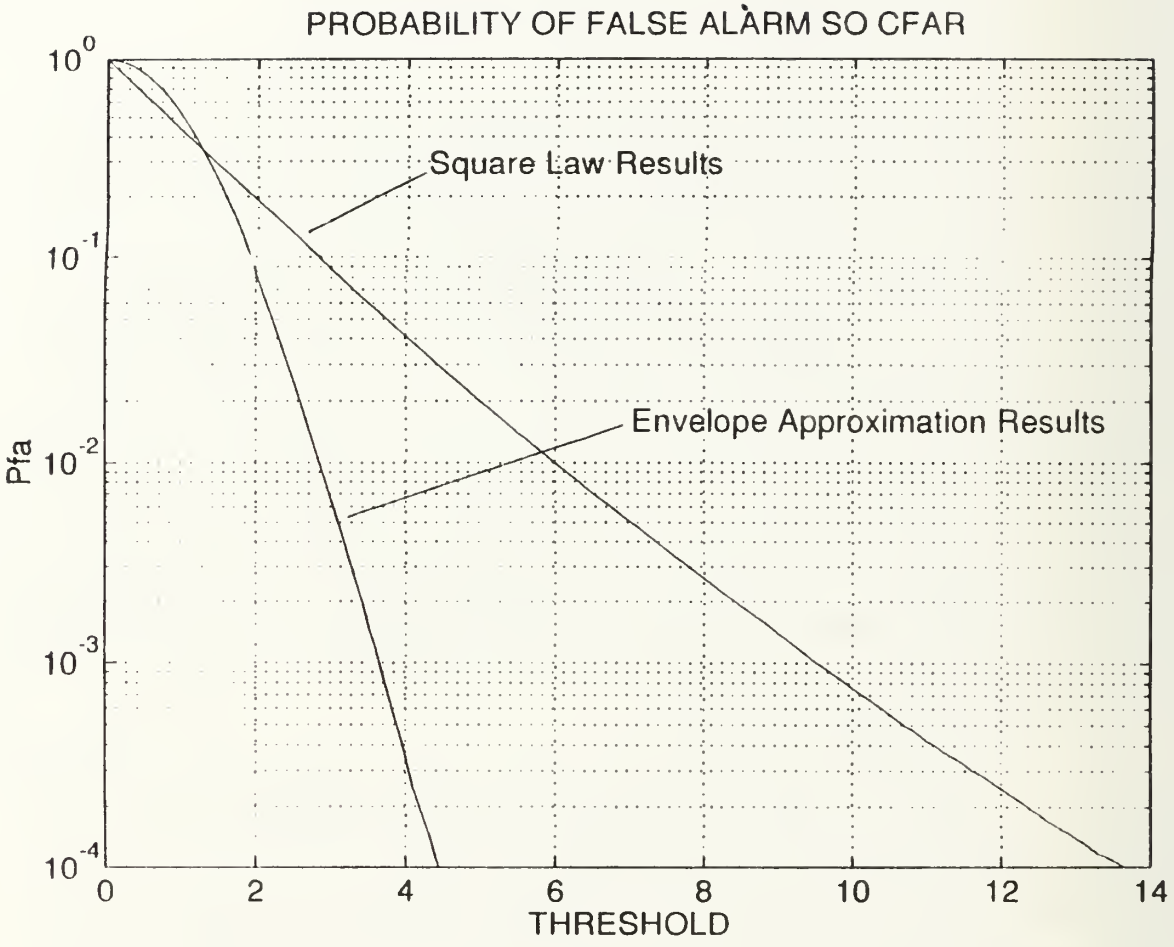

Figure 16. SO CFAR Probability of False Alarm

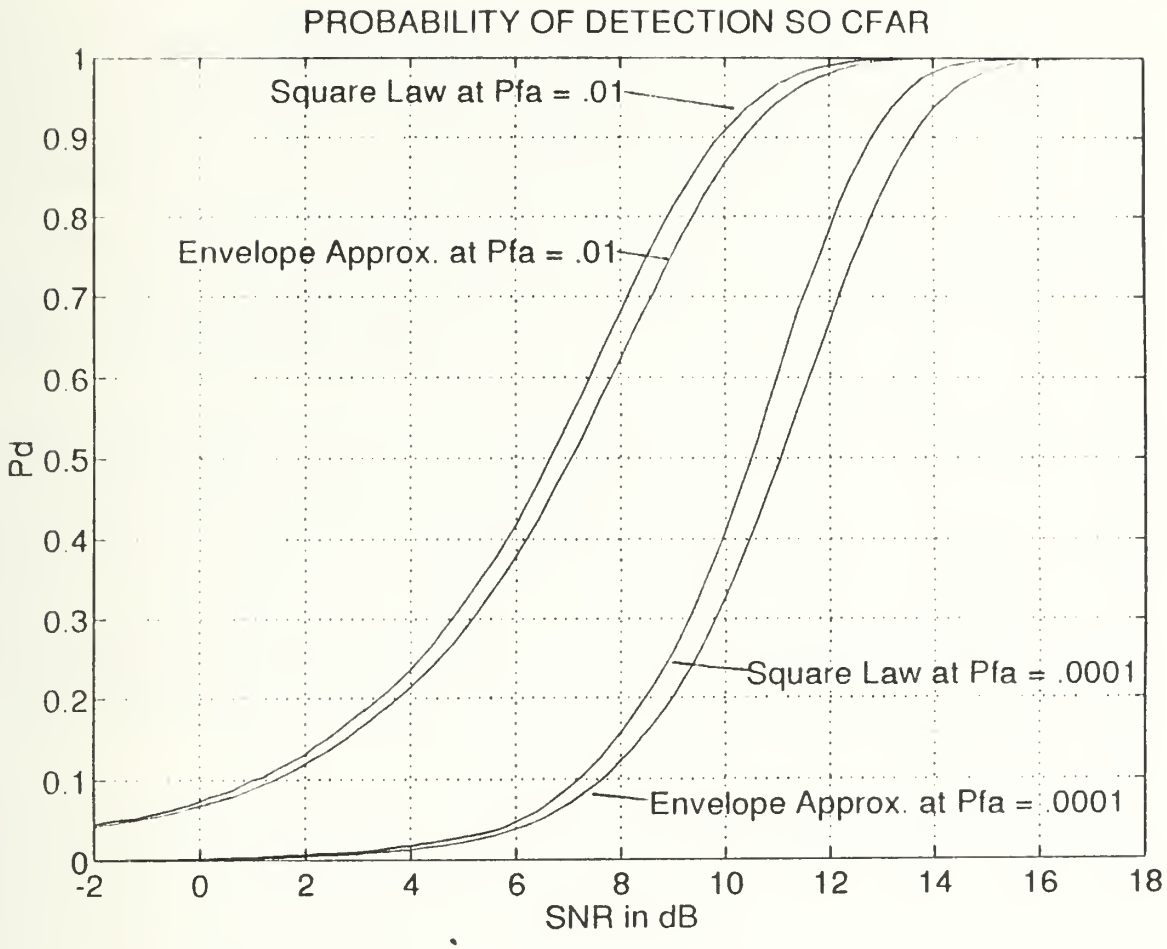

Figure 17. SO CFAR Probability of Detection

shown that the detectability loss of the SO CFAR scheme is approximately 11 dB for the N = 4 case but only 0.7 dB at N = 32 (P_{fa}).

C. RANK ORDERED CFAR PROCESSORS

1. Ordered Statistics CFAR

a. Background

The Ordered Statistic (OS) CFAR processor was designed to overcome the loss in detection performance suffered by CA CFAR when interfering targets were located among the background cells. Introduced by Rohling in 1983 [Ref. 27], OS CFAR provides inherent protection against drastic reductions in performance in the presence of interfering targets. The OS technique rank orders the background voltages encountered in the neighborhood areas according to their magnitude and then selects a certain predetermined address from this sequence. This address value can be the median, the minimum, the maximum or any other value. OS techniques have been proven to work satisfactorily in both multiple target and non-uniform clutter areas, although they present a small increment in detection loss. OS CFAR methods overcome many difficulties which arise in various situations of multiple targets in clutter, but many detection problems in special clutter regions remain to be solved.

b. System Description

The schematic of the OS-CFAR system is shown in Figure 18. In this system the values of the reference cells are first sorted by magnitude. The ordered sequence thus achieved is represented by the indices in the parenthesis.

$$X_{(1)} \leq X_{(2)} \leq \ldots \leq X_{(M)} \qquad 34$$

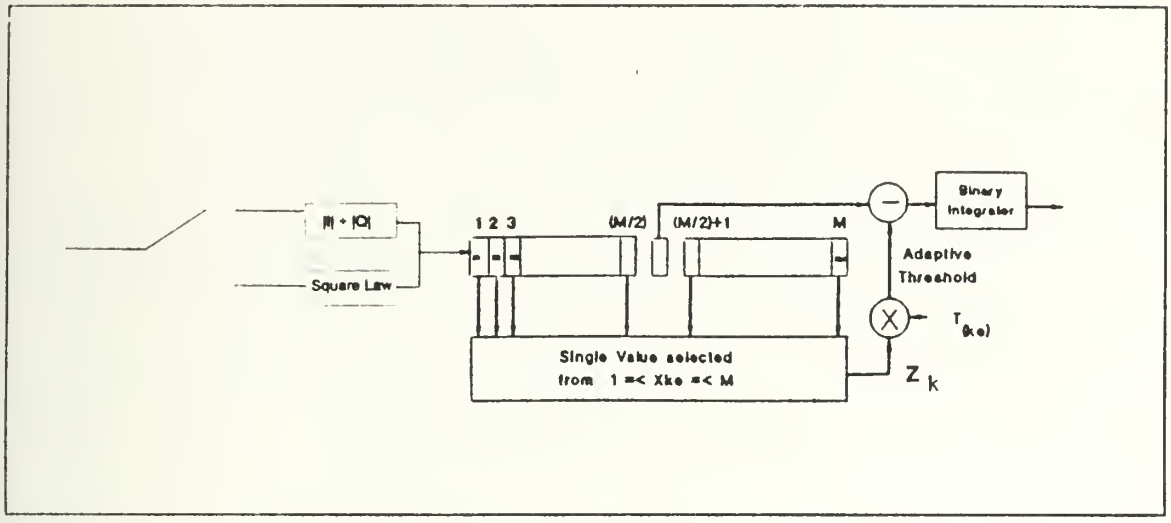

Figure 18. OS CFAR Schematic

The main premise of OS CFAR is to use some rank selection from the ordered sequence for use as the estimate for the average noise power in the entire reference window. The variable K identifies the rank or the address of the cell whose input is selected for further processing. The threshold level V_t is then obtained by multiplying the input from the Kth ranked cell by the scaling factor T so that

$$V_t = TZ_k \tag{35}$$

is a random variable and its PDF is a function of the PDF of Z_k. The use of statistics in OS CFAR processing does not define a single CFAR method but rather a series of several CFAR methods. For any given choice of Z_k, a distinct CFAR processor is established. Rohling pointed out that the choice of the representative cell K will effect the performance of the OS CFAR without interfering targets. For example, in a 16 cell reference window with a single target, the detection rates for a K = 10 system are markedly different then for a K = 14. Generally, with no interferers, performance increases as K is increased. However, with two interferers, K = 14 has an additional 1 dB loss as compared to the K = 10 case. The poor performance in the presence of interferers stems from the fact that we reach the point where M minus the number of interferers (J) equals K, implying that the representative cell becomes the highest ordered target free reference cell.

c. Statistics and Performance

The statistical representation of rank ordered CFAR becomes more complex and difficult to grasp as the CFAR architectures expand. The OS CFAR analysis is the basis for all other rank ordered systems and is shown. Using the previous notation, the PDF of the threshold random variable will be shown, as well as equations for P_{fa} and P_d. The optimum choice of K is the number of reference cells (M) minus the anticipated number of interferers (J). The following analysis of OS CFAR was taken from Levanons work [Ref. 2]

$$K = M - J \qquad (K \leq M) \tag{36}$$

$$V_t = TZ_K. \tag{37}$$

When Z is a random variable with a pdf p(z) and a distribution function P(z), the Kth ranked sample has a PDF

$$p_K(z) = K\binom{M}{K}\left[P(z)\right]^{(K-1)}\left[1 - P(z)\right]^{(M-K)} p(z), \tag{38}$$

where

$$p(z) = \exp^{(-z)}, \tag{39}$$

and the distribution function is therefore

$$P(z) = \int_0^z \exp^{(-z)}\, dz = 1 - \exp^{(-z)}. \tag{40}$$

Using 38, 39, and 40 the PDF of the Kth sample is found to be

$$p_K(z) = K\binom{M}{K}\ \exp(-z)^{M-K+1}\left[1 - \exp^{(-z)}\right]^{(K-1)}. \tag{41}$$

The probability of a noise input in the cell under test crossing the voltage threshold is

$$P(Z \geq V_t \mid V_t) = \int_{V_t}^{\infty} \exp^{(-z)}\, dz = \exp^{(-V_t)}. \tag{42}$$

The threshold V_t is a function of the random variable z_k. Thus the P_{fa} can be derived by averaging 42 with V_t expressed as a function of z_t

$$P_{fa} = \int_{0}^{\infty} \exp^{(-Tz_K)}\, p(z_K)\, dz_K \tag{43}$$

or

$$P_{fa} = \int_{0}^{\infty} \exp^{(-Tz)} p_k(z)\, dz. \tag{44}$$

Using Equations 41 in 44 the P_{fa} becomes

$$P_{fa} = K\left(\frac{M}{K}\right) \frac{(T + M - K)!(K - 1)!}{(T + M)!} \tag{45}$$

In order to derive the P_d we can use the same expression used for the P_{fa} by replacing the T with T' where

$$T' = \frac{T}{1 + SNR} \tag{46}$$

thus

$$P_d = \int_{0}^{\infty} \exp^{(-T'z)} p_K(z)\, dz. \tag{47}$$

or

$$P_d = K\left(\frac{M}{K}\right) \frac{(T' + M - K)!(K - 1)!}{(T' + M)!} \tag{48}$$

The P_{fa} for the envelope approximation OS CFAR is shown in Figure 19. As shown, a false alarm rate of 10^{-2} is found at a threshold multiplier value of approximately 2.3 and a 10^{-4} false alarm rate has a multiplier value of approximately 3.6. The square law results yield threshold multipliers of approximately 5.0 and 11.3 to ensure the 10^{-2} and 10^{-4} false alarm rates. Figure 20 displays the resulting P_d curves for the envelope approximation and square law systems at the false alarm rates of 10^{-2}, and 10^{-4}. This figure shows that a 0.6 detection probability requires approximately 8 dB SNR at the 10^{-2} rate, and approximately 12 dB is required for the 10^{-4} case. These values will be used in the following chapter to compare the different detector types. These Monte Carlo solutions are the result of the simulation where the value of K was set as the 20th position of the ordered sequence.

d. Strengths and Limitations

In general, the presence of one or more interfering targets among the reference cells causes the adaptive thresholds to increase erroneously. In OS CFAR this increase is relatively small. A reference cell with an input from a strong target will be ranked at the top, namely, it will occupy the Mth out of M cells. Thus the interfering target effectively reduces the number of reference cells to M-1. In the presence of J strong interfering targets, the effective number of reference cells drops to M-J. As stated by Levanon [Ref. 28], the detection loss due to the increase in threshold is not extensive as long as $J \leq M - K$.

Unfortunately the OS CFAR system suffers from two main limitations. First, small targets are easily missed in the presence of multiple targets. Clearly, the chosen K will detect the large targets but will set the V_t at a value too high for small or distant targets to cross. A second limitation of OS CFAR is its inability to perform at clutter edges. Any sharp clutter edge gives a clear rise in the system false alarm rate with respect to the false alarm rate that would be obtained in uniform clutter.

2. OSGO and OSSO CFAR

a. Background

In this section two modified OS CFAR architectures are analyzed. The OSGO (Ordered Statistic - Greatest Of) and the OSSO (Ordered Statistic - Smallest Of). OSGO CFAR has all the advantages of standard OS CFAR in the nonhomogeneous and multiple target situations with a negligible additional CFAR loss in the homogeneous environment. The OSSO CFAR's sole advantage is that it has the equivalent processing speed as an OSGO. Unfortunately, the OSSO can not control the false alarm rate and it also behaves poorly in the nonhomogeneous clutter situations [Ref. 29].

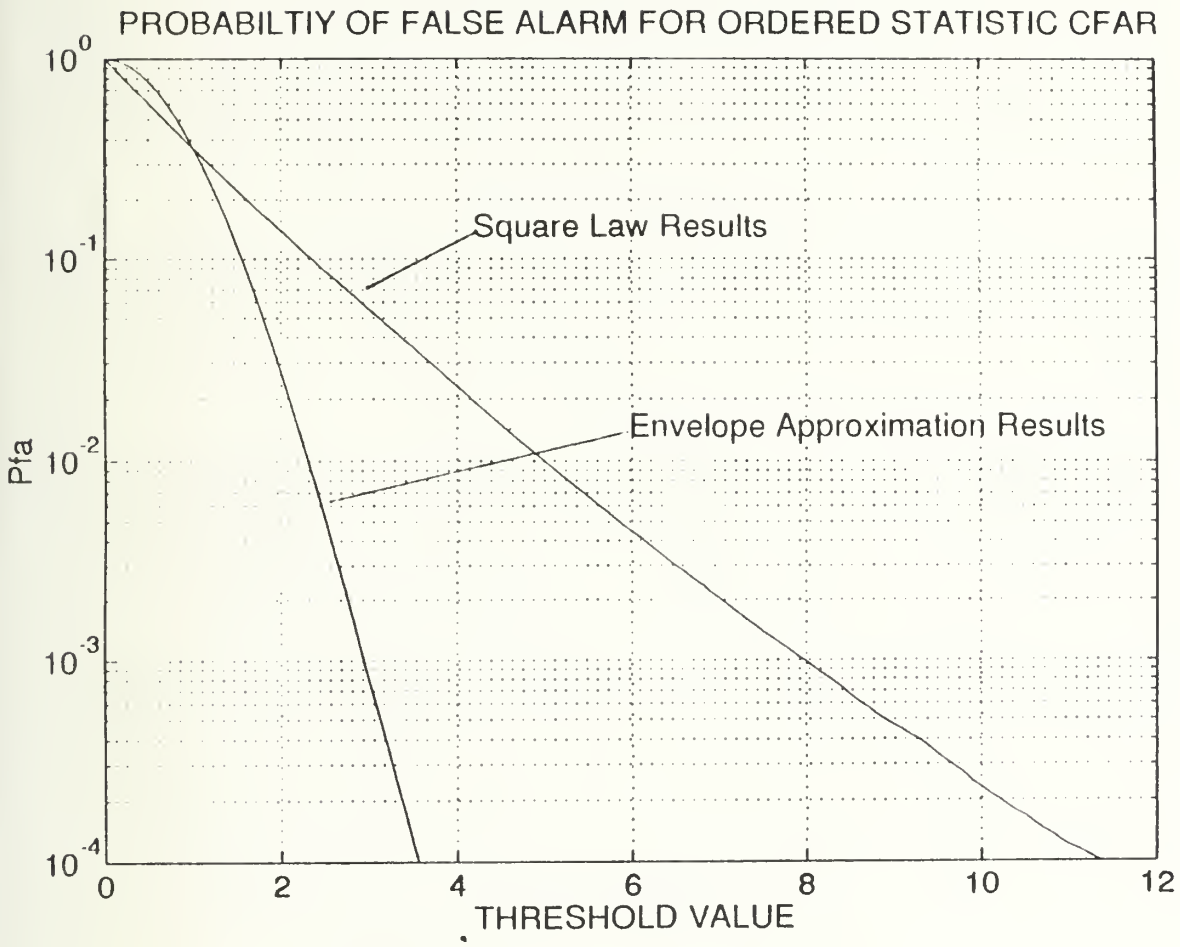

Figure 19. OS CFAR Probability of False Alarm

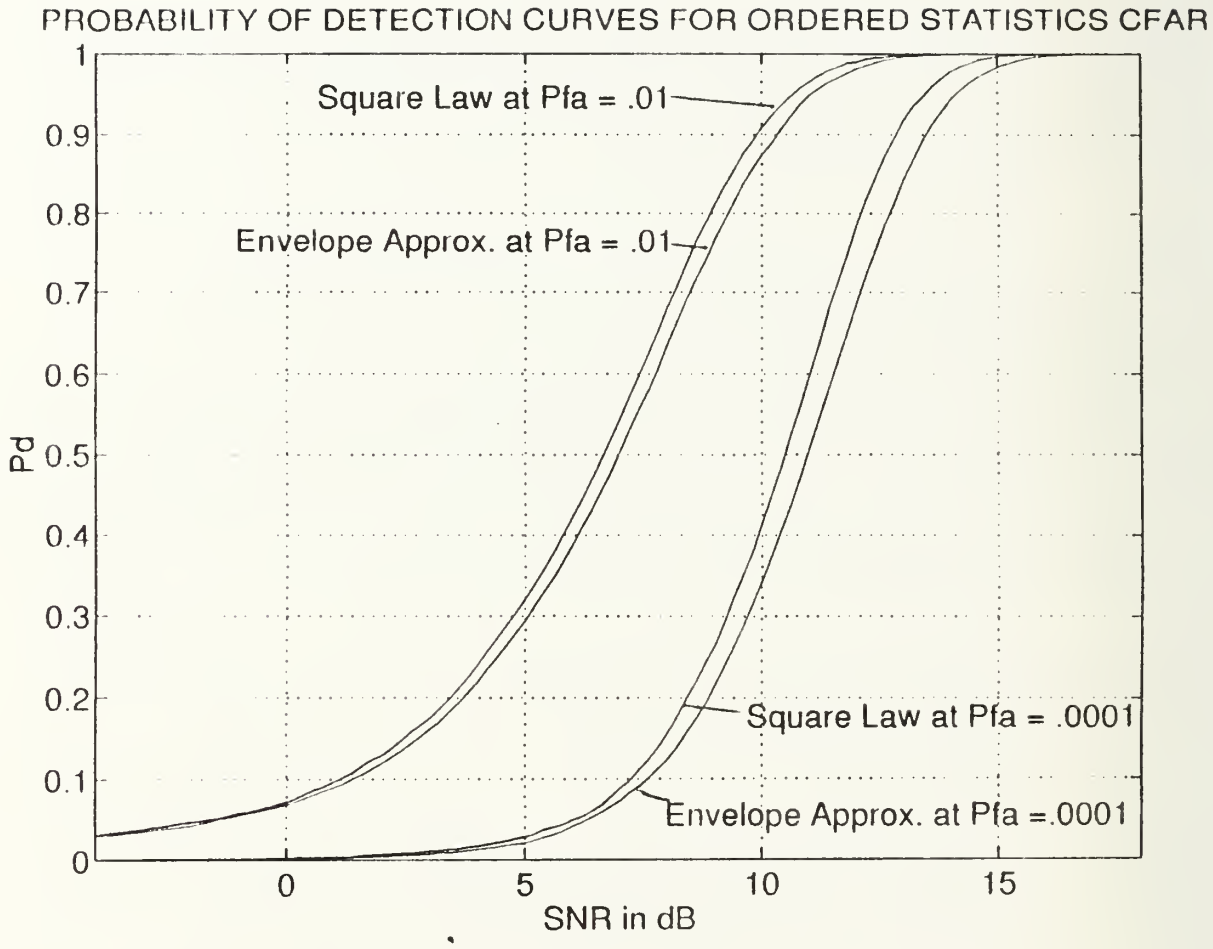

Figure 20. OS CFAR Probability of Detection

b. System Description

The schematic for the OSGO and OSSO system is shown in Figure 21. The OSGO and OSSO algorithm is based upon two assumptions. First that the noise estimation reference cells have an exponential PDF; and second that, noise in the cells are independent and homogeneously spread. The OSGO CFAR algorithm consists of taking the greater value of the two samples (leading reference cell is K_1, lagging reference cell is K_2). Obtained from Order Statistic techniques applied to the two neighborhood regions independently. The random variable Z is therefore found as

$$Z = \max(K_1, K_2). \tag{49}$$

For an OSSO system the algorithm takes the smaller value of the two representative cells so that

$$Z = \min(K_1, K_2). \tag{50}$$

From this point the OSGO/SO systems perform their operations identical to that of the standard OS system.

c. Statistics and Performance

Using Rohlings [Ref. 27] expression for the pdf for a kth representative cell of a set of M/2 cells, Elias-Fuste [Ref 29] analyzed the OSGO and OSSO functions yielding :

$$P_{fa}^{OSGO} = 2k^2\binom{\frac{M}{2}}{k}^2 \sum_{j=0}^{\frac{M}{2}-k} \sum_{i=0}^{\frac{M}{2}-k} \binom{\frac{M}{2}-k}{j}\binom{\frac{M}{2}-k}{i} \times \frac{(-1)^{M-2k-j-i}}{\frac{M}{2}-i} \frac{\Gamma(M-j-i)\Gamma(T+1)}{\Gamma(M-j-i+T+1)} \tag{51}$$

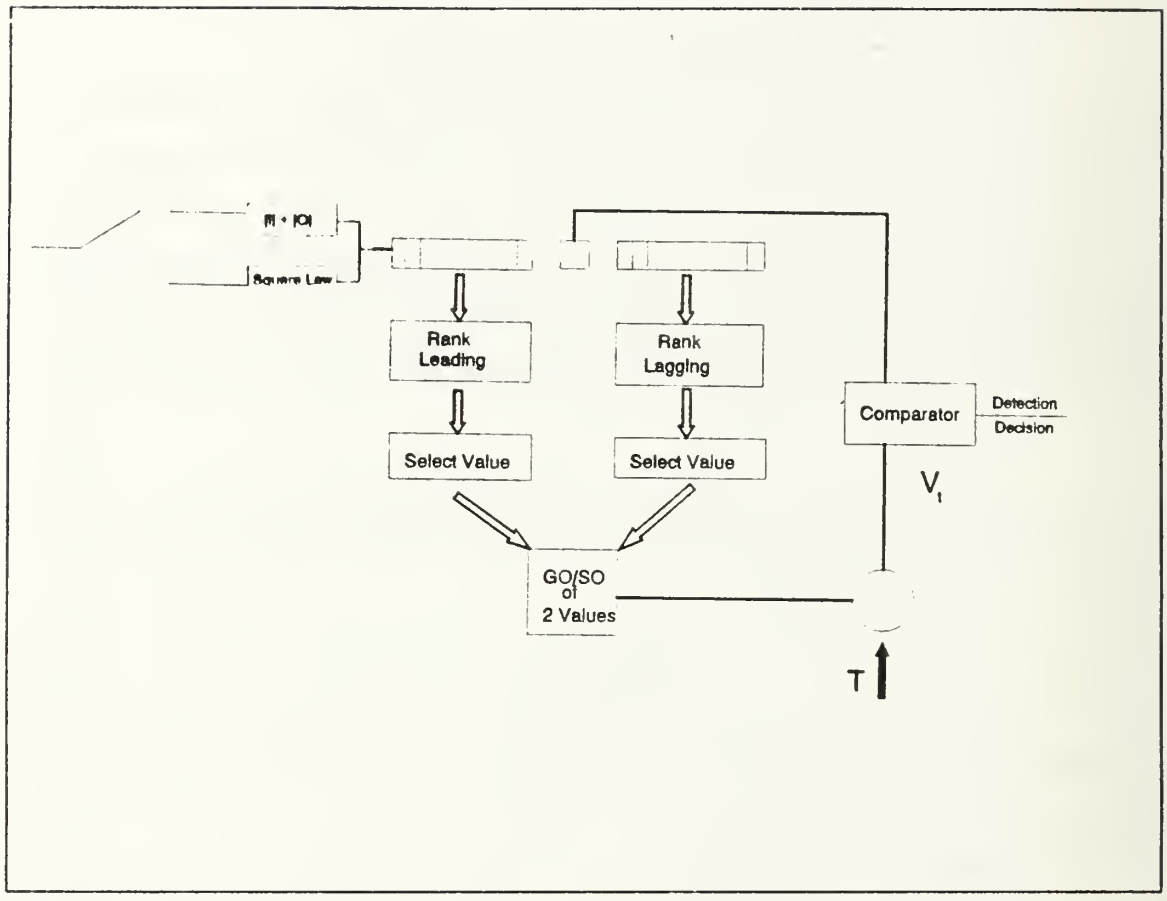

Figure 21. OSGO and OSSO CFAR Schematic

$$P_{fa}^{OSSO} = 2k\binom{\frac{M}{2}}{k}\frac{\Gamma(k)\Gamma(T+\frac{M}{2}-k+1)}{\Gamma(T+\frac{M}{2}+1)}$$
$$-k\binom{\frac{M}{2}}{k}\sum_{j=0}^{\frac{M}{2}-k}\sum_{i=0}^{\frac{M}{2}-k}\binom{\frac{M}{2}-k}{j}\binom{\frac{M}{2}-k}{i} \qquad 52$$
$$\times\frac{(-1)^{M-2k-j-i}}{\frac{M}{2}-i}\frac{\Gamma(M-j-i)\Gamma(T+1)}{\Gamma(M-j-i+T+1)}$$

$$P_d^{OSGO} = 2k^2\binom{\frac{M}{2}}{k}^2 \sum_{j=0}^{\frac{M}{2}-k} \sum_{i=0}^{\frac{M}{2}-k} \binom{\frac{M}{2}-k}{j}\binom{\frac{M}{2}-k}{i} \times \frac{(-1)^{M-2k-j-i}}{\frac{M}{2}-i} \frac{\Gamma(M-j-i)\Gamma(\frac{T}{(1+SNR)}+1)}{\Gamma(M-j-i+\frac{T}{(1+SNR)}+1)} \quad (53)$$

$$P_d^{OSSO} = 2k\binom{\frac{M}{2}}{k} \frac{\Gamma(k)\Gamma(\frac{T}{(1+SNR)}+\frac{M}{2}-k+1)}{\Gamma(\frac{T}{(1+SNR)}+\frac{M}{2}+1)} - k\binom{\frac{M}{2}}{k} \sum_{j=0}^{\frac{M}{2}-k} \sum_{i=0}^{\frac{M}{2}-k} \binom{\frac{M}{2}-k}{j}\binom{\frac{M}{2}-k}{i} \times \frac{(-1)^{M-2k-j-i}}{\frac{M}{2}-i} \frac{\Gamma(M-j-i)\Gamma(\frac{T}{(1+SNR)}+1)}{\Gamma(M-j-i+\frac{T}{(1+SNR)}+1)} \quad (54)$$

Figures 22 thru 25 display the performance characteristics of the OSGO and OSSO envelope approximation and square law systems. Figures 22 and 23 show the false alarm rate versus threshold multipliers. As shown the OSGO envelope approximation system obtains a 10^{-2} value at an approximate 2.2 threshold value and a 10^{-4} value of approximately 3.3. The OSGO Square Law system shows the 10^{-2} and 10^{-4} rates at multipliers of approximately 4.1 and 9.35. The OSSO Envelope Approximation systems reach a 10^{-2} and 10^{-4} rates at the higher values of 2.5 and 4.05. The OSSO Square Law system shows the 10^{-2} and 10^{-4} rates at multipliers of approximately 6.1 and 14.8. As shown in the previous CFAR systems, the Square Law system yields a superior detection rate as compared to its Envelope Approximation counterpart. Figures 24 and 25 show the OSGO and OSSO detection rates. In these Monte Carlo simulations, the GO or SO of the 10th cell (out of 16) was chosen between the leading and lagging ordered sets to be used as the representative noise estimate.

d. Strengths and Limitations

Both OSGO and OSSO systems have a key advantage in that they both reduce processing time in half. This is due to two specialized sorting processors working

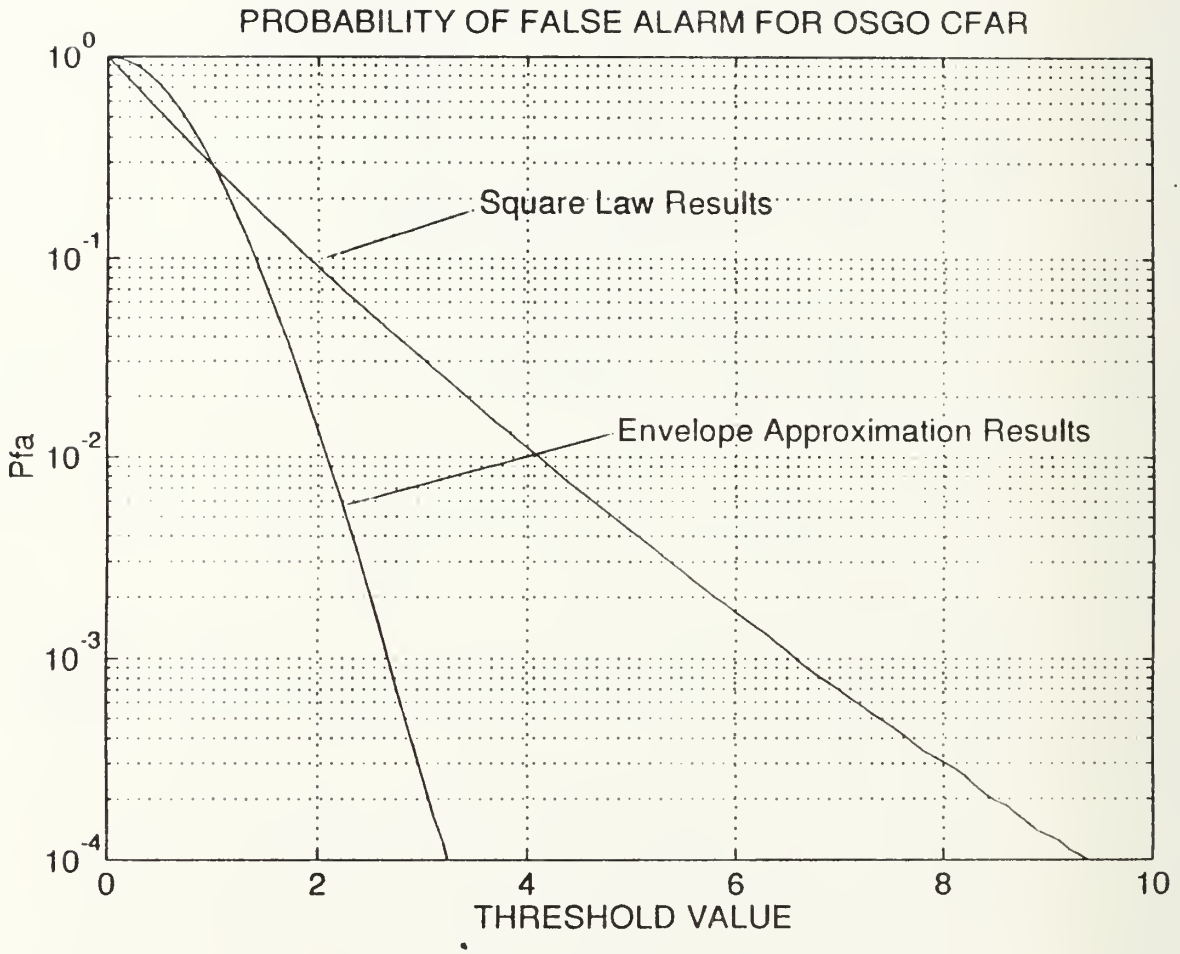

Figure 22. OSGO CFAR Probability of False Alarm

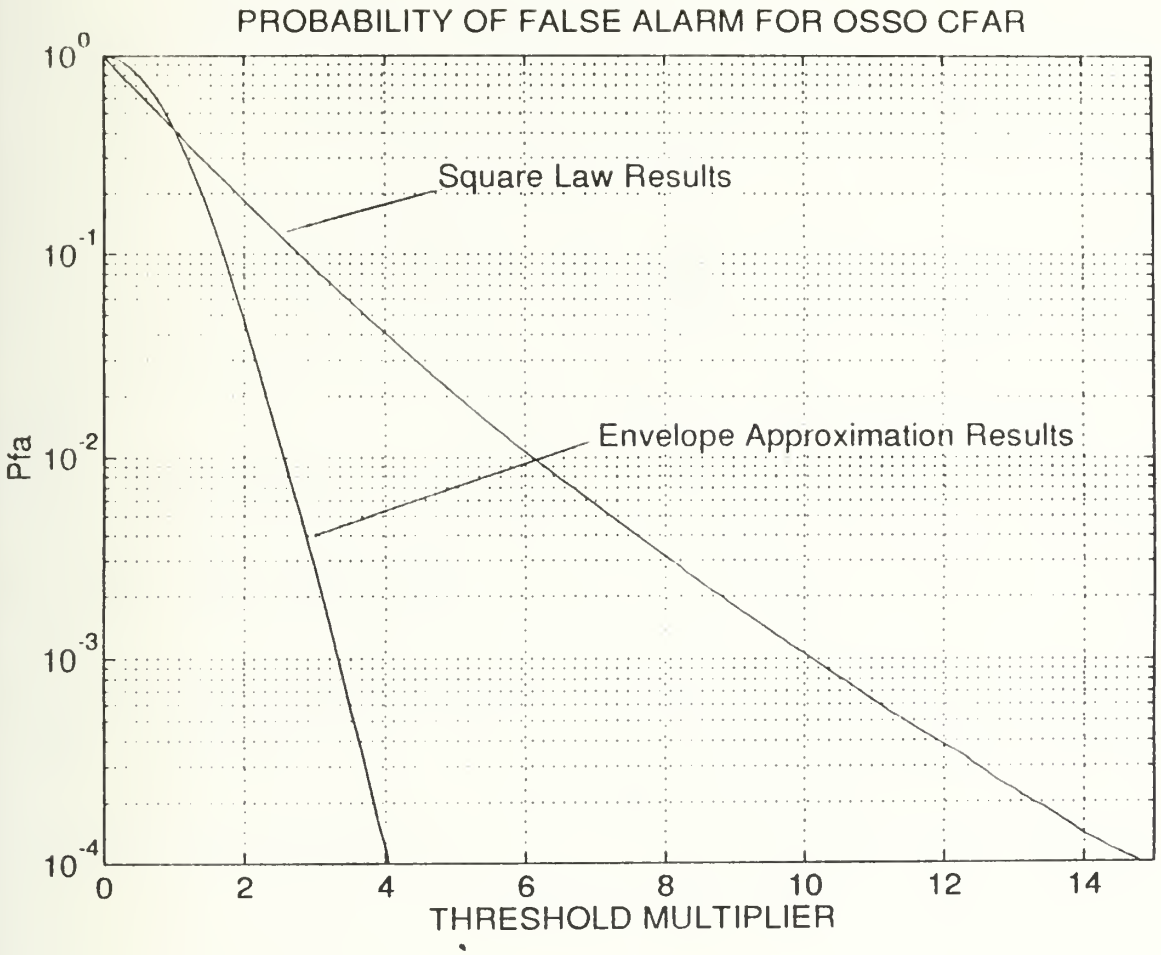

Figure 23. OSSO CFAR Probability of False Alarm

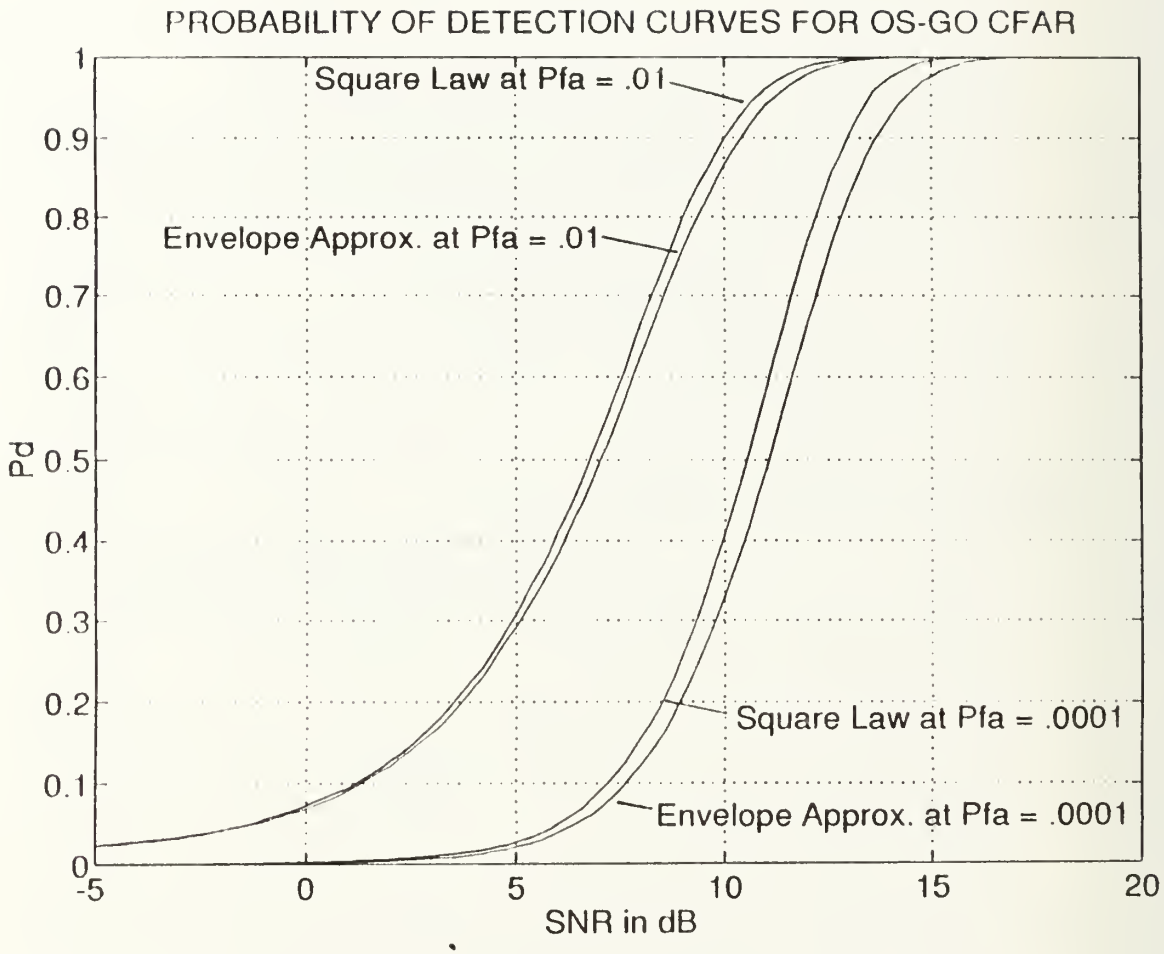

Figure 24. OSGO CFAR Probability of Detection

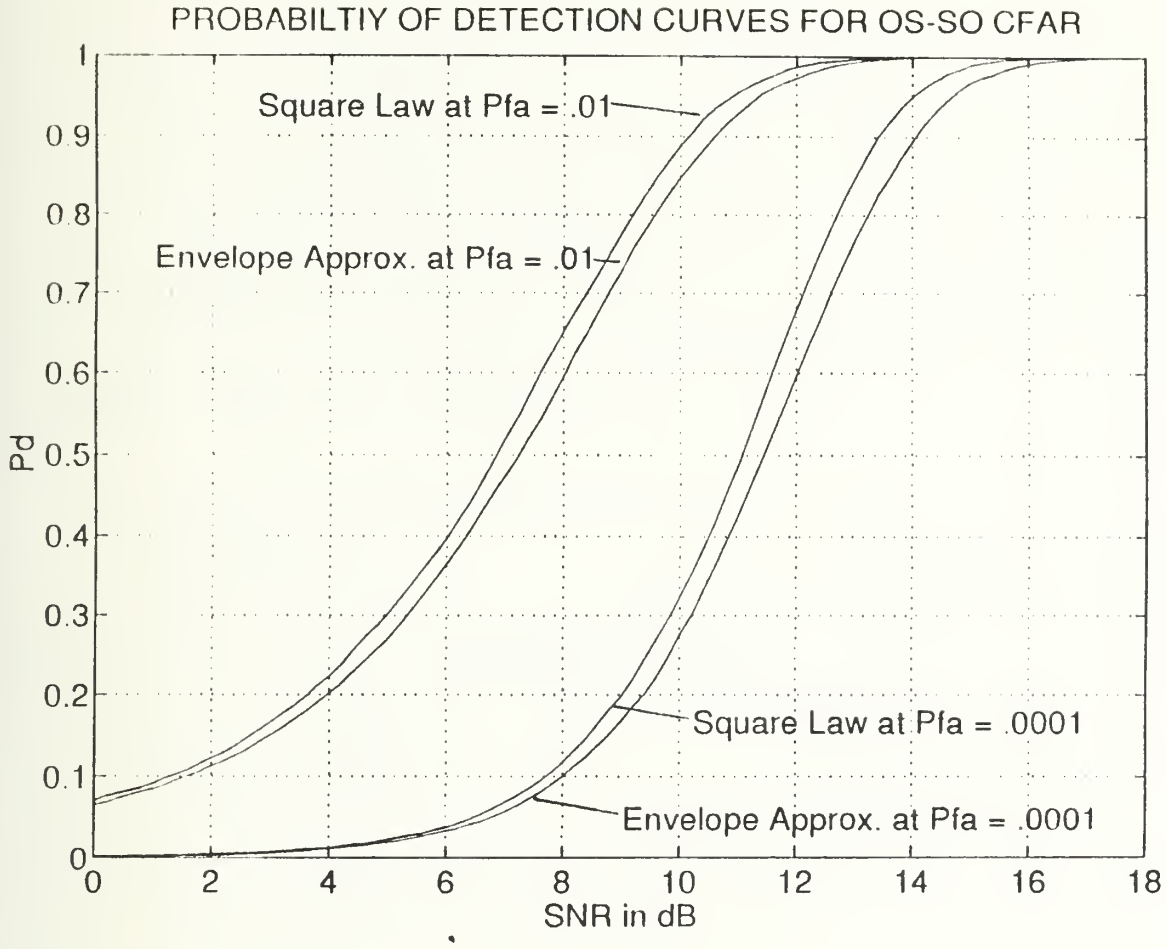

Figure 25. OSSO CFAR Probability of Detection

independently on the leading and lagging reference cells. Figures 26 and 27 show the capabilities of these two systems in a test environment that includes interfering targets and clutter edging. Taken from Elias-Fuste [Ref. 29], this test contains 256 reference cells, 2 clutter edges of 30 dB extending from the 30th to 190th cells, and three targets with SNR values of 19, 54, and 19 dB. The interferers are located in cells 100, 105 and 110. An additional target of 22 dB is located at position 215 outside the clutter cloud. As Figure 26 (OSGO system) clearly shows the adaptive threshold level (dashed line) always maintains a value greater than the noise plus clutter level (even at the edges). Also, all four targets are detected as they cross the threshold boundary. In Figure 27 (OSSO system) it is shown that all four targets are also detected but with an unacceptable false alarm rate due to an inability to handle clutter edge effects.

The OSGO CFAR appears to be a fine substitution for the standard OS CFAR since it maintains the key OS system strengths and reduces processing time. The OSSO system on the other hand, with its inability to control the false alarm rate, makes it a poor CFAR system for many applications.

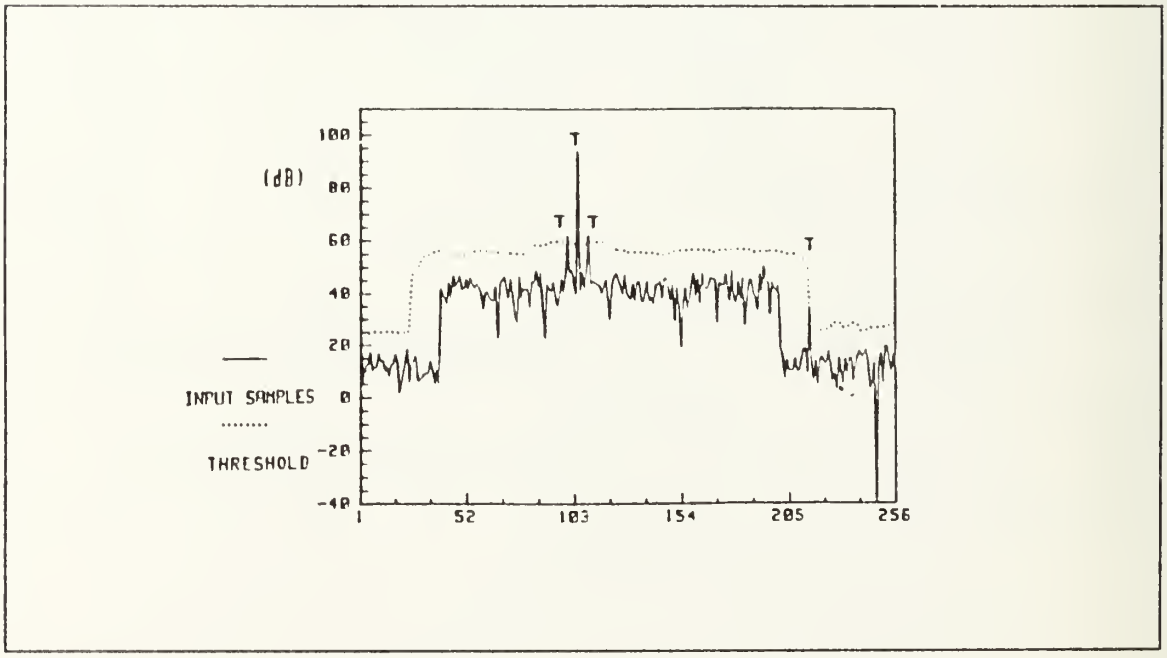

Figure 26. OSGO CFAR Performance in a Test Environment

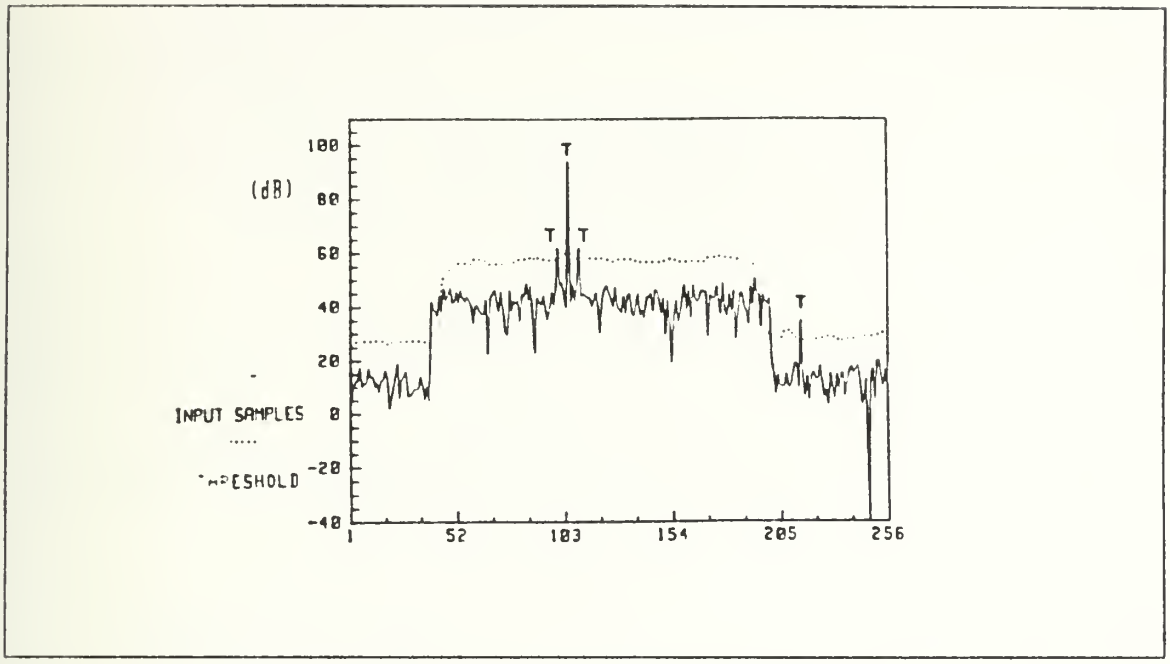

Figure 27. OSSO CFAR Performance in a Test Environment

3. Censored Mean Level Detector (CMLD) CFAR

a. Background

The CMLD system was proposed by Rickard and Dillard in 1977 [Ref. 6] and is a generalization of the traditional CA CFAR detector with modifications that provide robust performance in the multiple target environment. This is accomplished by censoring a select number of input samples from the ordered group. Like the MLD family, CMLD obtains its noise information estimate from neighboring resolution cells. This combination of OS and CA concepts uses an average of all but the first (or first and second) largest noise reference samples (i.e. the largest inputs are censored from the averaging routine). The result of this combination system is an architecture that has robust properties that offers superior performance in multiple target environments.

b. System Description

The schematic of the CMLD system is displayed in Figure 28. As always, the reference window may contain noise and or return echoes from an interfering target. The primary target return echo is observed in the cell under test. The output of the reference cells $[q_i]$, i= 1,2,...,M are fed into a ranking device which outputs the samples in ascending order according to their magnitude to yield the M ordered samples

$$q_{(1)} \leq q_{(2)} \leq \cdots \leq q_{(M)}. \qquad 55$$

At this point the largest K (1 or 2) samples are censored. The remaining M samples are combined to form an estimate of the noise level in a procedure identical to that of CA CFAR. The estimation is then multiplied by a constant T (threshold multiplier) to yield the adaptive threshold against which the cell under test will be compared.

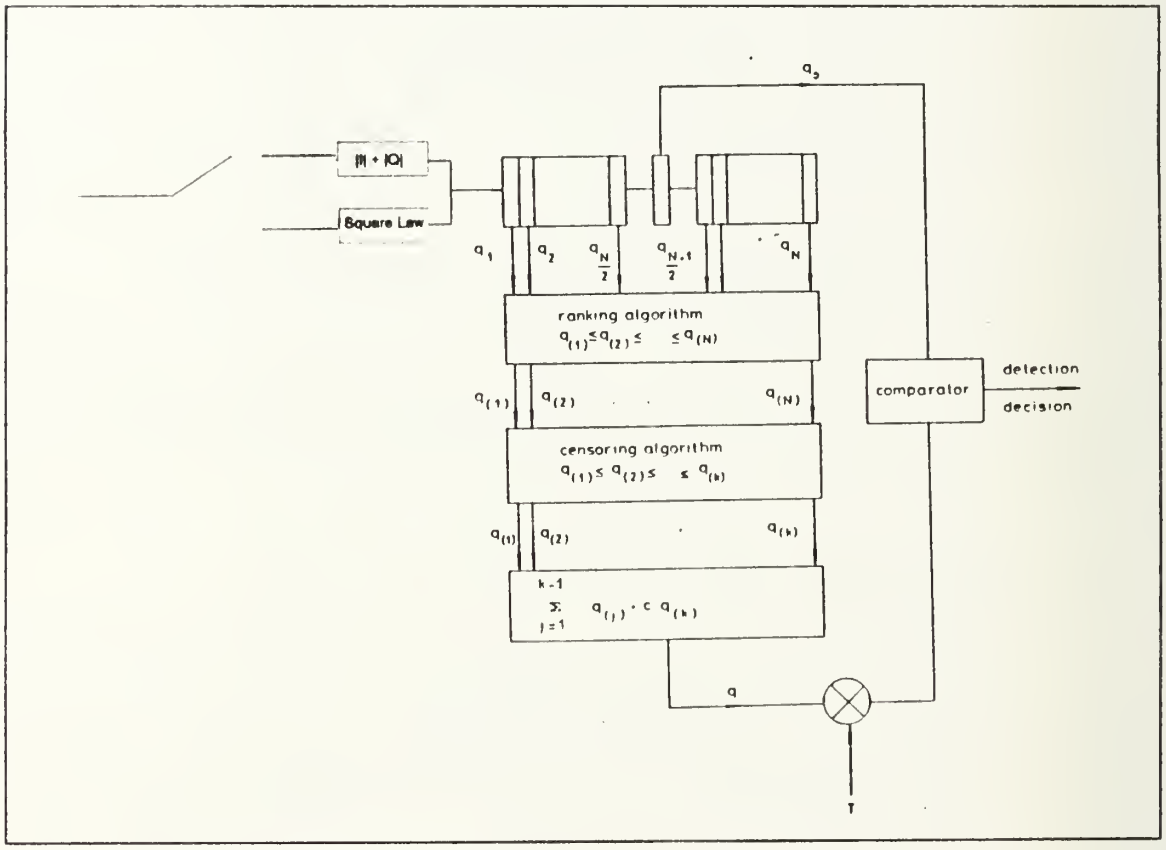

Figure 28. CMLD CFAR Schematic

c. Statistics and Performance

The analysis for the CMLD detection and false alarm probabilities was originally completed by Barkat [Ref. 30]. The following lists the CMLD systems false alarm and detection probability equations.

$$P_d = \Psi[T\theta(SNR)] - T\frac{\mu\dfrac{SNR}{2}}{(1+\dfrac{SNR}{2})^2}\left[\frac{d}{dw}\Psi(T\theta(SNR))\right]. \qquad 56$$

where μ is the *inverse* of the noise power. The detection probability uses the moment generating function (Ψ) where

$$\Psi(x) = \frac{\mu^2(SNR)(x+\mu)}{\mu[\theta(SNR)+x]^2}, \tag{57}$$

and

$$\theta(SNR) = \frac{\mu}{1+\frac{SNR}{2}}. \tag{58}$$

The probability of false alarm can be determined by setting the SNR to zero yielding

$$P_{fa} = \Psi(T\mu). \tag{59}$$

Figures 29 and 30 display the P_{fa} and P_d plots for the CMLD system. The envelope approximation system has a 10^{-2} false alarm rate at the threshold multiplier of approximately 2.7, and a 10^{-4} value at approximately 4.1. The square-law system shows corresponding values of approximately 5.7 and 11.8. In Figure 30, the Monte Carlo driven detection curves show SNR versus detection rates at 10^{-2} and 10^{-4} P_{fa} . To achieve a detection probability of 0.6, a SNR of approximately 7.5 dB is required at the 10^{-2} rate, approximately 11 dB at 10^{-4} for the envelope approximation system. The square law system shows slightly improved performance over the envelope approximation system. In the Monte Carlo simulation that generated these curves, two of the larger ordered values were censored. This in turn led to 30 reference cells being used in the noise estimation process.

d. Strengths and Limitations

The performance of the CMLD system exhibits only small additional losses in the homogeneous environment (as compared to CA CFAR) but was shown to be quite robust when a single large interferer is presented into the reference window. The major limitation to CMLD is that the number of cells used for noise estimation should be equal to the total number available (M) minus the actual number of outlying interferers (J) in the reference window to ensure superior detector performance. It has been shown by Barkat [Ref. 30] that the CMLD performance is seriously degraded if the exact number of interferers is not censored. This requires *a priori* knowledge. As expected , the more interfering targets censored results in poorer performance. It is clear

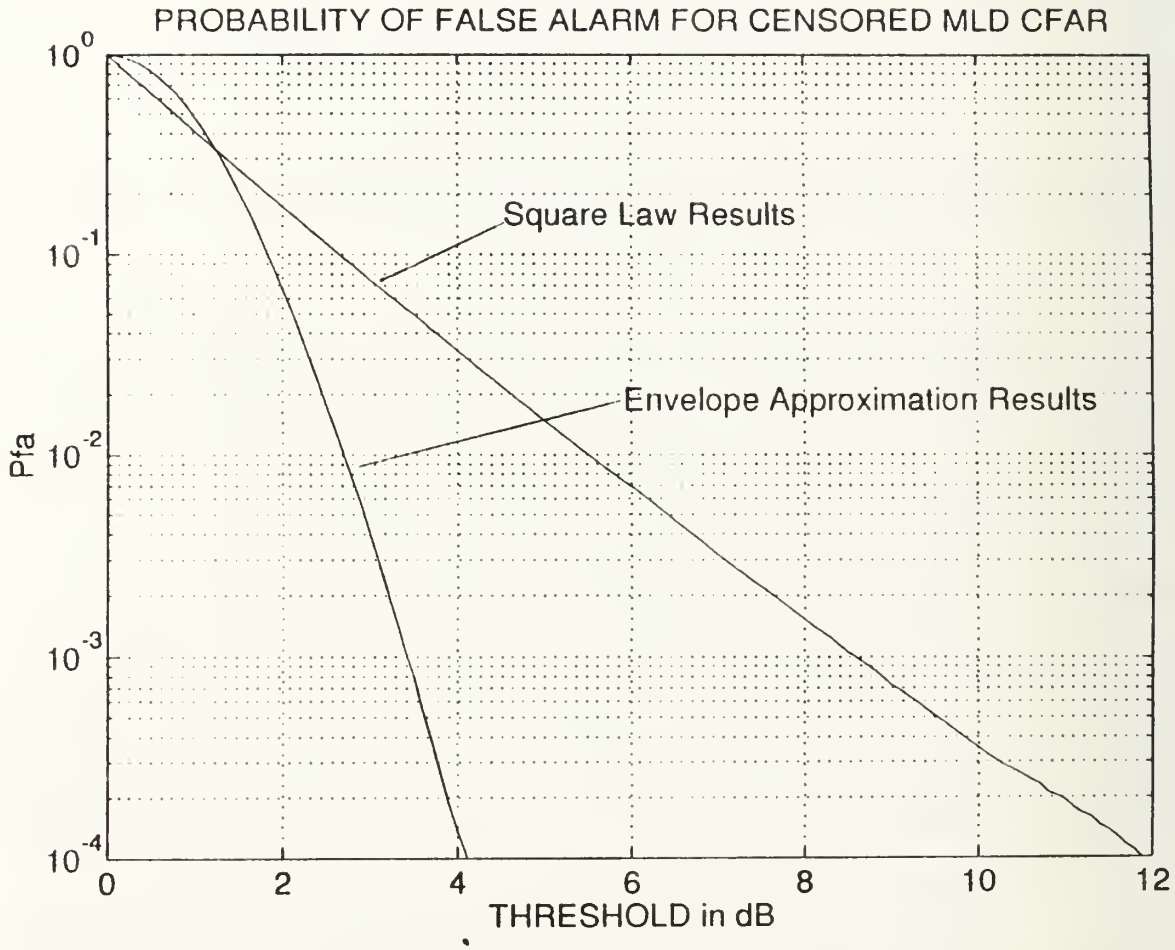

Figure 29. CMLD CFAR Probability of False Alarm

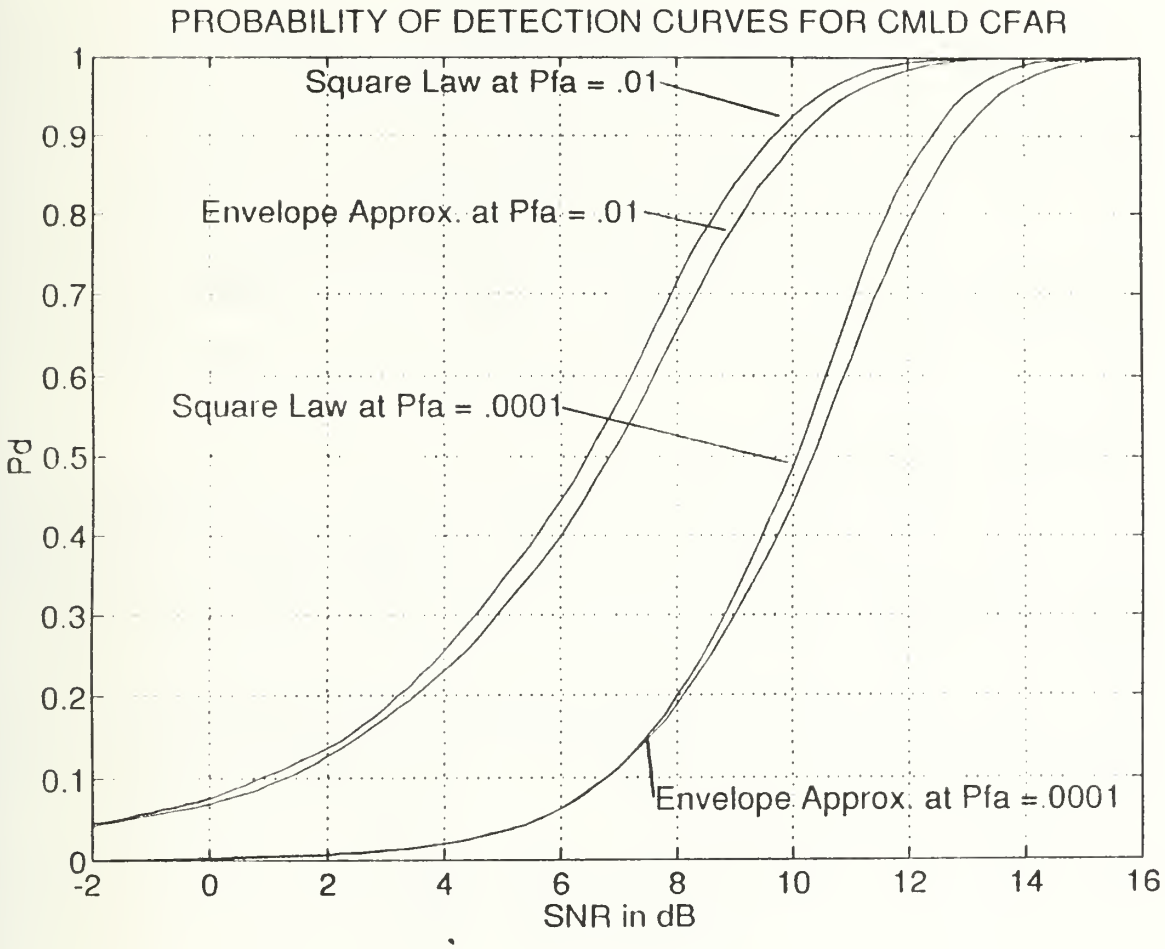

Figure 30. CMLD CFAR Probability of Detection

the if the number if interferers is unknown, the CMLD will not only lose its robustness but also its CFAR properties as well. For example, if the ordered list is undercensored, then the noise estimate will be contaminated and result in a degraded detector. On the other hand, if overcensoring occurs, the noise estimate is underestimated and an excessive number of false alarms occur.

4. Trimmed Mean CFAR

a. Background

The Trimmed Mean (TM) CFAR scheme is a generalization of the OS scheme in which the noise power is estimated by a linear combination of ordered samples. In the TM CFAR processor, a symmetric or asymmetric number of cells are trimmed or censored from both the upper and lower ends of the ordered list. The threshold is then estimated by forming the sum of the remaining cells. In TM CFAR, as in CMLD CFAR, the censoring points are preset. Again, this implies that some *a priori* knowledge about the background environment is required to sensor efficiently the unwanted samples [Ref. 31].

b. System Description

The schematic of TM CFAR is shown in Figure 31. The TM system first sorts the outputs of all the reference cells by magnitude. Then, it judiciously censors the K_1 lower and K_2 higher ordered samples in the reference window irrespective of the actual background environment. When $K_1 = K_2$, the system symmetric and when these values differ the system follows asymmetric trimming. The noise level estimate for the cell under test is then set to be the normalized sum of the uncensored samples, that is

$$V_t = \sum_{j=K_1+1}^{N-K_2} \frac{x_j}{(N-K_1-K_2)}. \qquad 60$$

Gandhi has shown through testing that the choice of K_2 plays the critical role in a TM system performance. Table 5 [Ref. 26] displays the effect that different values of K_1 and K_2 have on the adaptive threshold multiplier level (M = 24 and $P_{fa} = 10^{-6}$) for both symmetric and asymmetric systems. As shown, when the K_2 censoring value is too high, system performance suffers. This is clearly shown by the high valued threshold multipliers required to maintain the false alarm rate. As shown, th TM system performance is most interesting when asymmetric trimming is employed. As shown, with a fixed K_1

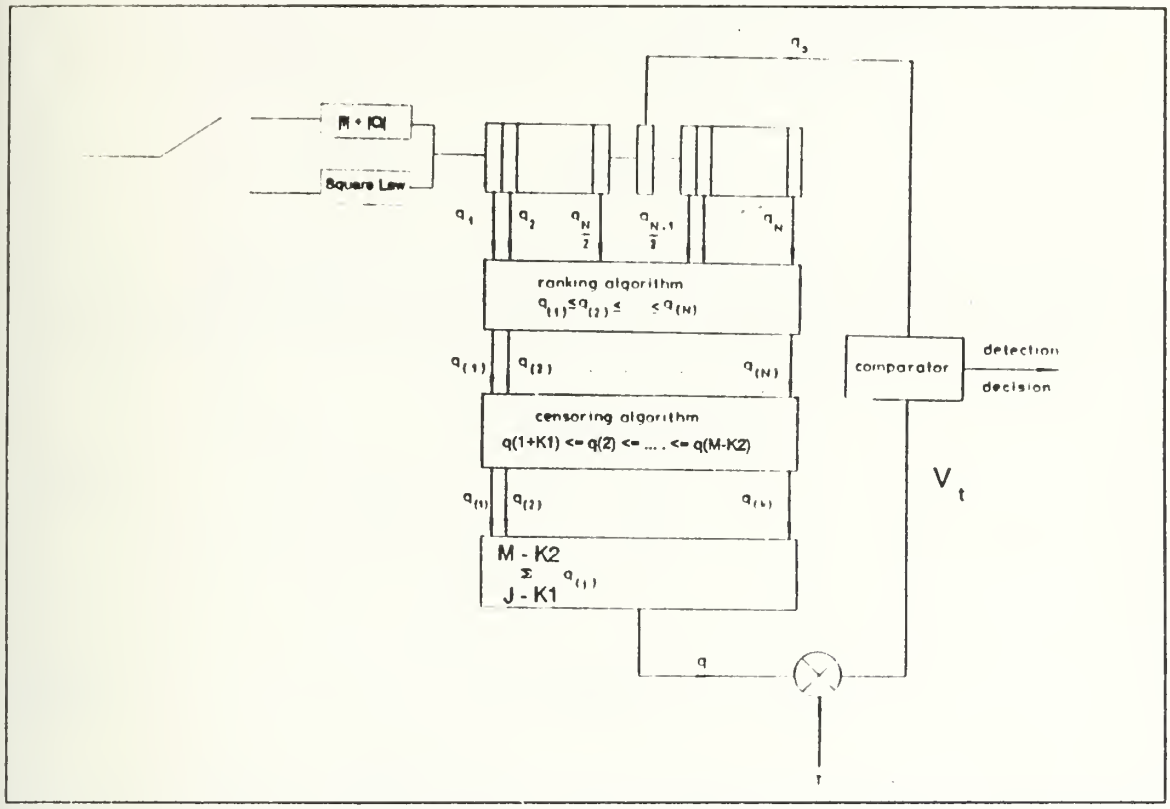

Figure 31. TM CFAR Schematic

Table 5. SYMMETRIC AND ASYMMETRIC TRIMMING EFFECTS

K1	K2	Thresh Mult	K1	K2	Thresh Mult
0	0	0.778	2	4	1.548
1	1	0.941	2	7	2.566
2	2	1.121	2	10	4.590
3	3	1.329	2	15	17.60
4	4	1.585	2	17	40.50
5	5	1.907	4	2	1.140
6	6	2.338	7	2	1.200
7	7	2.941	10	2	1.313
8	8	3.841	14	2	1.643
9	9	5.340	17	2	2.280

K_2 is increased. On the other hand, only minimum degradation occurs when K_2 is fixed and K_1 is increased. [Ref. 26]

c. Statistics and Performance

The following analysis of TM CFAR was taken from Gandhi's work [Ref. 26]. Beginning with the estimate Z given by

$$Z = \sum_{i=1}^{N-K_1-K_2} x_i \qquad 61$$

The mgf (moment generating function) of Z is therefore the product of the individual mgf of the x_i's. Therefore the false alarm rate is found to be

$$P_{fa} = \prod_{i=1}^{N-K_1-K_2} \Psi_{x_i}(T) \qquad 62$$

where

$$\Psi_{x_i}(T) = \frac{a_i}{a_i + T}, \qquad 63$$

where a_i = (N - K_1 - i + 1) / (N - K_1 - K_2 - i + 1). The detection probability P_d is obtained by replacing the threshold multiplier T with T/(1 + SNR).

Figures 32 and 33 display the performance plots of the TM CFAR system. The probability of false alarm and detection data were Monte Carlo simulated. As shown in Figure 32, a threshold multiplier of approximately 2.6 is required to maintain a 10^{-2} false alarm rate and a value of 4.0 is necessary to maintain a 10^{-4} rate for an envelope approximation system. The square law results that a threshold multiplier value of 5.6 and 12.3 are required to maintain the false alarm rates of 10^{-2} and 10^{-4} The detection plots shown in Figure 33 show SNR versus detection probability at 10^{-2}, and 10^{-6} P_{fa}. As shown, a 0.6 probability of detection can be found at a SNR value of approximately 7.5, and 11.5 for the two respective false alarm rates. In the square law system a 0.6 detection rate can be found at corresponding SNR values of approximately 7.0 and 11.0 dB. These values are very similar to the CMLD system. They were generated by symmetrically trimming the two largest and two smallest ordered reference cells. This resulted in 28 remaining cells to be used for system noise estimation.

d. Strengths and Limitations

A main limitation of the TM system is that as trimming increases, both the scaling factor T and the CFAR loss increase. To compound this problem, *a priori* in-

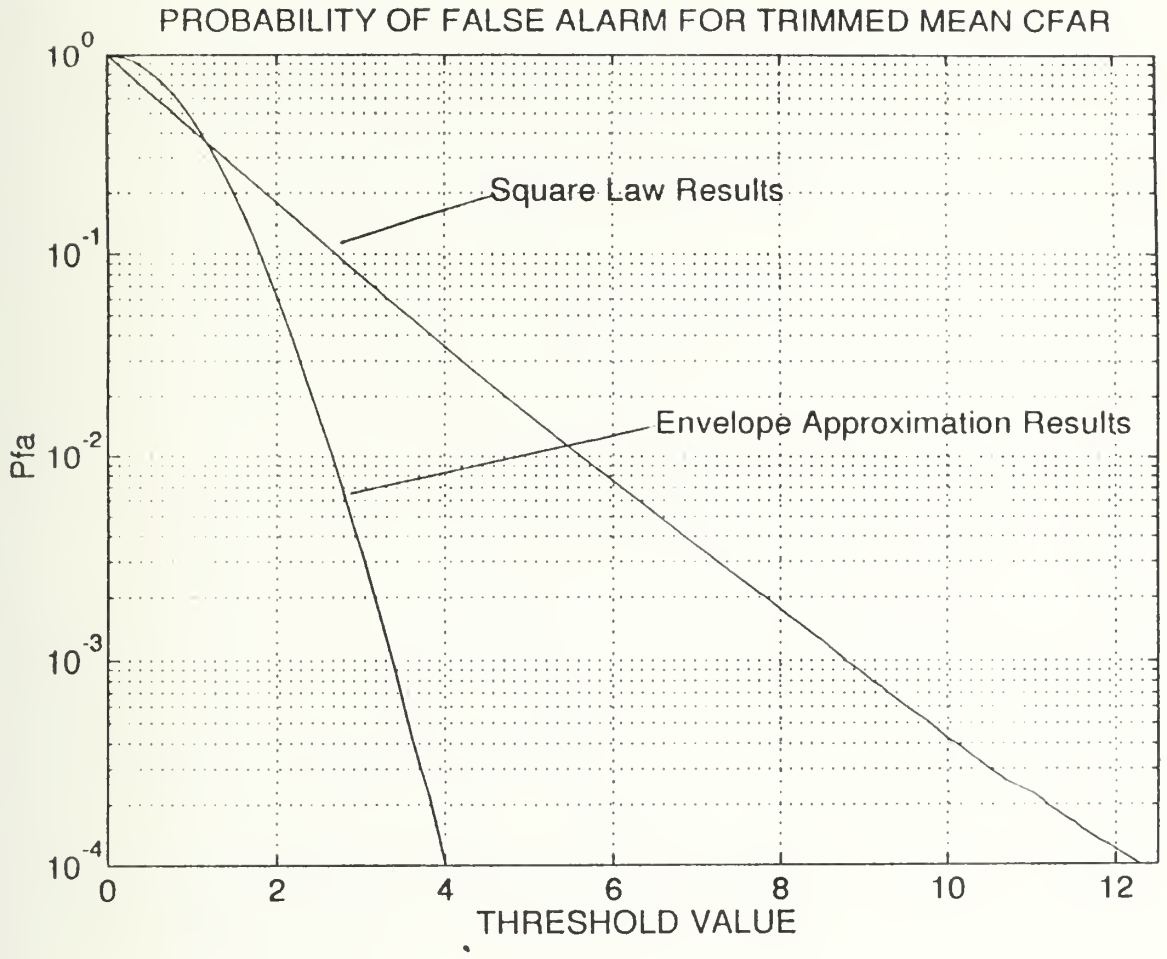

Figure 32. TM CFAR Probability of False Alarm

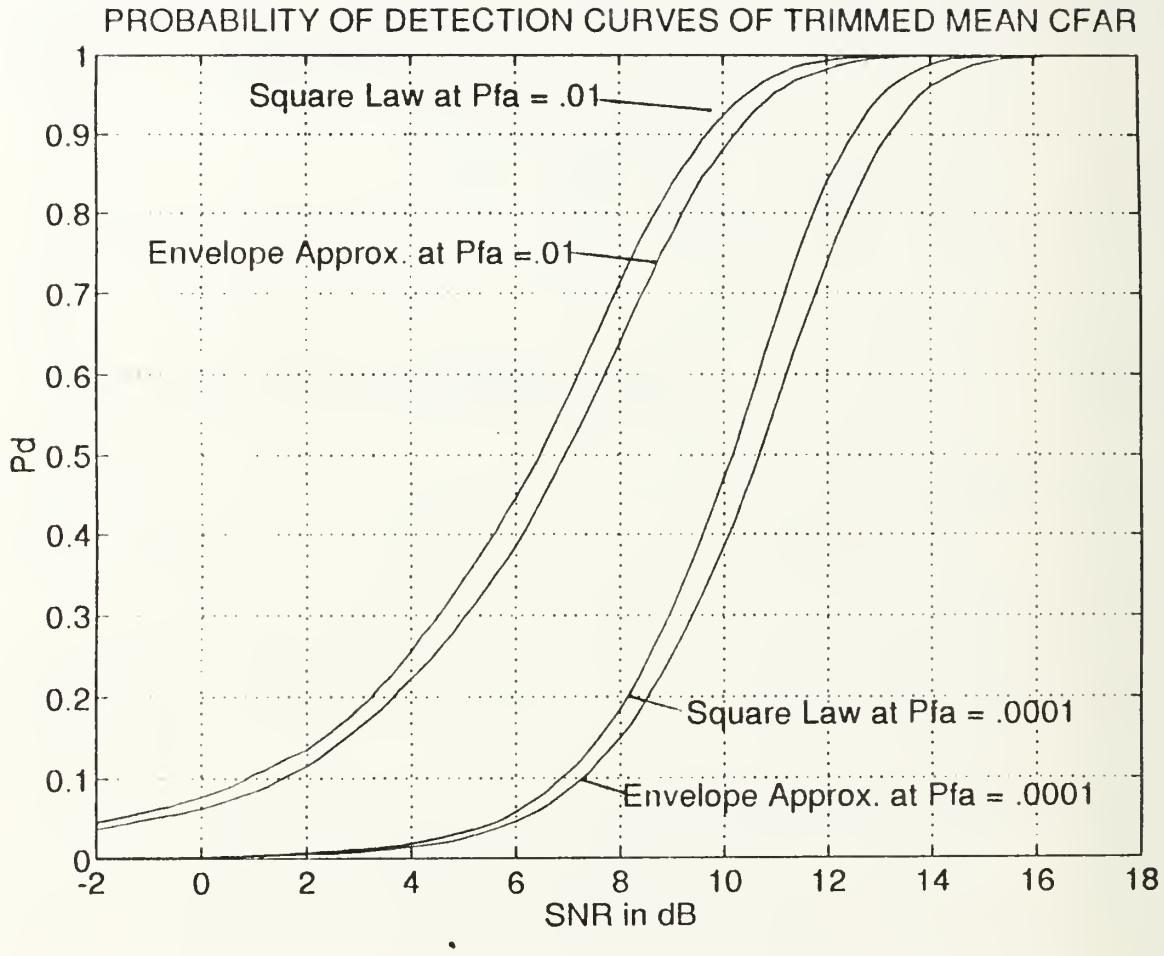

Figure 33. TM CFAR Probability of Detection

formation is critical in order to properly choose trim rates. Consider the situation where the leading half of the reference window contains cells from clutter plus noise and the lagging half from a clear background. The noise power estimate will include both clear region and clutter plus noise background regions. The corresponding threshold will then not be high enough to regulate the false alarm rate if the test cell contains a return from the clutter plus noise area. Also in a non-uniform background, a compromise must be made in determining the proper trimming parameters. In order for the process to be less sensitive to interfering targets, K2 should be set to a value greater than zero, and the value of K1 should be small in order to attain good detection performance in the homogeneous background. If the concern however is to handle clutter edges, K1 should be large and K2 should be small. Unfortunately in most cases we are interested in regulating the false alarm rate in both clutter edge and multiple target environments. This balancing act is near impossible to maintain in any dynamic radar operating environments making TM performance quite variable.

D. NON-ADAPTIVE THRESHOLD CFAR TECHNIQUES

1. Introduction

Although the focus of this thesis is on the optimization of adaptive threshold CFAR architectures, other important systems that perform CFAR functions also exist. Discussed here are two such systems. The first technique to be discussed is Clutter Mapping (which uses temporal rather than spatial information to control the false alarm rate). The second technique is a Non-Parametric CFAR that is generally insensitive to environmental background changes. Although these systems will not be covered in great depth, they are introduced to the reader for completeness.

2. Clutter Mapping

a. Background

The Clutter Mapping (CM) system is a specialized CFAR device which averages radar returns temporally over several scans to form an estimate of the mean background noise levels. This system is quite different from the adaptive schemes that use spatially differing inputs. The CM CFAR device compares present returns in each cell to a background estimate for that specific cell based on past inputs from that cell only. Past inputs refer to previous radar scans. For effective operation, the CM CFAR device requires temporal rather than spatial stationarity and is thus ideally suited for CFAR problems over land [Ref. 32].

Due to the typically large amount of cells to be processed, the required processing speed and high cost of digital memory, early clutter maps were typically of the blanking type. This system operated with a simple counter that measured how often clutter appeared in a specified cell. When this counter reached a preset level, all returns in that cell region were blanked. Today, reduced costs of digital memory and technical advancements in signal processing equipment has resulted in a recharged interest in high resolution CM CFAR processing.

b. System Description

The CM technique sets independent threshold levels in each map cell to yield a CFAR. As shown in Figure 34, [Ref. 32] this technique operates by dividing the radar space into cell units.

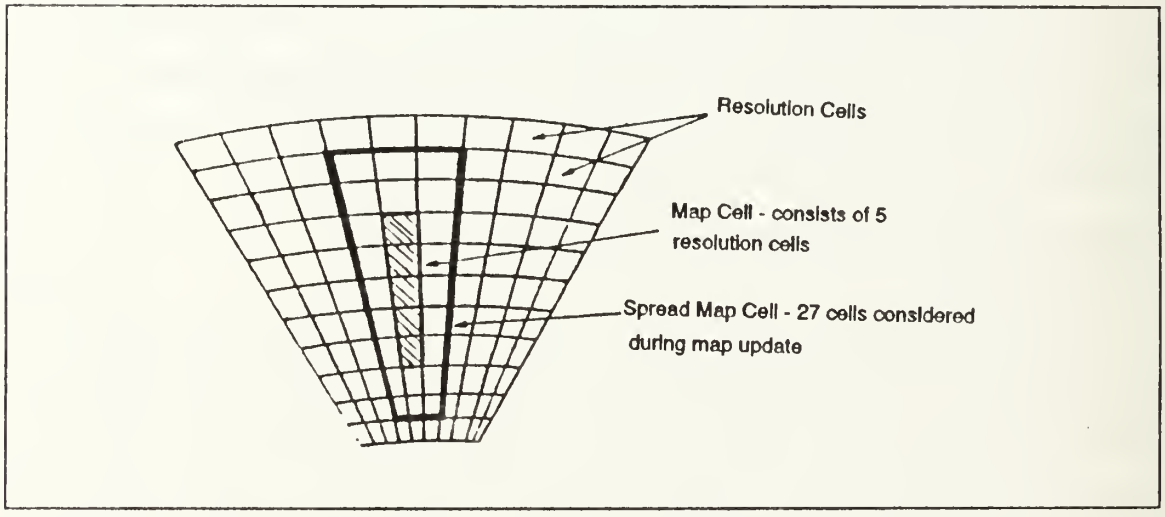

Figure 34. Clutter Map Range and Azimuth Cells

Each cell represents in range and azimuth one resolution cell. As shown, the five high lighted cells represent one clutter map cell. The spread map cells denote the area considered during the map update process. Although only five cells compromise a CM cell, due to map spreading a total of 27 cells are considered during map update.

The CM process consists of a number of steps. First, for each CM cell the map spreading logic selects for map update the greatest amplitude of all resolution cells within the map cell as well as the additional spreading set that borders the map cells. This amplitude is then stored in the proper location of the measurement map. The process continues with averaging the content of the measurement map with the current stored value in the Clutter Map. The average amplitude in each cell is estimated by a

low pass, digital filtering of the input data. Target detection declarations then follow the CA CFAR logic form. If the CM cell value exceeds that mean background estimate, a target is declared.

c. Design Issues

The design of a high resolution CM system is not necessarily feasible for any combination of radar parameters. Four key parameters are used in the determination of a CM design and include; compressed resolution cell size, radar update period, number of pulses noncoherently integrated, and detector law employed. According to Farina [Ref. 4], CM CFAR designs are based on :

- The geometry of the map: How the surveillance space is divided into cells (i.e. rectangular or polar).
- The map building process: The map changing process may be periodic with increasing and decreasing counters or by amplitude averaging. Also, assuming a map cell larger than the radar cell, the data obtained in one radar cell may be used alone or in combination with data from nearby cells.
- The approach taken: Different action can be decided on the basis of the content of the CM. Such actions include blanking zones, switching to different processing channels, resetting detection thresholds in each cell, and tracking clutter points.

d. Strengths and Limitations

A primary reason for employing a CM CFAR system is for its excellent interclutter visibility. Interclutter visibility is the ability to detect and track targets in shadow areas where clutter is normally absent. Another favored capability of a CM system is that it generally provides better detectability of targets in near tangential flight paths over clutter regions [Ref. 7]. Finally, CM systems also may be employed to sense locations where clutter echoes are too strong to be suppressed by other signal processing systems such as doppler filters.

The major limitation, or drawback of CM CFAR is the assumption that clutter statistics are temporally stationary (over five to ten scans of the radar). Rainstorms, jamming, and other nearby radars thereby cause excess false alarm rates. Also large differences in system capability become apparent even with low velocity point clutter. At only two knots velocity, there is a four orders of magnitude difference between the false alarm rate as compared to zero knots. Even with a land based radar where there should be no apparent velocity between the land clutter and a radar, changes in the atmospheric index, multipath and systems instabilities all lead to small positional shifts resulting in unacceptable false alarms.

3. Non-Parametric CFAR

a. Background

Throughout the discussion of the adaptive threshold CFAR techniques, an emphasis was placed on optimal detectors requiring an essentially complete statistical description of the input signals and noise. Thomas [Ref. 33] mentions three compelling reasons which lead to consideration of other 'nonoptimal' detectors. First, a complete statistical description of the input is rarely available; second, the statistics of the input data set may vary with time or may change from one radar application to another. Finally, optimal detectors may be too complex or costly to implement. Adaptive systems have developed and evolved to meet the first two conditions and can perform in a near optimal sense in a unknown or changing environment by proper adaptation of detector structure; however, such detectors tend toward greater complexity. Nonparametric or distribution-free detectors exhibit insensitivity to the environment rather than adapting to it and often exhibit simplicity in implementation.

In the Non-Parametric (NP) device it is assumed that the statistics of the interference are unknown. The rational of the approach is to somehow map the unknown PDF onto a known one where a fixed threshold produces CFAR [Ref. 4]. This technique enables CFAR performance against very broad classes of noise probability density functions [Ref. 22].

b. System Description

A wide assortment of NP processing techniques are available and present a the practical problem of choosing the proper technique for a particular need. A common and simple NP detector obtains a CFAR by order ranking the test cell among the reference cells [Ref. 34]. The smallest ranked value receives a rank of zero and the largest a rank of N. Under the hypothesis that the samples are independent with unknown PDF, the test cell has equal probability of taking on any of the N ranked values from zero to N. The rank detector is then constructed to compare the rank of the test cell against a preset threshold rank. If the cell under test rank is greater than that of the threshold rank, a target is declared. This simplistic system normally incurs a CFAR loss of approximately 2 dB but achieves a fixed false alarm rate for any noise density as long as the input sample stream remain independent.

c. Strengths and Limitations

The insensitivity to environmental noise density changes is the strong suit of any NP detector. Clear costs are paid for this action however. Besides the 2 dB loss, correlated samples result in a detector inability to maintain CFAR. Also, a large inter-

fering target may lead to target suppression, that is, if a large return is found in the reference cells, the test cell will not receive the highest ranking possibly resulting in a rank below the threshold rank. A final concern is that by maintaining only the rank orders, the system loses the actual signal amplitude information which may be used in other signal processing applications.

V. CFAR ARCHITECTURE COMPARISONS

A. INTRODUCTION

A great deal of literature has been written comparing the relative performance of various adaptive threshold CFAR systems, each paper dealing with only one to three different types. The goal of this chapter is to compare on a larger scale, all eight of the popular types of CFAR systems being used today. As always, there are tradeoffs in capabilities between systems; that is, even if one detector is superior in one scenario, it may be poorer in some other. The system comparisons will be on the basis of capability in 1) homogeneous noise, 2) clutter edging, and 3) interfering targets. It should be understood that these are but three idealized examples of the multitude of different situations which may occur in actual radar operation.

The comparisons made in this chapter will be restricted to the adaptive threshold systems previously discussed. The chapter begins with a comparison of the MLD family of detectors followed by a comparison of the rank ordered systems.

B. MEAN LEVEL DETECTOR COMPARISONS

The relative capabilities of the MLDs are tested under the three test environments of homogeneous noise, clutter edges, and multiple targets. As discussed, the CA CFAR is the optimum system in the homogenous noise environment. The modifications to CA CFAR (GO and SO) have been proposed to overcome the problems associated with the non-homogenous background. The GO system was designed to regulate the false alarm rate in the region of clutter transitions and the SO system was designed to resolve two closely spaced targets.

1. Homogeneous Noise

In the homogeneous environment, the threshold multiplier T can be used to judge a systems capability. Table 6 [Ref. 26] details the CA, GO, and SO (Square Law systems) threshold multipliers at various false alarm rates and different selections of N. The data in this table represents the noise only environment. As shown, the CA system has the lowest threshold multiplier in all cases which results in superior P_d values. The GO systems values are slightly worse and the SO system values are significantly poorer than that of the CA detector.

Figure 35 details detection probability curves for the MLD family via Monte Carlo simulation using an envelope approximation detector. The P_{fa} for these curves

Table 6. MLD THRESHOLD MULTIPLIERS (SQUARE LAW)

P_{fa}	N = 8 (CA)	N = 8 (GO)	N = 8 (SO)	N = 16 (CA)	N = 16 (GO)	N = 16 (SO)
10-4	2.162	3.600	10.88	0.078	1.360	2.444
10-6	4.623	7.780	36.00	1.371	2.420	5.131
10-8	9.000	15.30	117.90	2.162	3.860	9.905

was set at 10^{-4} with a total of 32 cells being used. As expected, the CA CFAR is the best system in this environment with the GO system showing approximately 0.2 dB additional loss and the SO system yielding a 0.7 dB additional loss.

2. Clutter Edges

The second comparison area considers detector performance in clutter regions. These regions can be caused by chaff, weather clutter distributed in range, and by patchy land clutter. The boundary of this interference (the clutter edge) will move into and out of the reference cells as the test cell approaches or leaves the clutter patch. Of prime concern is the detectors ability to regulate the false alarm rate caused by edging and not specifically with detector losses [Ref. 35]. In the troublesome scenario where the clutter edge occupies half of the reference cells, Moore [Ref. 35] states that the P_{fa} of the CA system increases by a factor of a 1000, whereas the P_{fa} of the GO system only increases by a factor of 17.5. This control of the false alarm rate is the prime advantage that the GO system maintains over CA CFAR. As expected, the SO CFAR system has the poorest performance in clutter edge regions. Trunk states [Ref. 23] that the SO processor performance worsens by more that 5 orders of magnitude when the clutter to noise ratio is greater that 15 dB. Figures 36-38 show the capabilities of the three MLD systems confronting a 'real' sea environment clutter edge. The adaptive threshold levels for each system are shown versus the actual clutter power levels. Figures 36 and 37 clearly show that the CA and GO algorithms handle the simulated clutter edge. However, the SO system shown in Figure 38 is unable to handle the leading and lagging edges of the clutter region leading to unwanted false alarms.

3. Multiple Targets

The final scenario to examine is how multiple target situations affect the MLD family. The SO CFAR system which was designed specifically for the multiple target scenario is nearly unaffected by a single interfering target while the suppression is serious

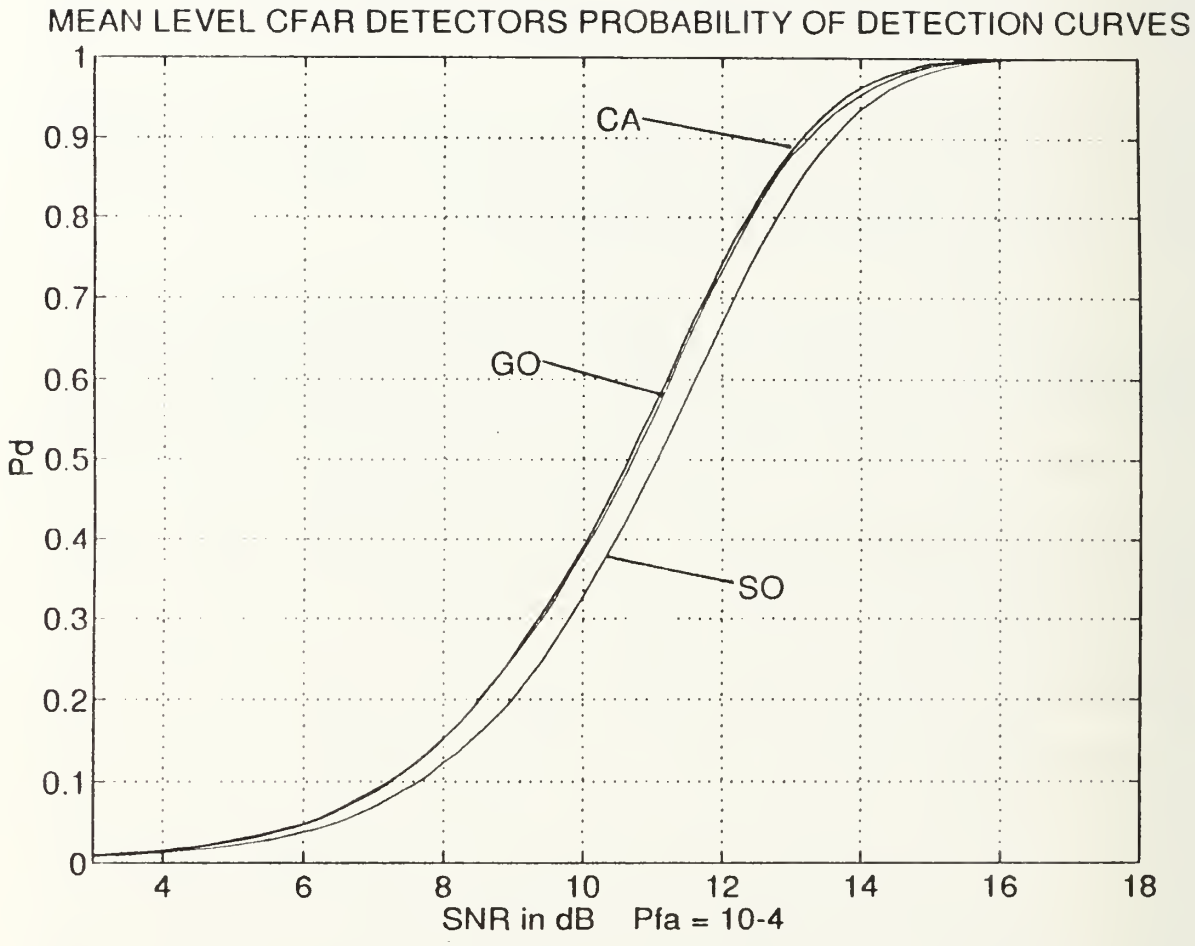

Figure 35. MLD Family Detection Curves

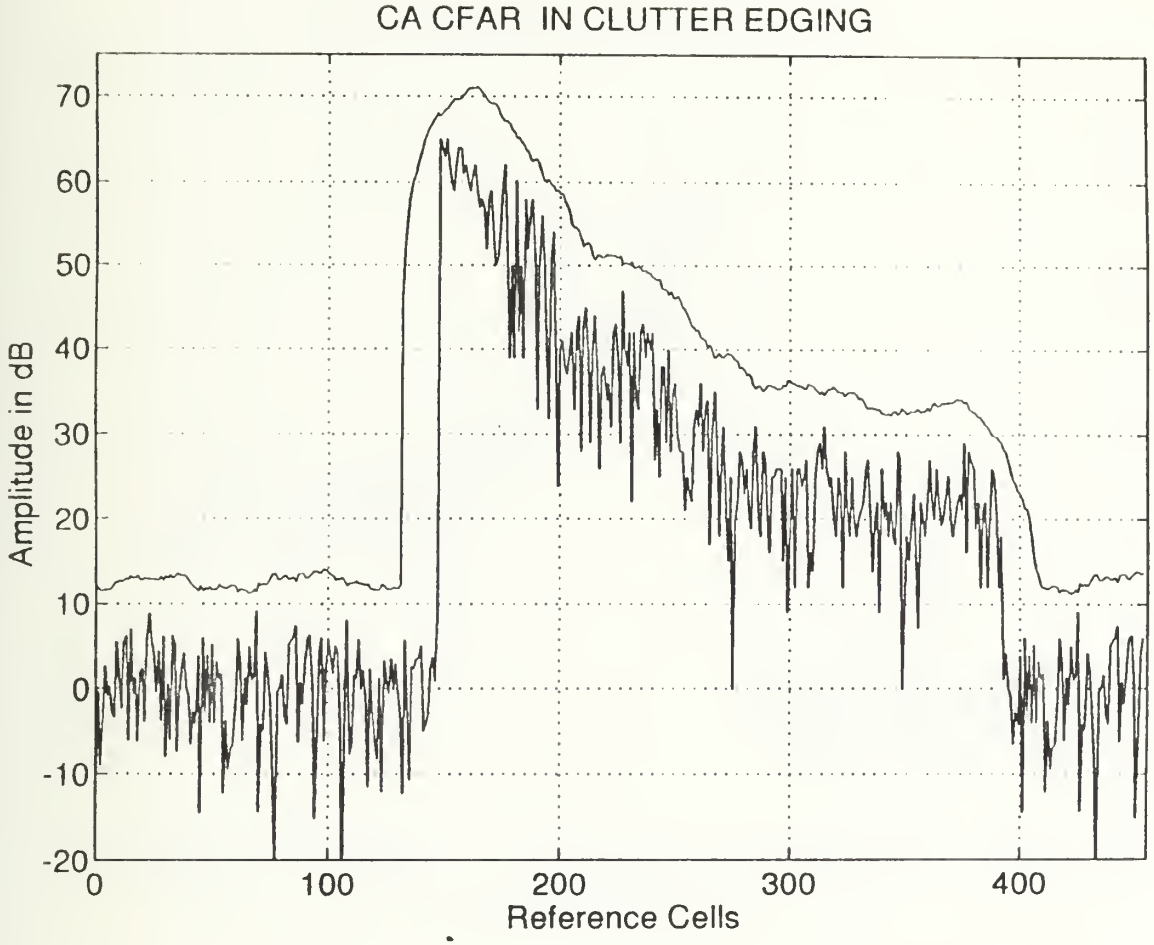

Figure 36. CA CFAR in Clutter Edges

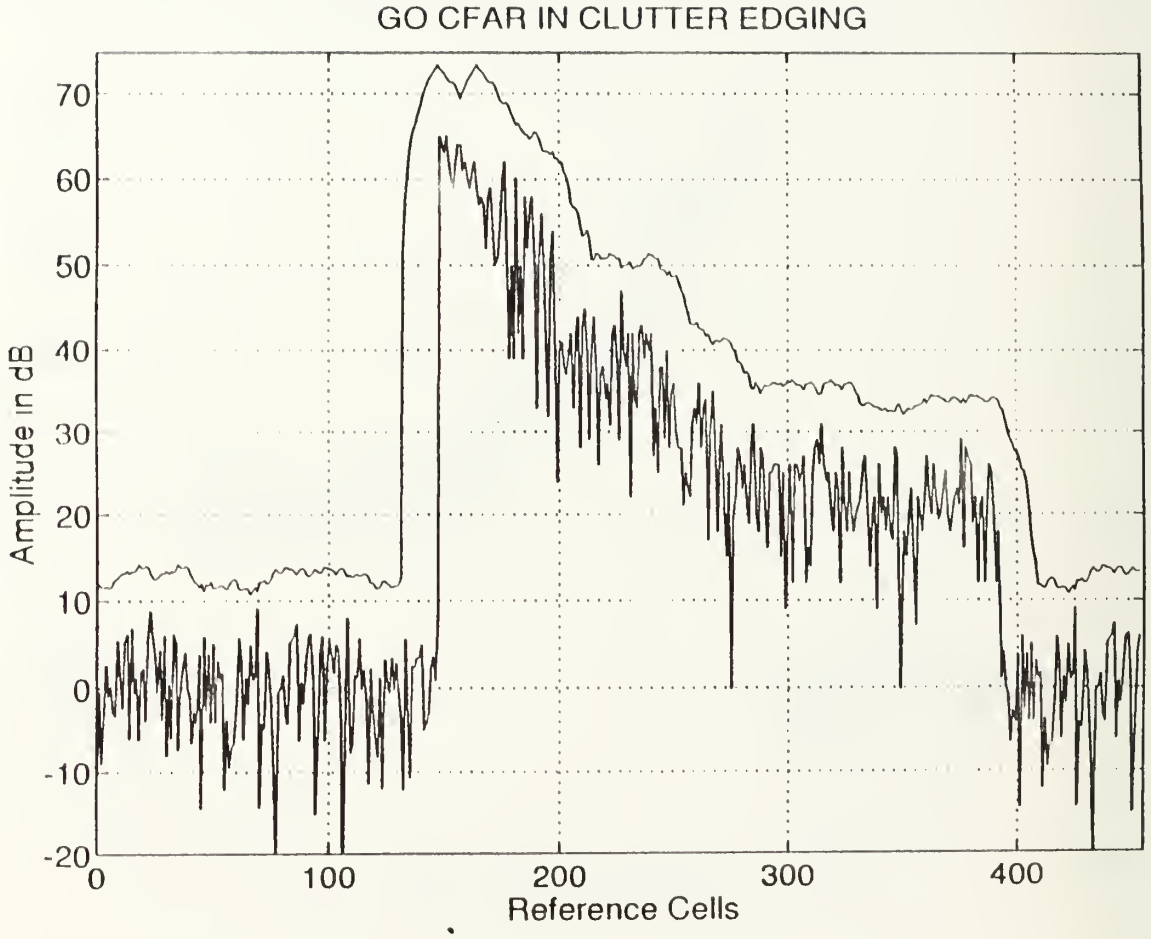

Figure 37. GO CFAR in Clutter Edges

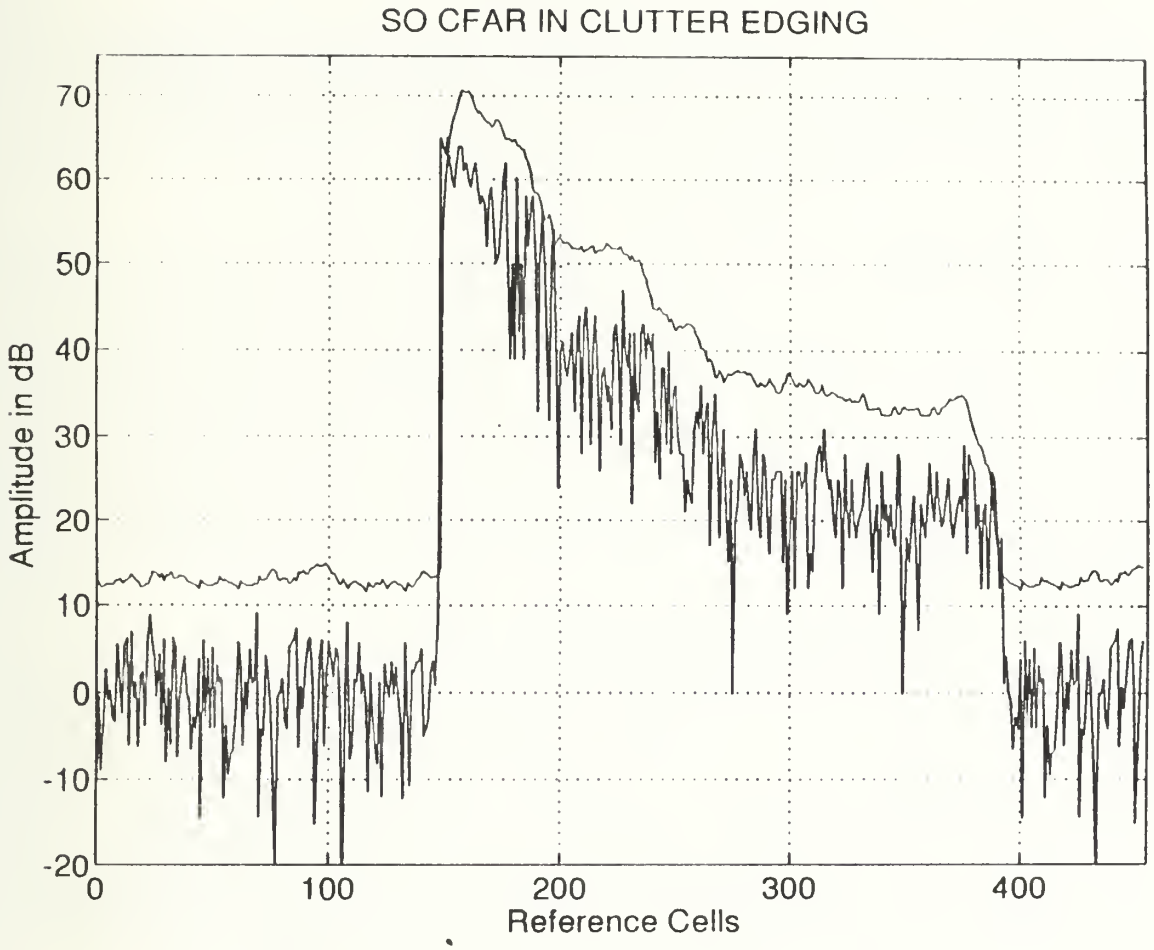

Figure 38. SO CFAR in Clutter Edges

in the CA CFAR and even worse in the GO. Practically, when the total number of reference cells is less than or equal to 16, detection of target pairs with a GO CFAR system is almost totally inhibited [Ref. 15].

Figures 39 and 40 show the effects of interferers on the envelope approximation MLD systems. In Figure 39 a single interferer is introduced into the reference cells. As anticipated the SO system has the best performance with a single interferer yielding the smallest additional CFAR loss of approximately 1 dB. The CA and GO system performances are significantly reduced yielding an additional loss of approximately 3 and 5 dB respectively. Figure 40 shows the effects of 2 interferers (both in the same reference cell neighborhood) on the MLD systems. Again, the SO system maintains its performance while the CA and GO systems perform poorly.

4. Conclusions

The tradeoffs to be compromised concerning the selection of the appropriate type of processor and adequate choice of N are highly dependent on the clutter and interference models the radar engineer chooses. An optimal and general performance CFAR detector can almost never be devised. Therefore it is of great importance to understand fully the operating environment of the radar system in order to correctly tailor or choose the proper CFAR system that will yield superior results for some particular application.

C. ORDERED STATISTICS VS. MLD COMPARISONS

As previously discussed, the OS processing scheme was introduced to alleviate the problems associated with the MLD family. Of significance is that a properly designed OS detector with interfering targets maintains its robustness with only gradual detection loss, while suffering only a minor degradation in the homogeneous environment. Like the MLD systems though, the OS processor is generally unable to prevent excessive false alarm rates at clutter edges unless the clutter appears in one single contiguous patch.

1. Homogeneous Noise

In the homogeneous environment the OS CFAR processor performance is inferior to that of both the CA and GO systems. The loss however is typically 0.5 dB ($K = 21$, $N = 24$, $P_d = 0.5$) [Ref. 26] and is quite tolerable. Figure 41 displays the Monte Carlo comparison of the CA, GO, SO and OS systems in homogeneous noise. The false alarm rate used was 10^{-4}, and the number of reference cells set at $M = 32$ with K set to 20 in the OS system. As shown, the OS system is only slightly poorer than the CA and GO systems but is slightly better than the SO.

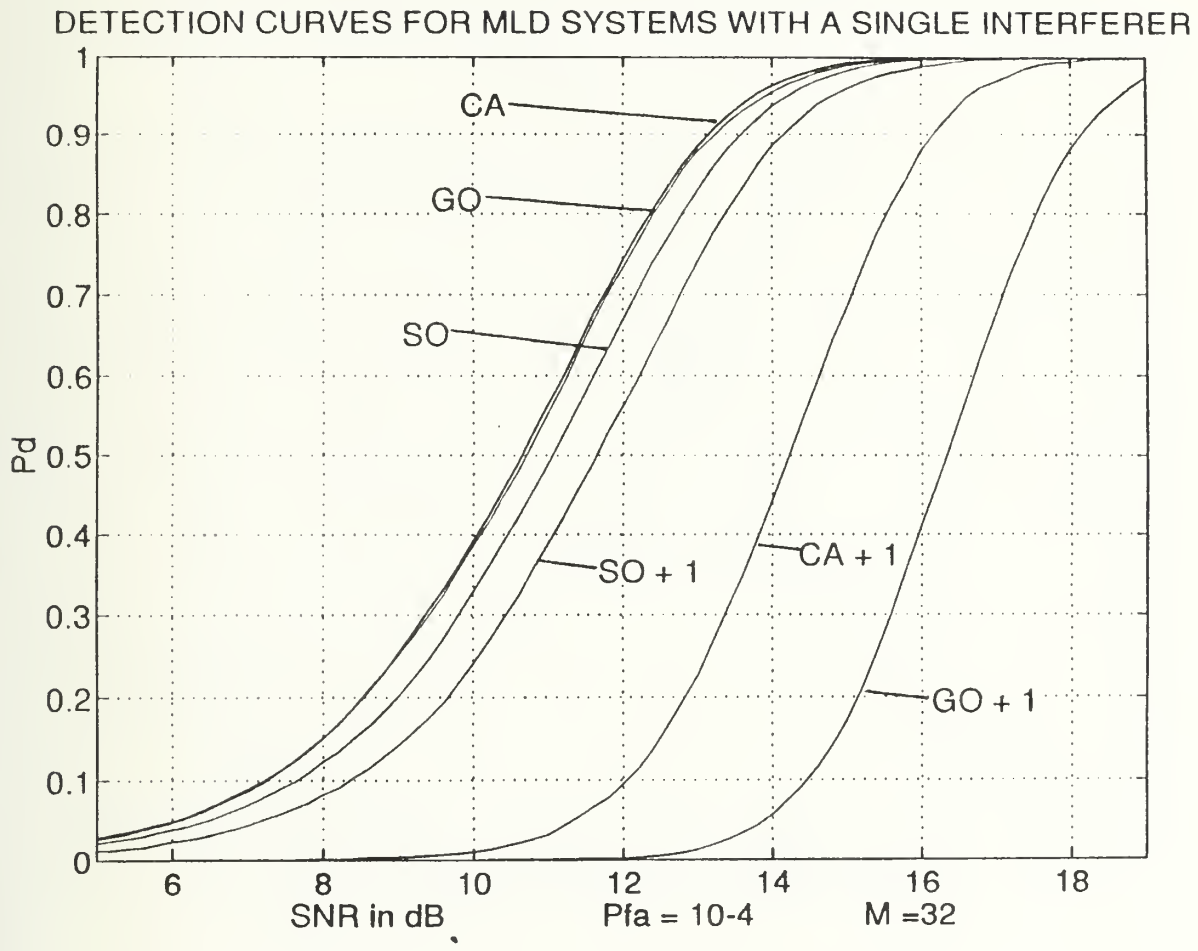

Figure 39. MLD Probability of Detection with a Single Interferer

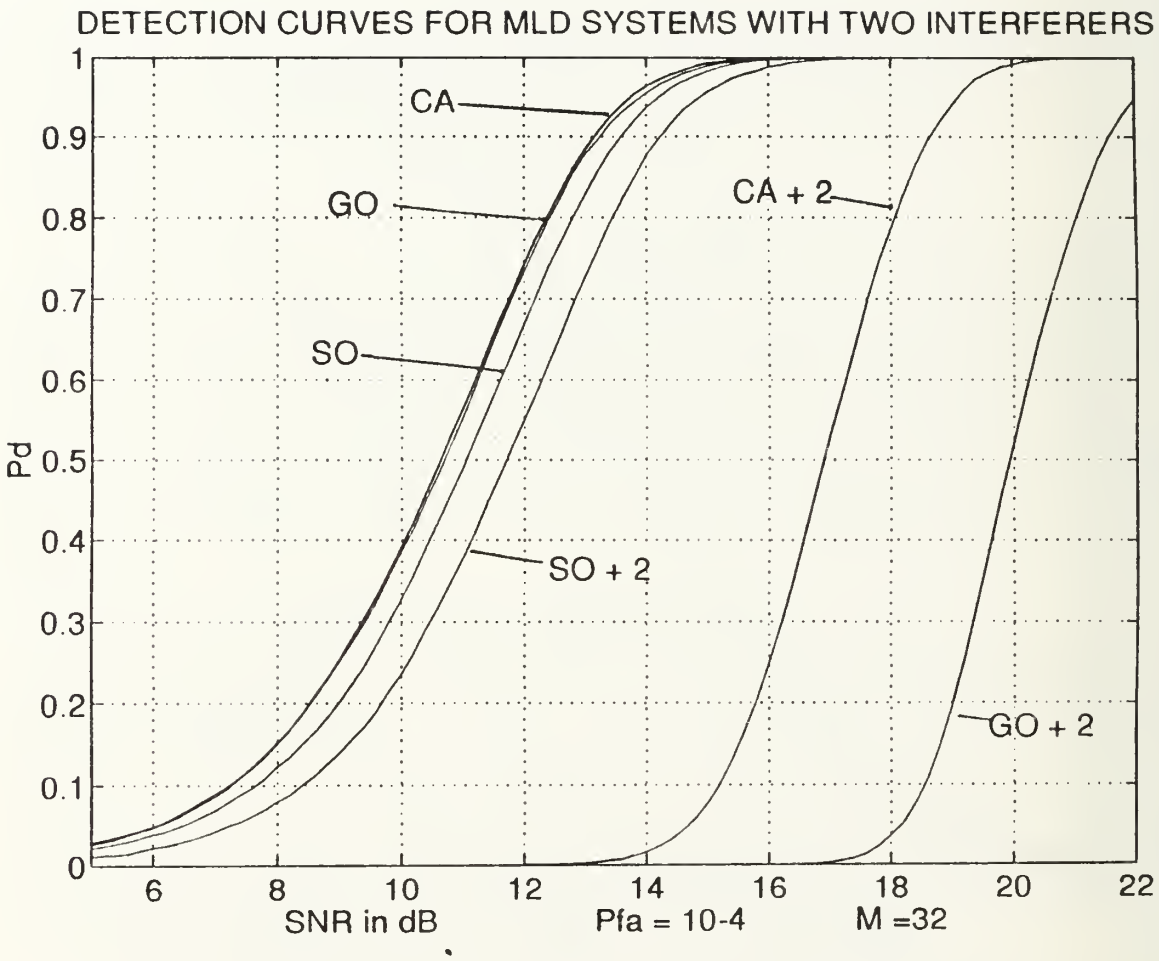

Figure 40. MLD Probability of Detection with Two Interferers

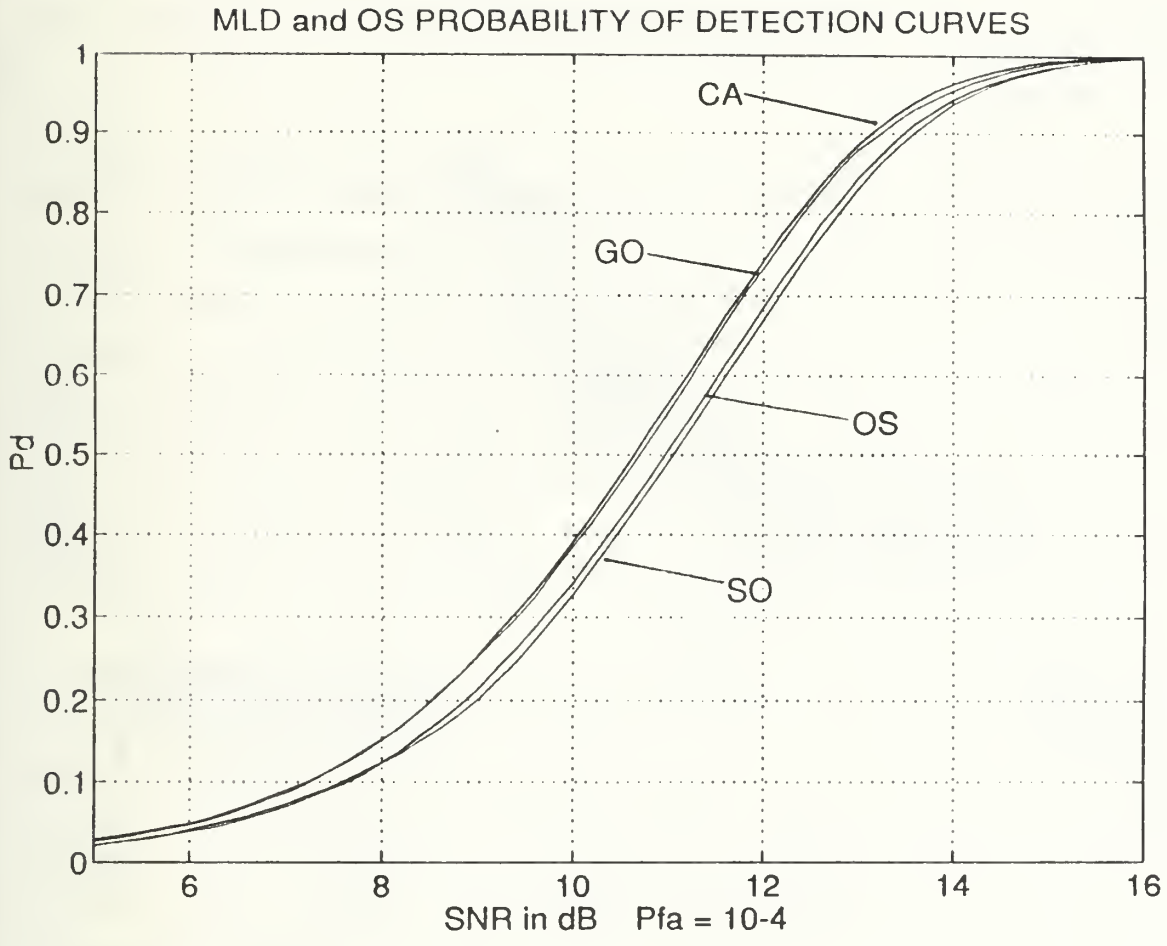

Figure 41. Ordered Statistics versus MLD Detectors in Homogeneous Noise

2. Clutter Edges

In considering the clutter edge problem, one would intuitively expect the OS CFAR performance to be relatively insensitive to edging. This is true only when the clutter returns have slowly varying amplitudes or appear in contiguous patches. The ability to handle these edges (such as weather clutter) are detailed in Figure 42. In this figure the OS system is able to handle the contiguous patch of sea clutter. Unfortunately, OS CFAR can not handle random clutter spikes as well. This is caused by clutter being found in the cell under test while the representative cell (K) is in the clear. This inevitably leads to an increase in the false alarm rate.

3. Multiple Targets

In general, the presence of one or more interfering targets among the reference cells cause the adaptive threshold to increase erroneously in the MLD family. In OS CFAR, this increase is relatively small resulting in a superior performance as compared to the MLD processors. As always, the OS processor performance is highly dependent on the value chosen for K. An optimum OS system is one where K = M - J, where J is the *a priori* known number of interferers. Figure 43 displays the inherent strengths of OS CFAR as compared to the multiple target handling capability of the SO (shown to be the best MLD system with interferers) The figure displays probability of detection versus SNR for envelope approximation systems. As shown, the OS system is favorably compared to the SO CFAR system. Both the OS and SO systems can easily handle two interferers with little additional CFAR loss.

To further stress the performance of a properly designed OS system Table 7 details the detection probability losses and relative CFAR loss of square law OS and CA detectors due to J interferers. In this table, both schemes use a false alarm rate of 10^{-4} and 64 total reference cells with a SNR of 20 dB for both the primary target and the interferers. The value of K is set at 54, allowing for a total of 10 interferers prior to system degradation. As expected, with no interferers, the CA system is superior. However, once interferers are introduced into the system the loss in probability of detection and the relative CFAR loss of the CA system are dramatic as compared to the robust OS detector.

As previously described in Chapter IV, the OSGO and OSSO are direct descendents of the OS system. In terms of comparison, OSGO CFAR has all the advantages of the standard OS system in nonhomogeneous clutter and in multiple target situations with a negligible CFAR loss in the benign environment. Of importance is that the OSGO system requires only half the processing time that the conventional OS sys-

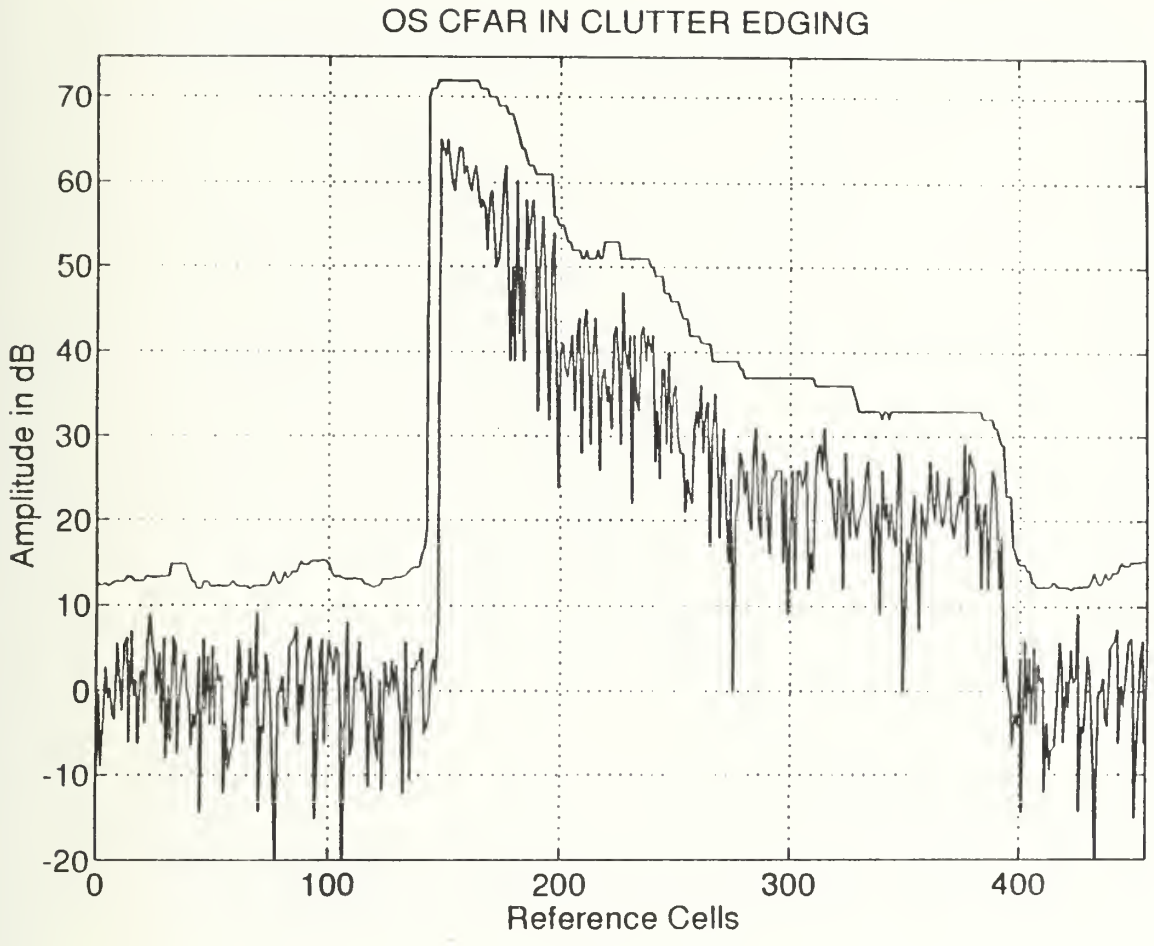

Figure 42. OS CFAR in Clutter Edges

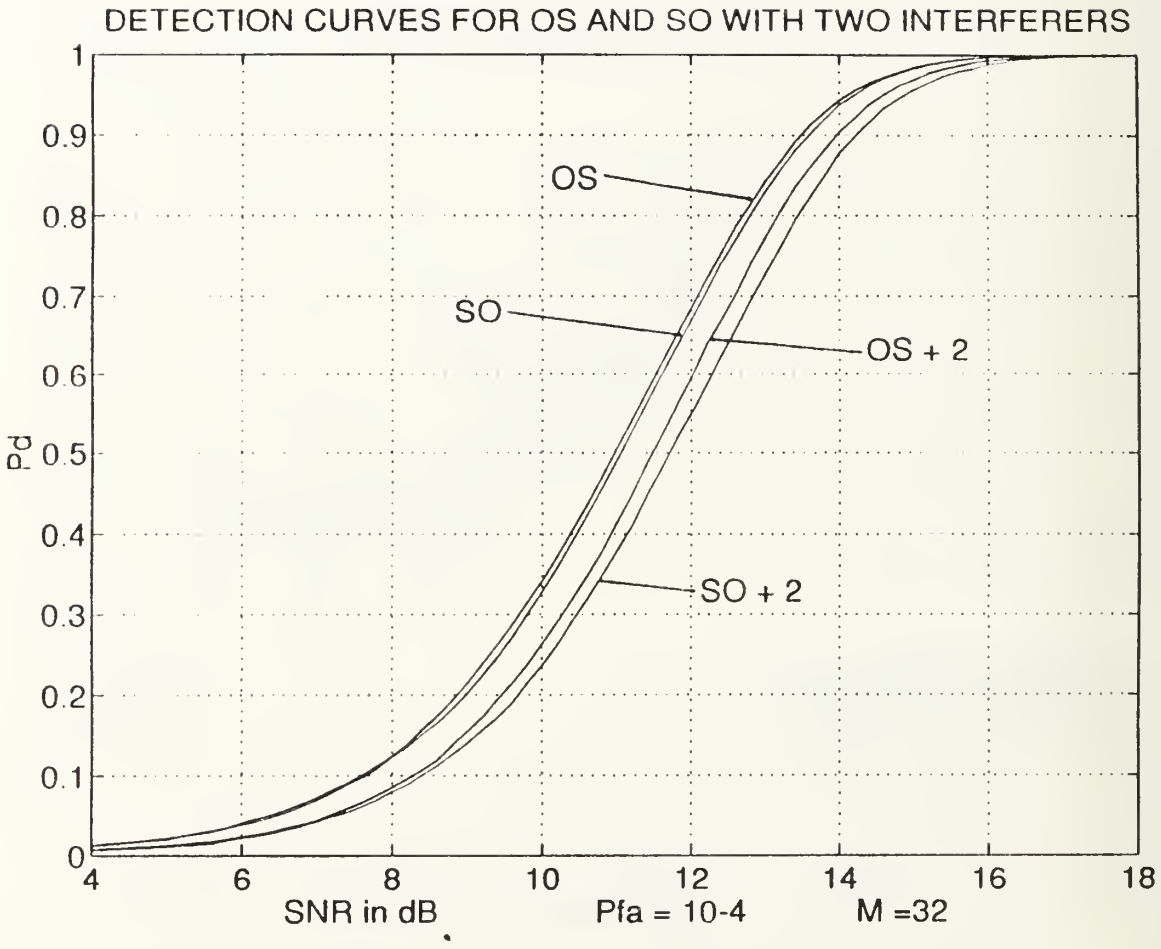

Figure 43. OS vs SO with Two Interfering Targets

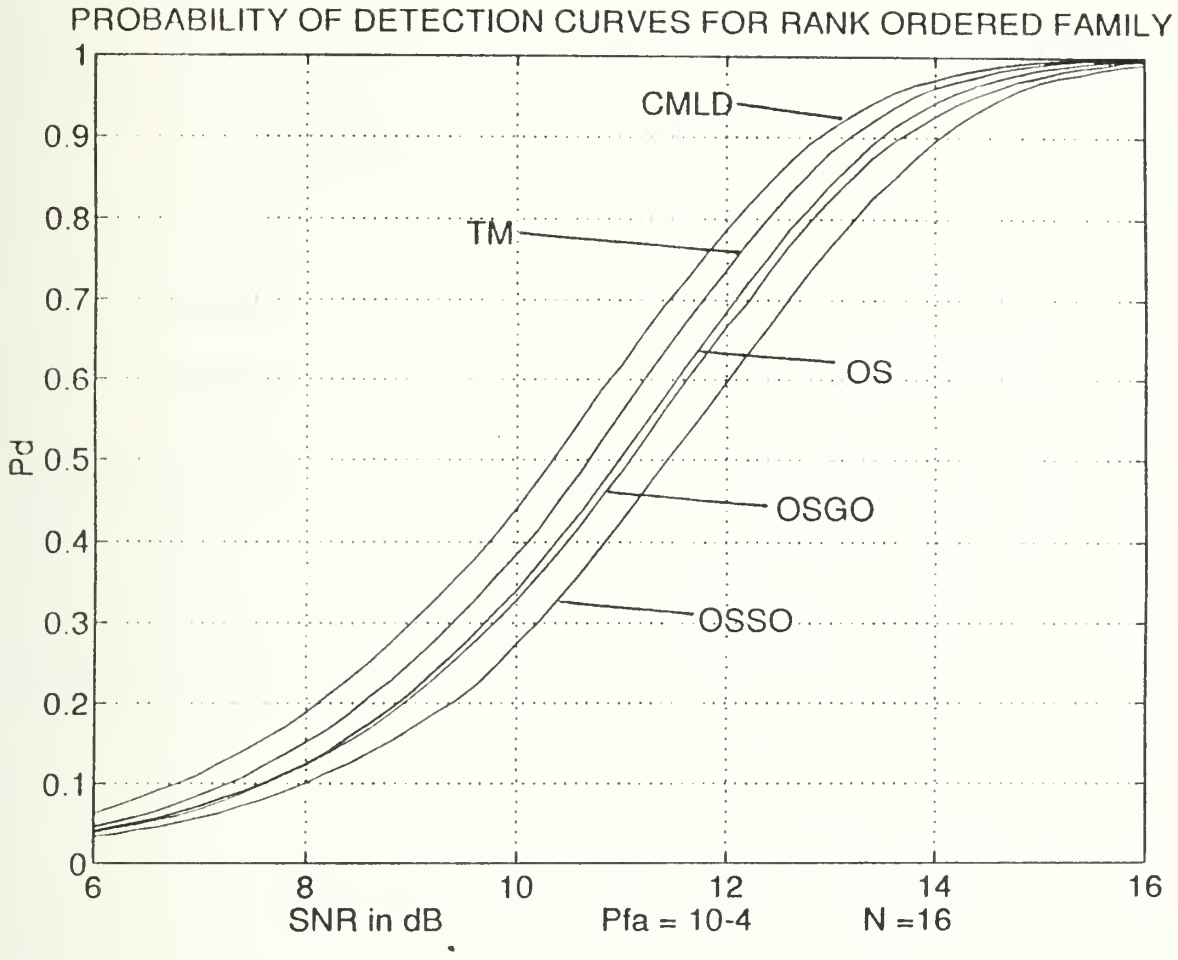

Figure 44. Rank Ordered System Comparison in Homogeneous Noise

Table 7. MULTIPLE TARGET EFFECTS ON CA AND OS CFAR

J	OS P_d	CFAR Loss (dB)	CA P_d	CFAR Loss (dB)
0	0.851	0.71	0.858	0.48
1	0.845	0.90	0.693	4.35
2	0.838	1.11	0.560	6.41
3	0.830	1.39	0.452	7.85

tems requires [Ref. 29]. Concerning the OSSO system, its only advantage is that it too requires less processing time yet it has much higher loss than the OS system and behaves poorly in the non-homogeneous situation. These conditions generally make the OSSO system a poor detector choice. Figure 44 shows the P_d curves for all the envelope approximation rank ordered devices. These Monte Carlo curves were generated at a false alarm rate of 10^{-4}. As shown, the OS system with a representative value of K = 20 is only slightly superior to the OSGO system with K = 10. The OSSO system, also with K = 10, yields the poorest system performance in this noise only environment.

From the results obtained so far, a clear conclusion of the OS system performance versus the MLD detectors can be drawn. Though the OS CFAR exhibits some additional loss of detection in the homogenous noise background, its far superior performance in multiple target environments makes this a seemingly desirable system. Of course, the proper value for K must be chosen to ensure these robust results. This generally requires *a priori* information not generally available, making these systems theoretically superior but operationally sub-optimum performers.

D. CENSORING SCHEME COMPARISON

The CMLD and TM schemes will be considered together since they are both censoring schemes that imply some required *a priori* knowledge to avoid unwanted samples. With this knowledge, the TM and CMLD censoring points would result in near equal optimal system performance. As previously mentioned, the value of K2 in the TM scheme (upper censoring point) plays the crucial role in determining detector performance. The non-zero K2 (TM) or K (CMLD) values dictated by robust detector performance in the multiple target environment conflicts with the requirement to maintain the false alarm rate in regions of clutter power transitions. A near zero value for K2 is necessary for this case.

1. Homogeneous Noise

In the homogeneous environment, TM and CMLD detectors overall performance is better than that of a properly designed OS system and performs nearly as well as a MLD system [Ref. 36].

Referring back to Figure 44, the CMLD and TM systems show near excellent performance in the noise only environment. In these curves the CMLD system censors two of the largest ordered cells and the TM censors the two largest and the two smallest. As shown in this 10^{-4} case, CMLD and TM outperforms the OS system by approximately 0.5 dB and is nearly equal to the optimum CA architecture.

2. Clutter Edges

The clutter edge problem for the CMLD and TM system varies directly with the censoring points chosen. As previously mentioned, a small censoring point may degrade the detection performance since high power clutter samples mask the target in the test cell. As always, the inverse problem of over censoring, results in additional CFAR loss. Since it is recognized that the GO system is the superior MLD system in clutter, it will be compared with the two censoring schemes. Himonas [Ref. 21] has shown that in high clutter power transition areas TM CFAR with K1 = 0 and K2 = 4 yield almost identical performance with that of a GO system when the actual number of clutter cells is four. The performance worsens however, as the number of actual clutter cells increases or decreases away from the preset values of 0 and 4. For small clutter power transition regions the detection performance of the TM (K1 = 0 and K2 = 4) system is actually superior to that of the GO system by approximately 2 dB.

Figure 45 shows the envelope approximation TM CFAR system performance in the sea clutter edge. Since the TM method sums all but the highest and lowest ranked reference cells, its curve is similar to the CA CFAR curve under the same clutter edge environment (Figure 36). As shown, the TM censoring scheme handles clutter edges quite successfully.

3. Multiple Targets

In a multiple target situation, prior knowledge of the number of interfering targets will result in superior performance of the TM and CMLD systems. As always, system performance decreases rapidly with an improper choice of censoring points. Figure 46 clearly proves this point. The envelope approximation CMLD CFAR system used in this simulation censors the two highest ranked reference cells. This enables the system to handle up to two interferers. As shown, the CMLD system with no interferers performs only slightly better than the CMLD system facing two interfering targets.

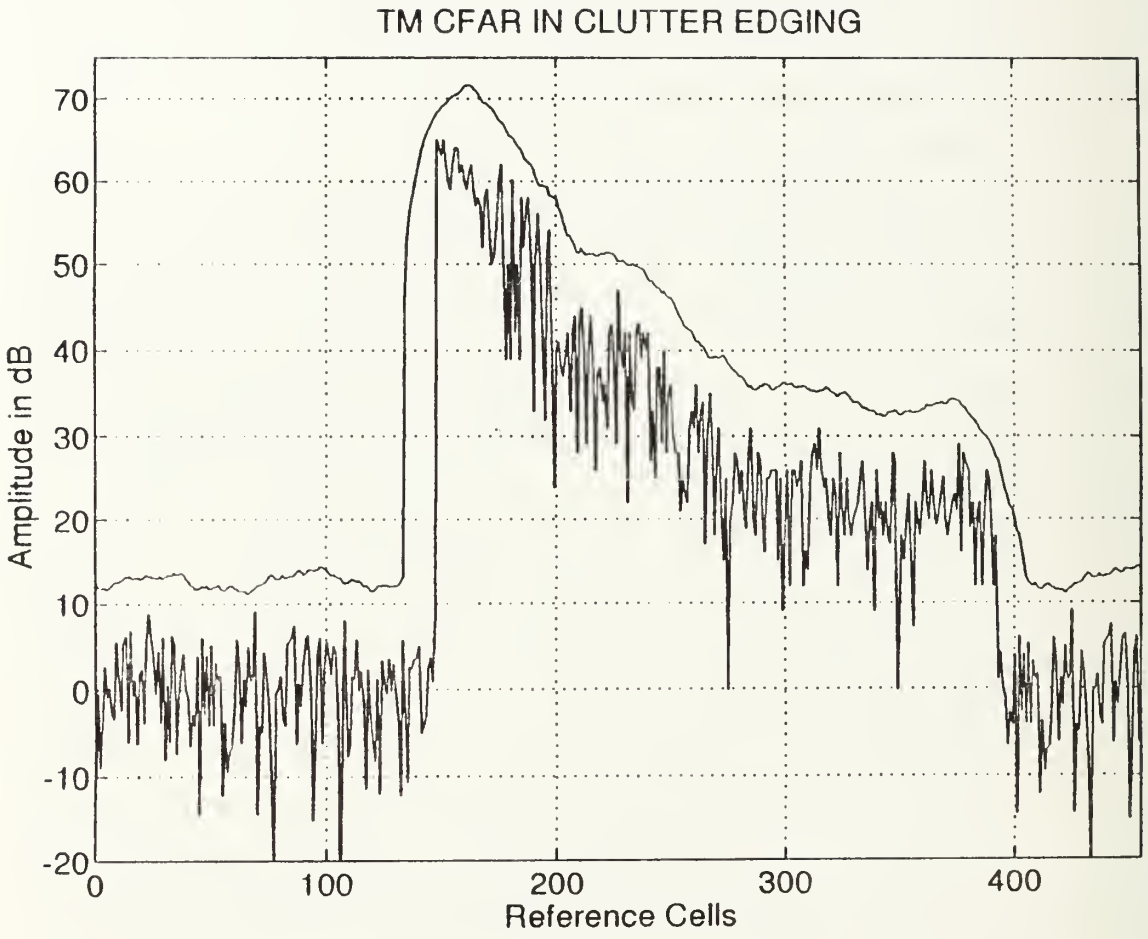

Figure 45. TM CFAR in Clutter Edges

However, once the quantity of interferers becomes greater than two, system performance suffers greatly. As shown, the CMLD system with four interferers shows a drastic reduction in capability. Figure 47 details the CMLD CFAR loss as a function of the number of interferers relative to the optimum Neyman-Pearson detector. In this plot, a CMLD system with N = 32, P_d of 0.9 and a designed false alarm rate of 10^{-4} is detailed. The CFAR loss shown is a result of the increase in false alarm probability caused by improper estimates of the actual number if interferers present. For example, if the actual number of interferers is four (the x axis) and our system is designed to handle two interferers (selecting the curve labeled 2), a CFAR loss of approximately 1.3 dB (read off the y axis) occurs.

4. Conclusions

The performance of the censoring CFAR systems are robust in all operating scenarios as long as the proper censoring points are chosen. When improperly selected, system performance degrades intolerably. In actual operating environments, these CFAR systems would possibly result in unacceptable detection and false alarm rates due to a lack of *a priori* information.

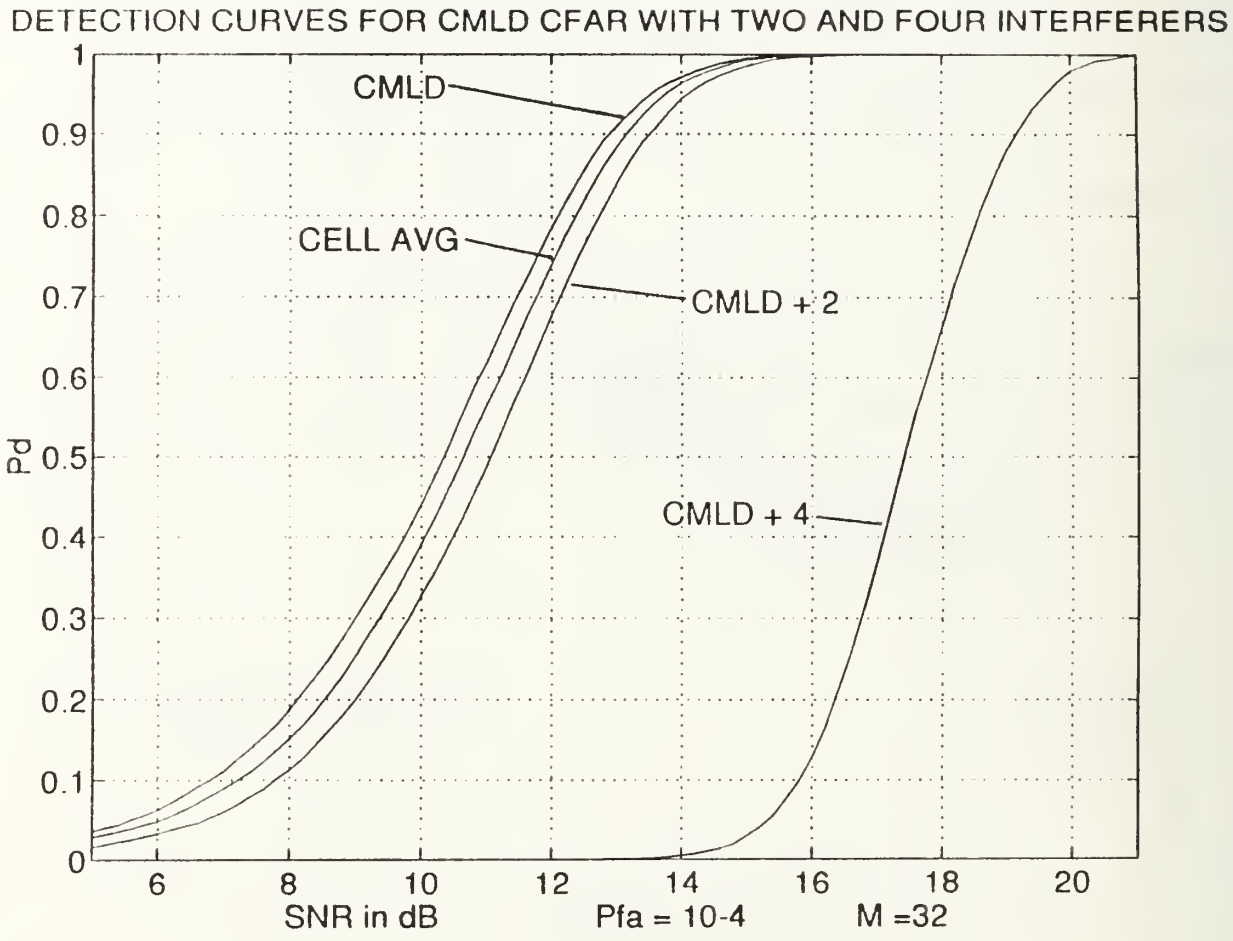

Figure 46. CMLD CFAR with 0, 2, and 4 Interferers

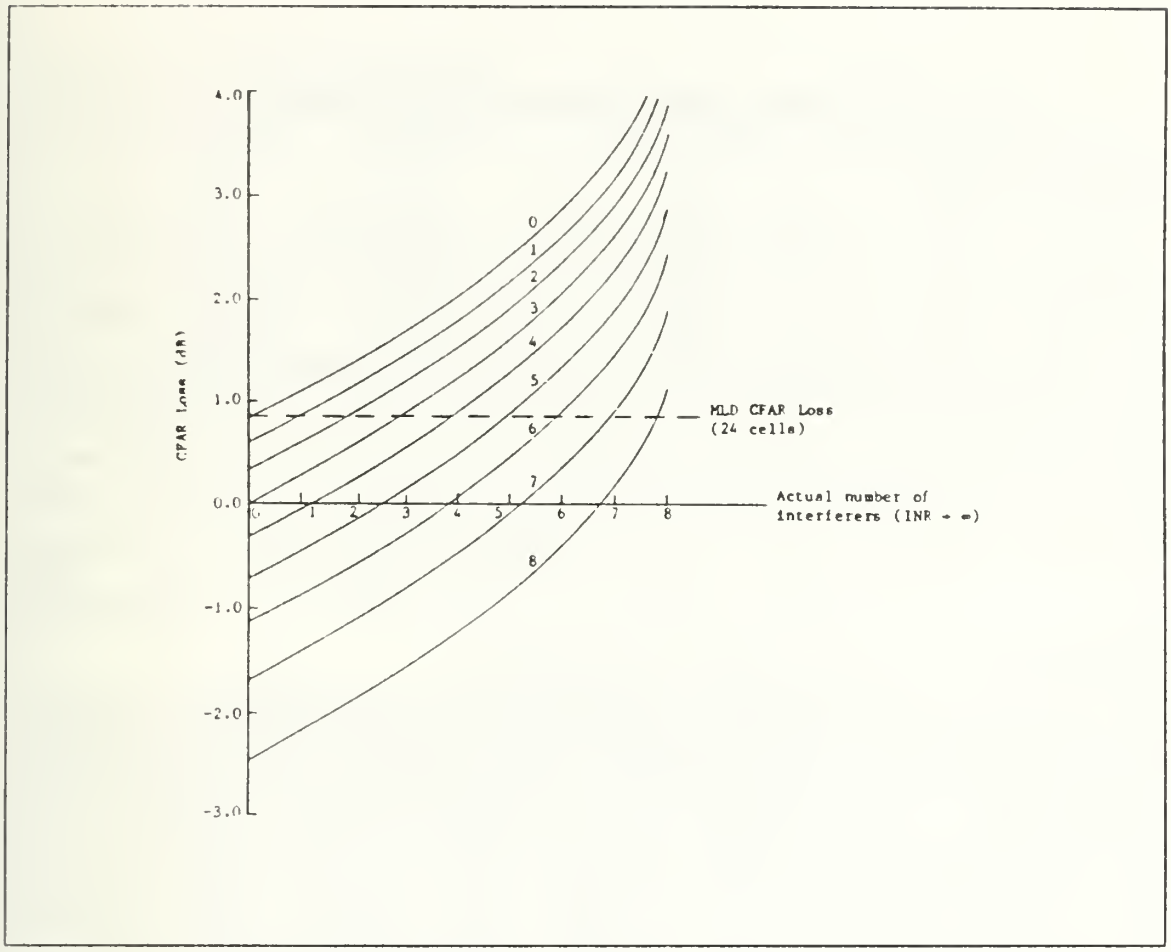

Figure 47. CFAR Loss for CMLD

VI. ENVELOPE APPROXIMATION RESEARCH

A. INTRODUCTION

As discussed earlier in Chapter Two, the input to a CFAR system is often the envelope detected in-phase (I) and quadrature (Q) channels of the baseband signal ($R = \sqrt{I^2 + Q^2}$). Since the digital computation of the square root of the sum of squares of the quadrature components is complicated and time consuming, various approximations to this operation have evolved. One less complex method of I and Q detection using absolute values is the envelope approximation method where the input is estimated as

$$R = a \times \max\{|I|, |Q|\} + b \times \min\{|I|, |Q|\}. \qquad 64$$

In this calculation, a and b are simple scaling coefficients.

The purpose of this chapter is to examine the performance difference this type of detector has on CFAR processors for seven different scaling factors. This examination uses a GO CFAR device. Results for the envelope approximation GO CFAR processor in terms of probability of false alarm [Ref. 37] and probability of detection [Ref. 38] are shown. The a and b multipliers are listed in Table 8 along with the average error and mean square error for the seven approximations. In the first five approximations, the multiplying coefficients are either one or simply binary fractions. The sixth approximation was designed to have zero average error which simultaneously minimizes the variance of the error. The last approximation was designed such that the end point error equals the absolute value of the peak error in the region $0 < \phi < \pi/4$ [Ref. 37],[Ref. 5].

B. PROCEDURE AND RESULTS

Monte Carlo simulations were created to test the seven scalar combinations listed in Table 8. The envelope approximation results have been devised for the six cases N = 2, 4, 8, 16, 32, and 64. The threshold multipliers used in these simulations were taken from Paces results to ensure a false alarm rate of 10^{-4}. Table 9 lists these threshold multipliers. Figure 48 shows the P_{fa} curve versus Threshold Multipliers. Shown are the seven combinations plotted along with the $\sqrt{I^2 + Q^2}$ results. Figures 49-54 detail the resulting detection probabilities versus SNR . As detailed in these performance curves,

Table 8. SCALING FACTORS

Case	a Scalar	b Scalar	Average Error	Mean Square Error
1	1.0	1.0	-27.3	30.0
2	1.0	0.5	-8.68	9.21
3	1.0	0.25	-0.65	4.15
4	1.0	0.375	-4.02	4.76
5	0.96875	0.375	-1.20	2.70
6	0.948	0.393	0.00	2.33
7	0.96043	0.39782	-1.30	2.70

the a = 1.0 and b = 1.0 case yields the highest system detection performance and the lowest P_{fa} for a given threshold multiplier. The a = 1.0, b = 0.25 yields the poorest performance.

Table 9. THRESHOLD MULTIPLIERS AT 10-4 PFA

M	CASE 1	CASE 2	CASE 3	CASE 4	CASE 5	CASE 6	CASE 7
2	12.20	13.40	16.60	14.40	14.30	14.00	14.1
4	5.90	6.50	7.80	7.00	6.90	6.80	6.80
8	4.40	4.70	5.50	5.05	5.05	4.95	4.95
16	3.90	4.10	4.70	4.32	4.35	4.30	4.30
32	3.70	3.90	4.30	4.05	4.05	4.01	4.01
64	3.60	3.80	4.20	3.95	3.95	3.90	3.90

C. CONCLUSIONS

A clear conclusion can be drawn from this study of the envelope approximation scaling coefficients. In all cases, a = 1.0 and b = 1.0 yields the best detection performance. The next chapter uses this information and presents a new CFAR architecture that overcomes the inherent deficiencies of the architectures examined previously.

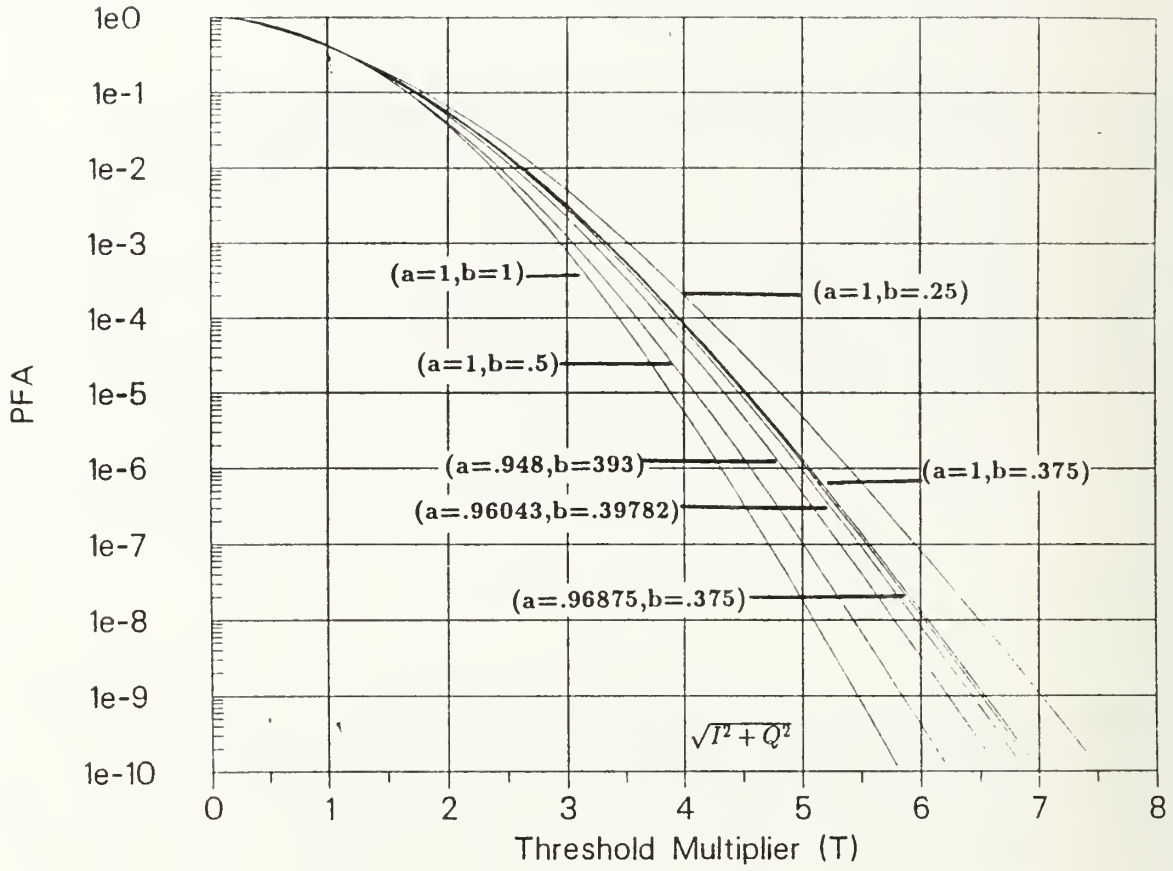

Figure 48. Probability of False Alarm for Envelope Approximation GO CFAR

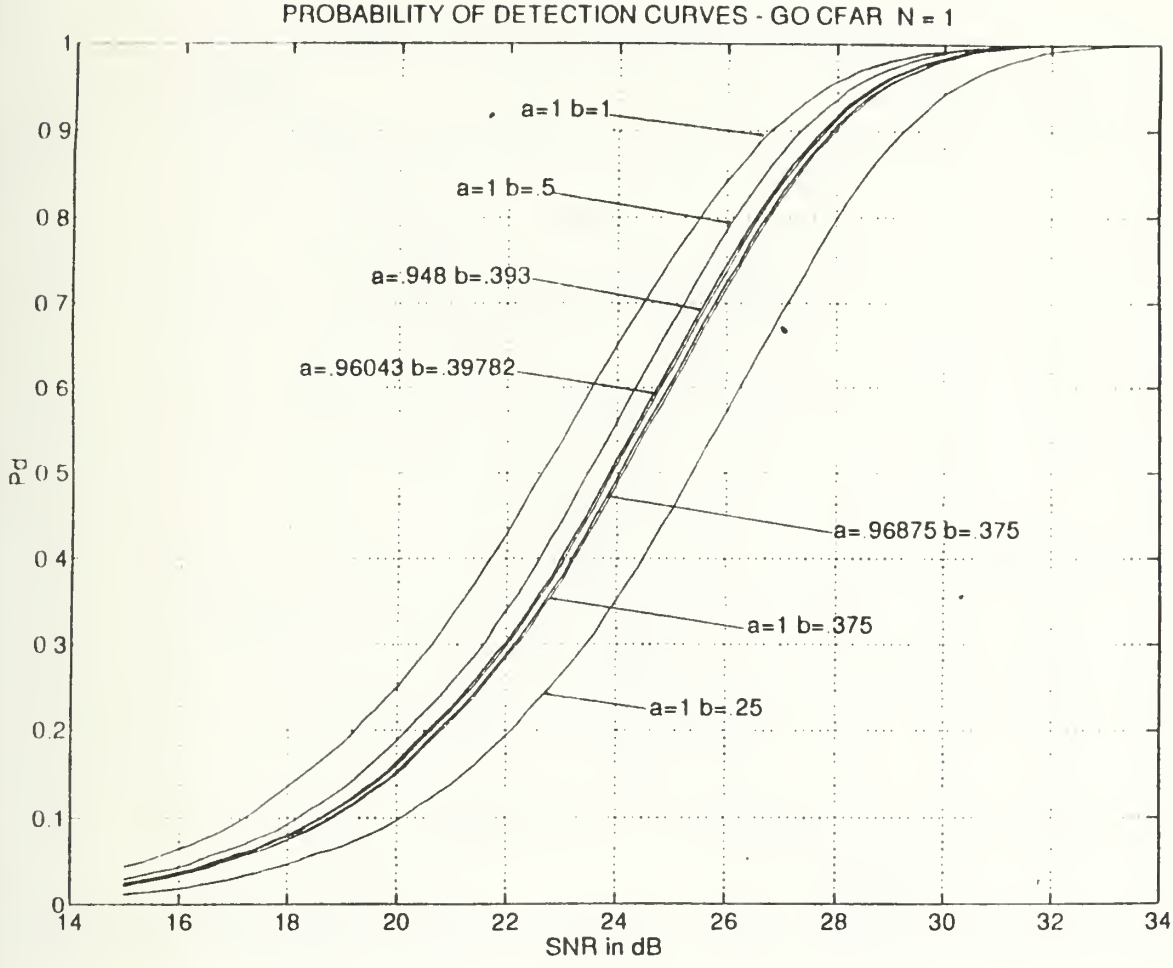

Figure 49. Envelope Approximation Curves with N = 1

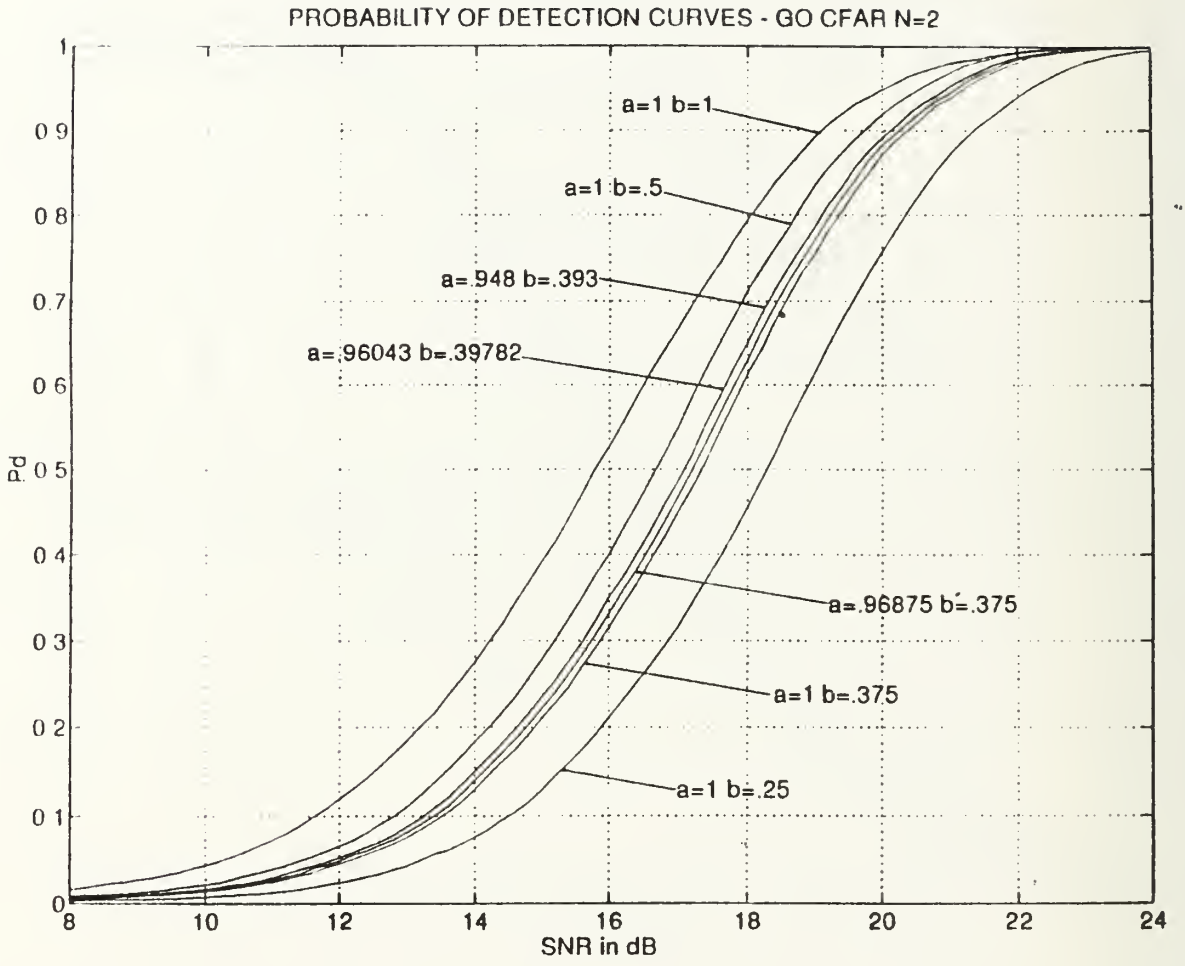

Figure 50. Envelope Approximation Curves with N = 2

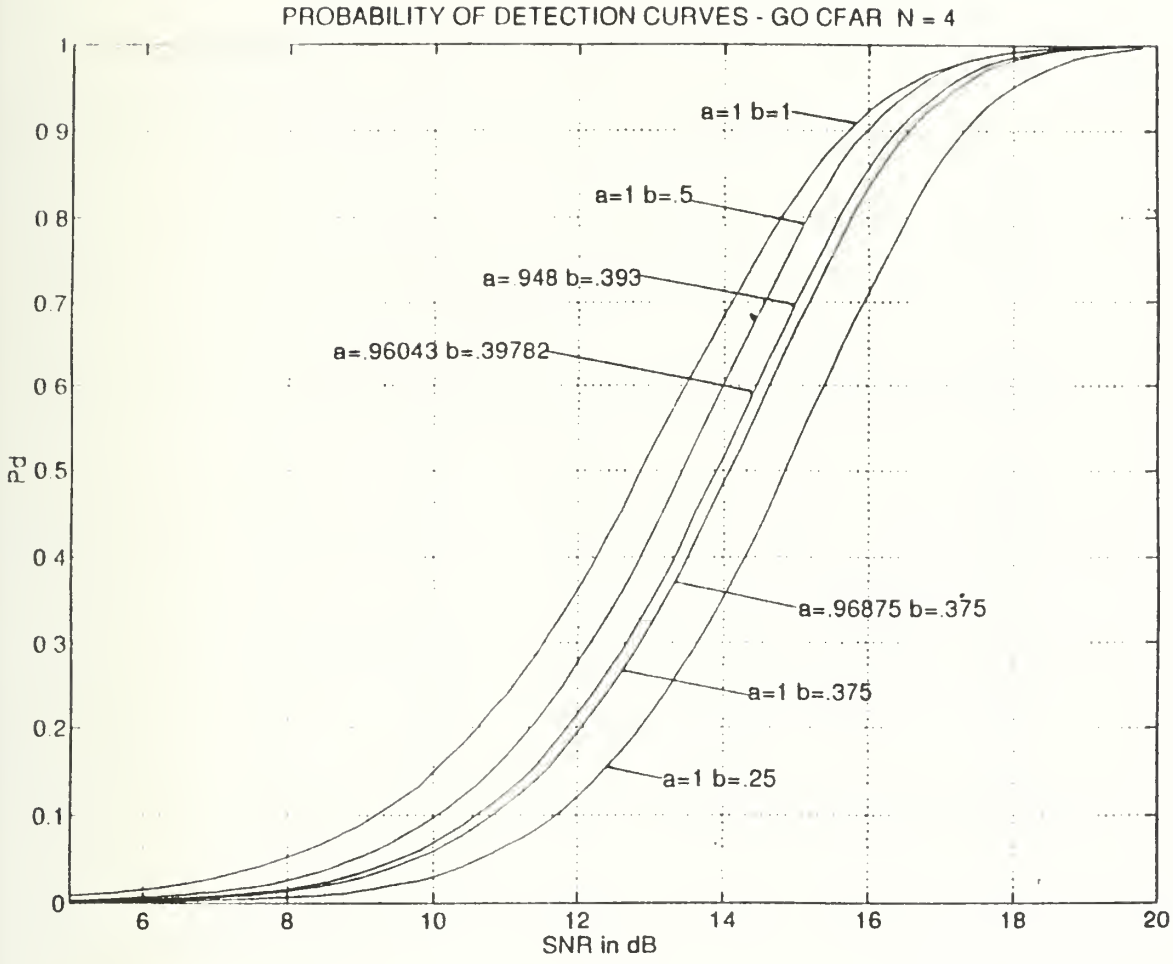

Figure 51. Envelope Approximation Curves with N = 4

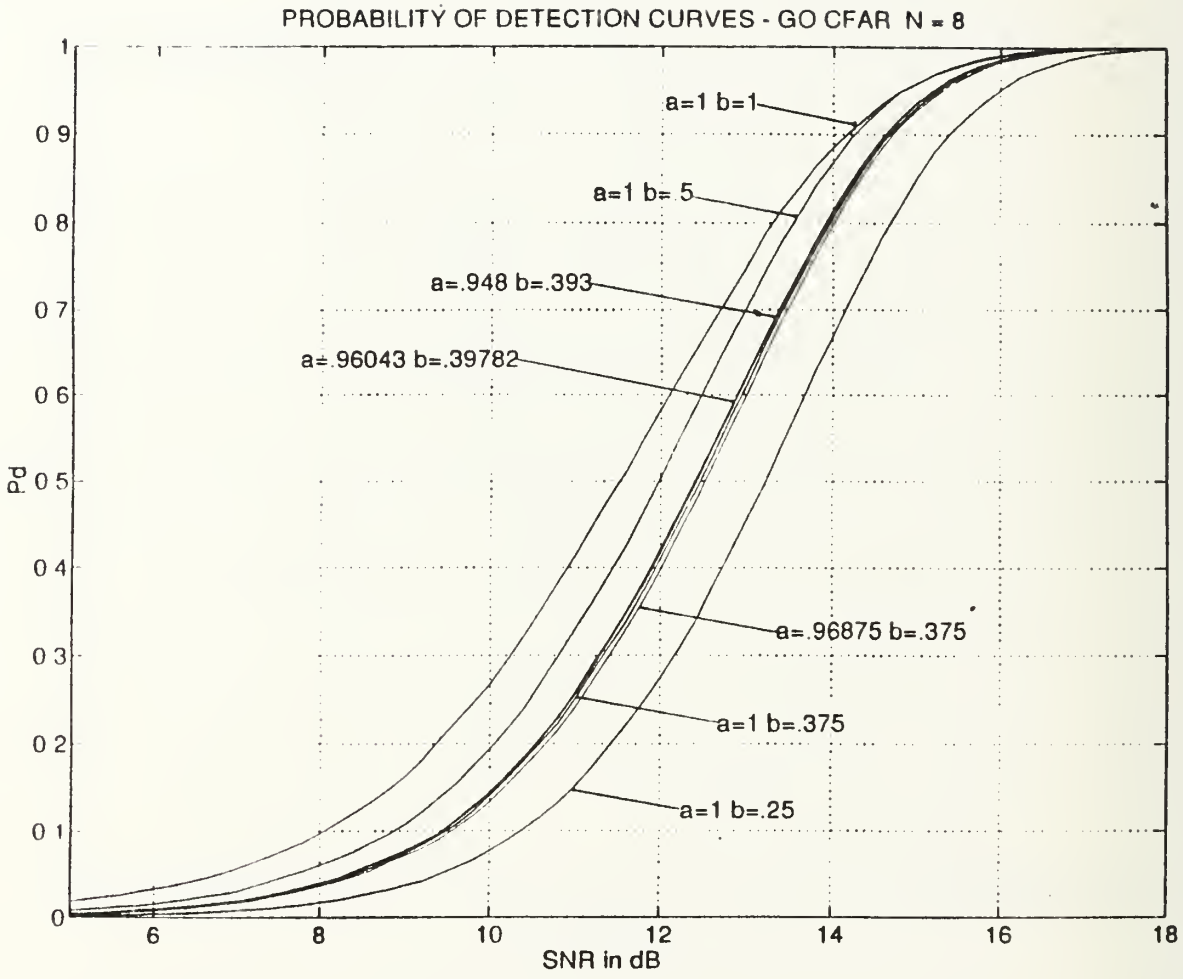

Figure 52. Envelope Approximation Curves with N = 8

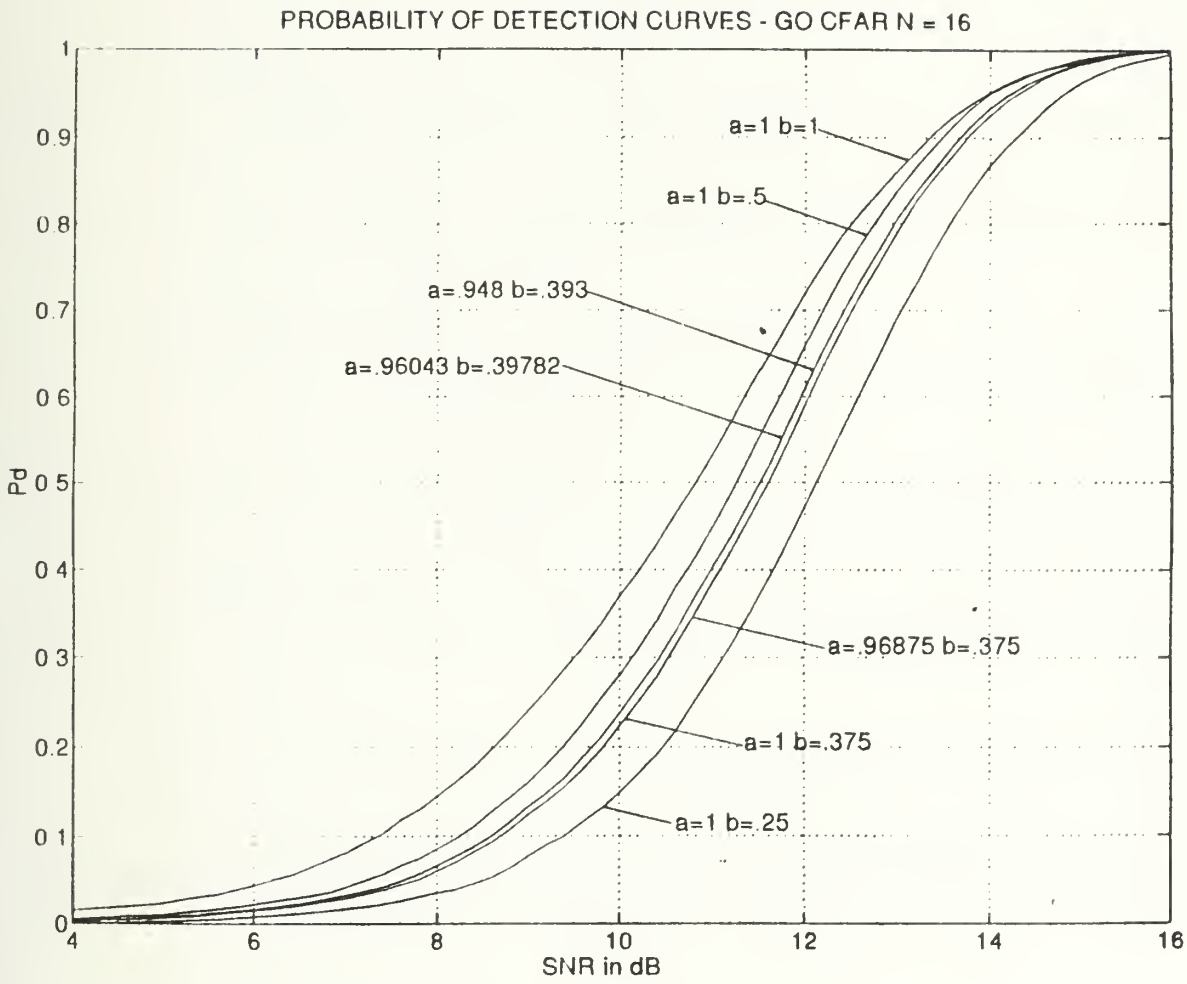

Figure 53. Envelope Approximation Curves with N = 16

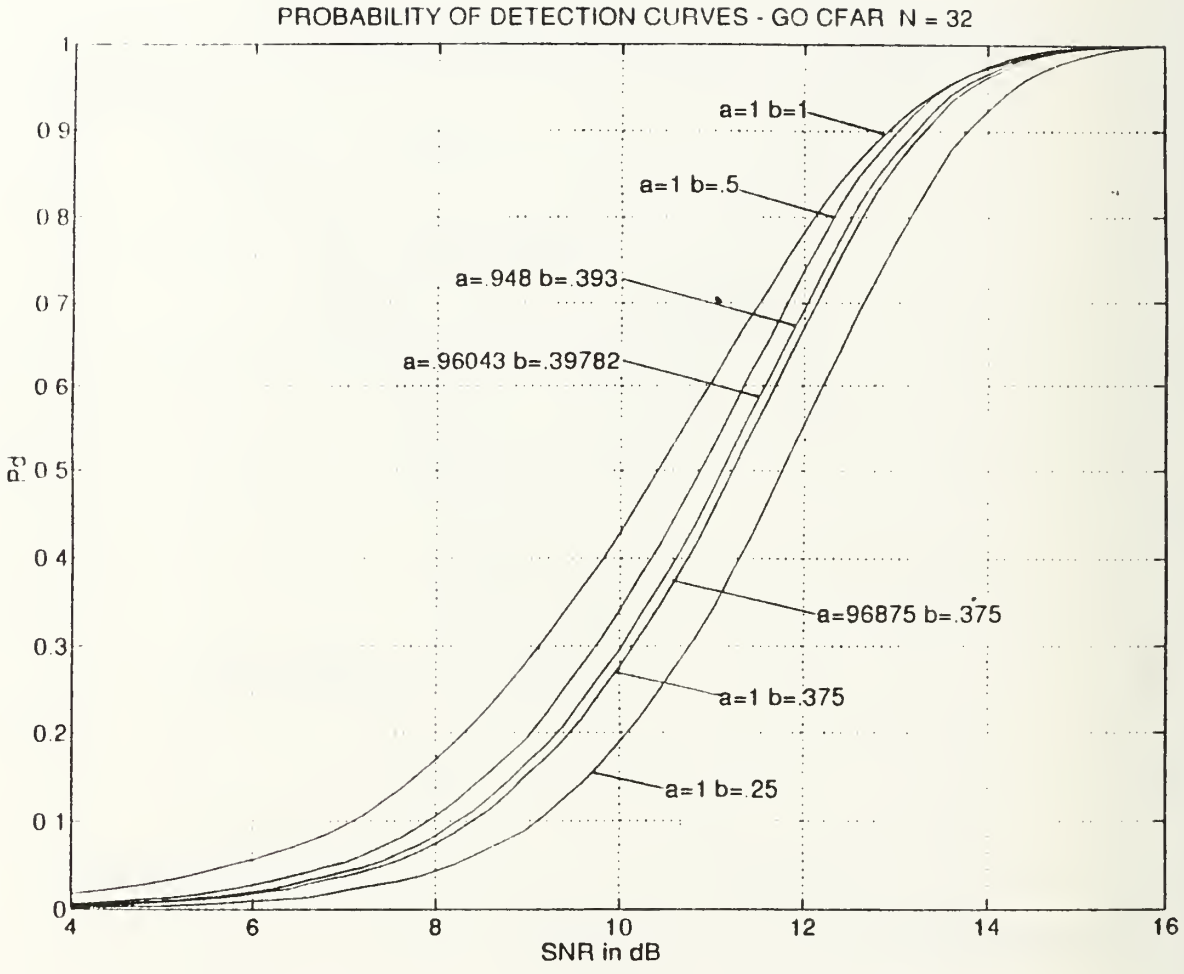

Figure 54. Envelope Approximation Curves with N = 32

VII. EXCISION GREATEST OF (EXGO) CFAR

A. INTRODUCTION

As presented throughout this thesis, numerous CFAR architectures have been developed to balance the conflicting goals of maintaining a high detection probability while enjoying a low false alarm rate. As shown, this difficult task is magnified in the presence of interfering targets and ECM. In this chapter a new CFAR device call 'Excision Greatest Of' (EXGO) will be presented. This system was designed to maintaining superior performance under clutter edge, multiple target and jamming environments. The concept of excising large interferers was initially introduced by Goldman and Bar David [Ref. 39]. for their cell averaging scheme.

B. SYSTEM DESCRIPTION

A schematic diagram of the proposed EXGO CFAR detector is shown in Figure 55. The EXGO processor uses envelope approximation to detect the inphase (I) and quadrature (Q) components of the signal. Scalar values of a = 1 and b = 1 are used since they have been shown to most closely match the results of a true envelope detector. Two additions to the standard GO MLD are shown in Figure 55. The first addition is the excision logic, and the second is the extended leading and lagging reference cells (shown with hashed lines).

1. Excision Logic

The purpose of the excision logic is to compare the relative magnitude of all utilized reference cells to an adaptive voltage threshold level (V_{t1}). The excision logic is shown in detail in Figure 56. The threshold level is the product of a preset scalar value (T_1) and the continuously updated running system noise average (R) given by

$$R = \frac{\sum_{j=1}^{k} x(j)}{k}, \tag{65}$$

where x(j) is the reference window input and k is the total number of inputs into the system over time. Thus, the initial threshold level is set as

$$V_{t1} = R \times T_1. \tag{66}$$

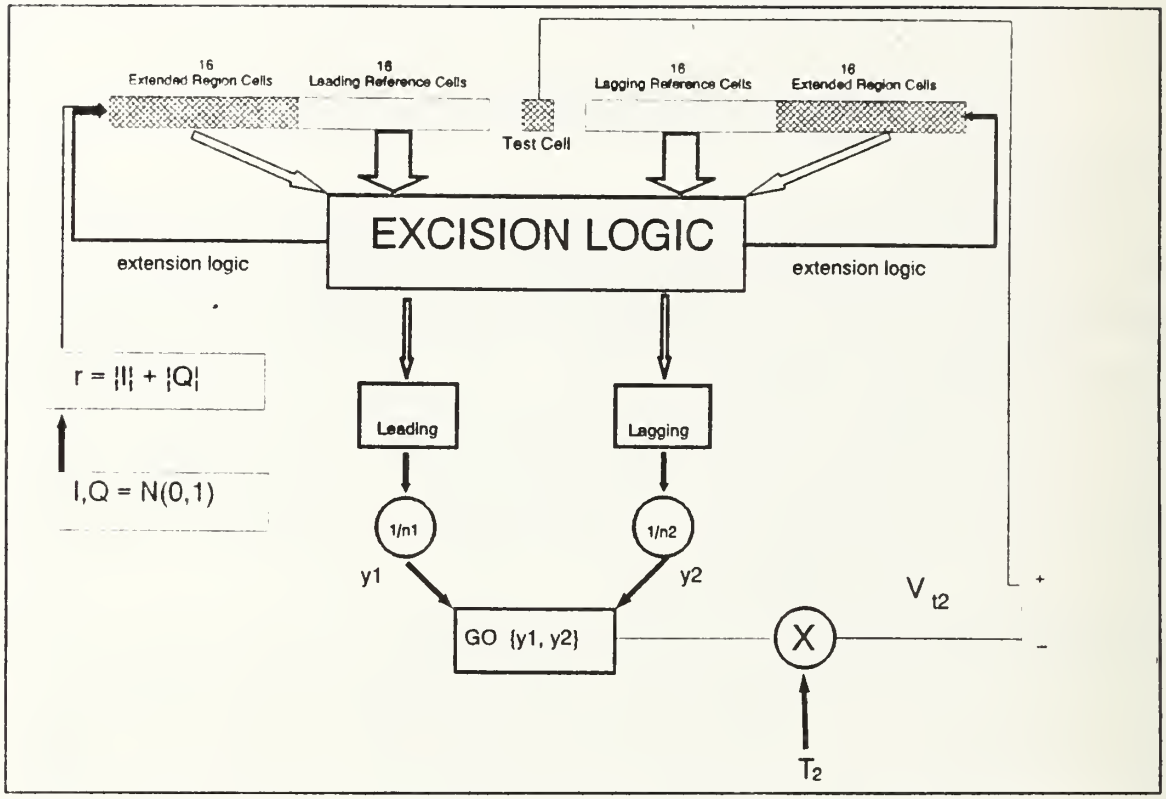

Figure 55. EXGO Schematic

If the magnitude of any individual reference cell is greater than V_{t1}, an interfering target is assumed to be present in that cell and therefore ignored from further use in the GO process. For example, with $T_1 = 2$, any reference cell that is greater in magnitude than twice the system noise average will be discarded from further GO processing. If the cell is less than twice the running noise level, the reference cell is then processed in a normal GO fashion. The selection of a proper threshold multiplier, T_1 is important. With too low a threshold, proper noise samples will be excised from the system, thus increasing the CFAR loss. Setting T_1 too high will cause some large interfering targets to pass the excision logic and thus contaminate the noise power estimate and degrade the probability of detection. A binary integration at the output of the excision logic counts the number of threshold crossings.

The EXGO architecture takes special precautions in order to maintain the proper false alarm rate in the presence of clutter edges. When at least one entire leading or lagging reference cell window is fully contaminated by clutter (recognized by greater

than 16 excisions), the system adapts by using the clutter cells to determine the overall system threshold level (V_{t2}). Thus, rather than excising the clutter, it is used to properly adjust the voltage threshold to maintain the false alarm rate. This is the same method employed by the GO system.

2. Extended Range Cells

The hashed lines in Figure 55 show an additional 16 cells straddling the original 16 leading and lagging reference cells. The additional cells are used only when a preset number of cells are excised from processing (indicating the possible presence of jammers) or when clutter edges dominate a reference window. This is the output of the binary integration. In general, only a marginal decrease in CFAR loss is obtained when going from a 32 to 64 cell system. This processing cost is well worth the effort however, when the system is under attack from multiple false target ECM systems. Thus, when the false target jamming is detected or when immersed in clutter, a full 64 cell system is engaged into the EXGO processor to maintain robust performance.

False target jamming (resulting in the 64 cell system) is declared by the excision logic once some predetermined number of excisions take place. For example if between eight and sixteen excisions take place among the original 32 leading and lagging cells, the system declares false target jamming. Since system performance of a standard 32 cell system is seriously degraded when high excision rates are used, the reference windows are expanded to the full 64 cell system. Thus, if every fourth cell contains a false target, the 64 cell system would excise 16 cells yet still maintain 48 cells for noise estimation.

3. System Operation

Other than the extended reference cells and the excision logic architecture, the EXGO processor behaves exactly as a GO CFAR. After the cells pass though the excision logic, all remaining cells are summed by neighborhood and normalized by the proper number of non-interferer cells (n1, n2). The resulting values, y1 and y2 are then input to the 'GO' logic for determination of the largest value. The 'GO' output is then multiplied by the threshold multiplier T_2, yielding a comparator threshold voltage, V_{t2}. The cell under test is then compared to this value. If the test cell's amplitude exceeds V_{t2} then a target is declared.

When the system is in the clutter edge mode, the normal 'GO' process continues. Since the clutter cells are purposefully passed through the excision logic, they inevitably become the 'GO' selection yielding the properly inflated adaptive threshold level that maintains the false alarm rate.

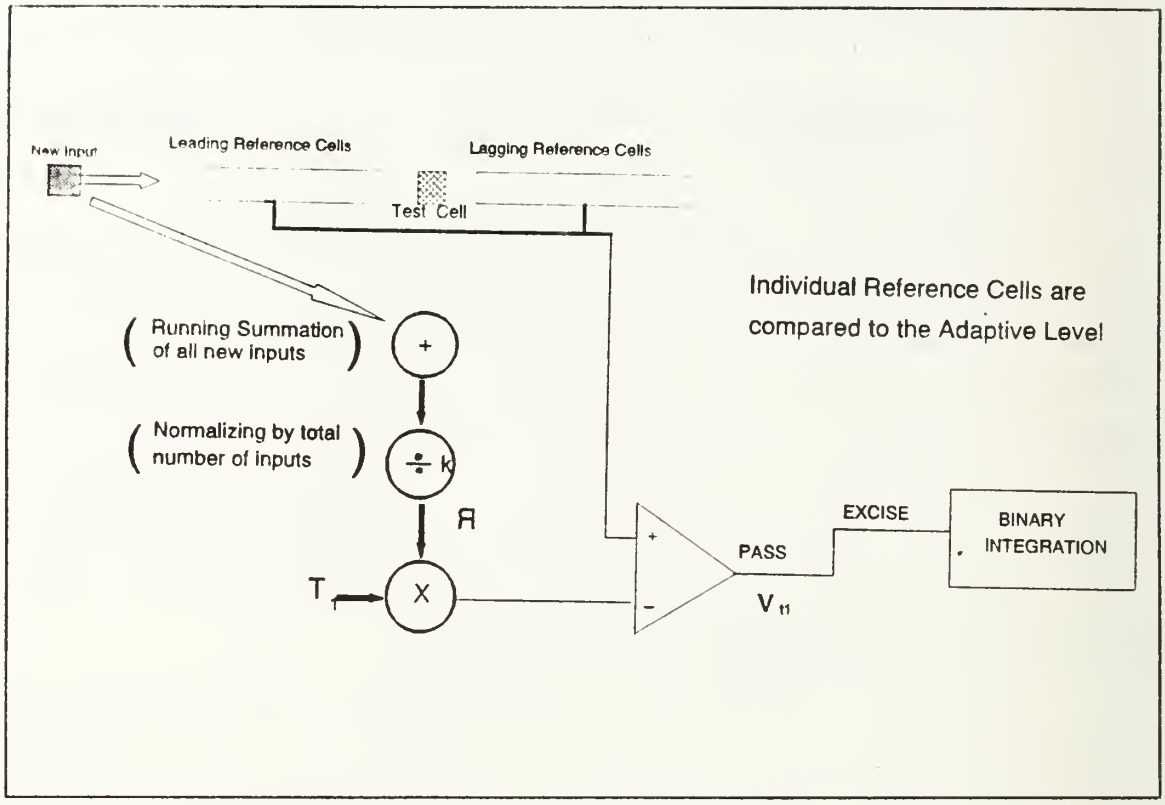

Figure 56. Excision Logic

C. PERFORMANCE ANALYSIS

As a member of the GO family, the EXGO detector maintains the key advantages of GO logic. The EXGO system has the advantage of low CFAR loss in the homogeneous environment, but more importantly maintains a GO systems ability to control the false alarm rate in the presence of a clutter edge. In this analysis, we will show that the EXGO system clearly overcomes the GO system's inherent vulnerability to multiple target situations. The price paid for this significant improvement is a small increase in system complexity and an additional CFAR loss ($\approx$ 0.1 dB) in homogeneous environments caused by excising legitimate noise samples. In addition, problems could occur when the processor is in a clutter region and multiple false targets appear.

The input noise samples to the EXGO are normally distributed N(0,1). The Monte Carlo probability of false alarm versus T_2 is shown in Figure 57. Figure 58 shows the probability of detection curves using the threshold multipliers that offer false alarm rates of 10^{-2}, 10^{-4}, and 10^{-6}. Excision logic threshold multiplier (T_1) was chosen to be three

times the running average noise level for these simulations This level led to an excision rate of approximately five percent of the input noise samples.

Figure 59 shows the ability of the EXGO system to handle the clutter edge problem. Adaptive level 1 (excise level) and adaptive level 2 are detailed in this figure. As shown, adaptive level 1 is higher than almost all the noise only peaks, yet is continually crossed in the clutter region. This graphically shows why excisions do not occur once the system recognizes that it is in a clutter edge. Adaptive level 2 shows the ability of the system to handle both the leading and lagging edges of this simulated sea clutter; thereby maintaining the false alarm rate.

System operation in the multiple target environment is shown in Figures 60 to 65. In each of these plots, a P_{fa} 10^{-4} was chosen along with $T_1 = 3$. All interfering targets have a SNR of 15 dB. In Figure 60, the EXGO system P_d curves show relatively no change between the two interferer scenario and the noise only environment. Figure 61 contrasts these curves by displaying the dramatic loss in capabilities of the standard GO CFAR with the same two interferers. For example, when the SNR of the primary target is 12 dB, the EXGO system maintains a detection probability of 0.72 whereas the GO CFAR yields a detection probability of 0.28. Figure 62 and 63 shows the loss in performance caused by four interfering targets and Figure 64 and 65 shows the performance caused by six interferers. In these plots the EXGO performance remains robust facing additional interferers whereas the GO system degrades significantly.

To demonstrate the EXGO system in a multiple false target situation, 15 dB interferes were injected into every fourth reference cell window. In this situation, the extended leading and lagging cells are engaged since between eight and sixteen excisions occur. This performance is shown in Figure 66. The resultant EXGO system has only and additional 0.2 dB CFAR loss whereas the GO CFAR performance is extremely poor.

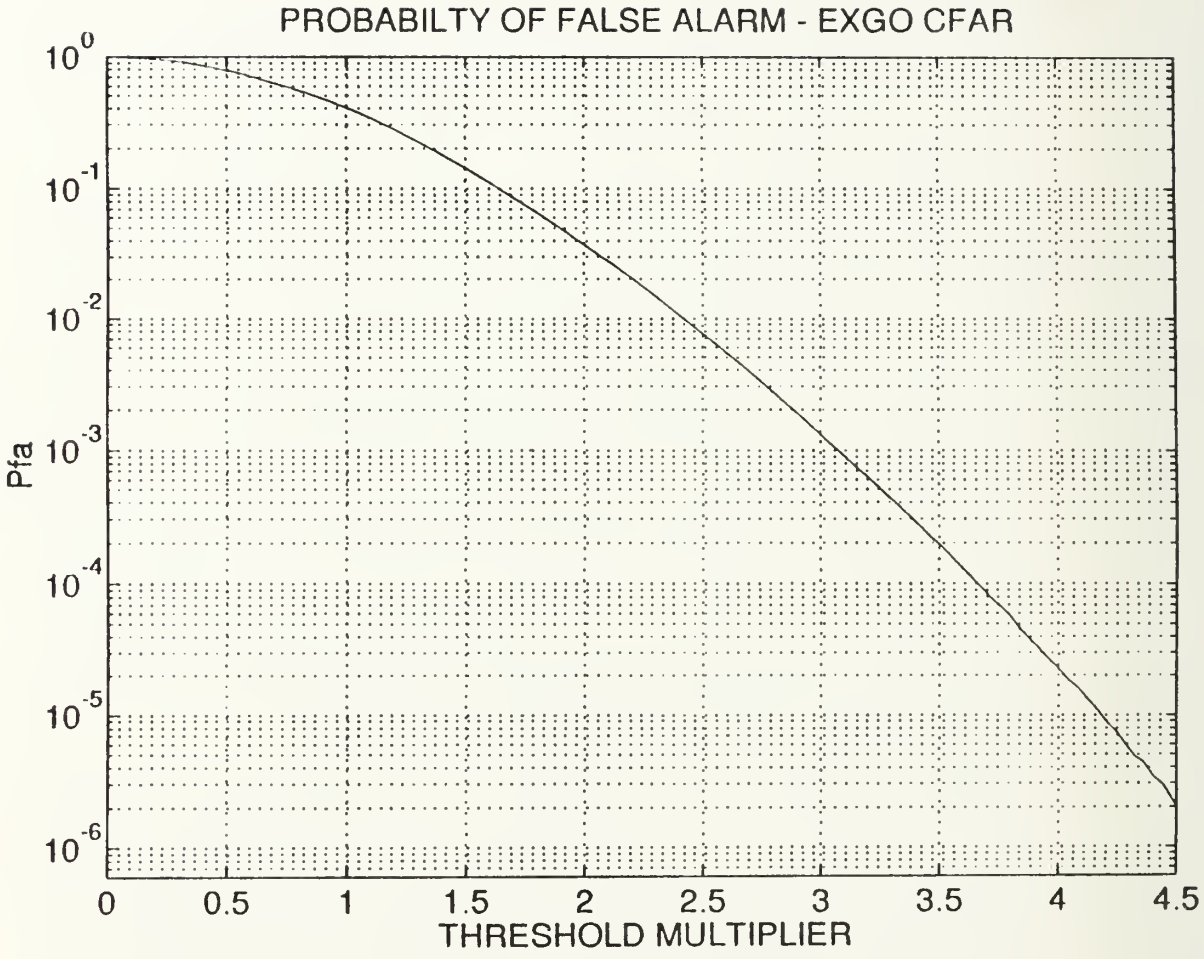

Figure 57. EXGO Probability of False Alarm Curve

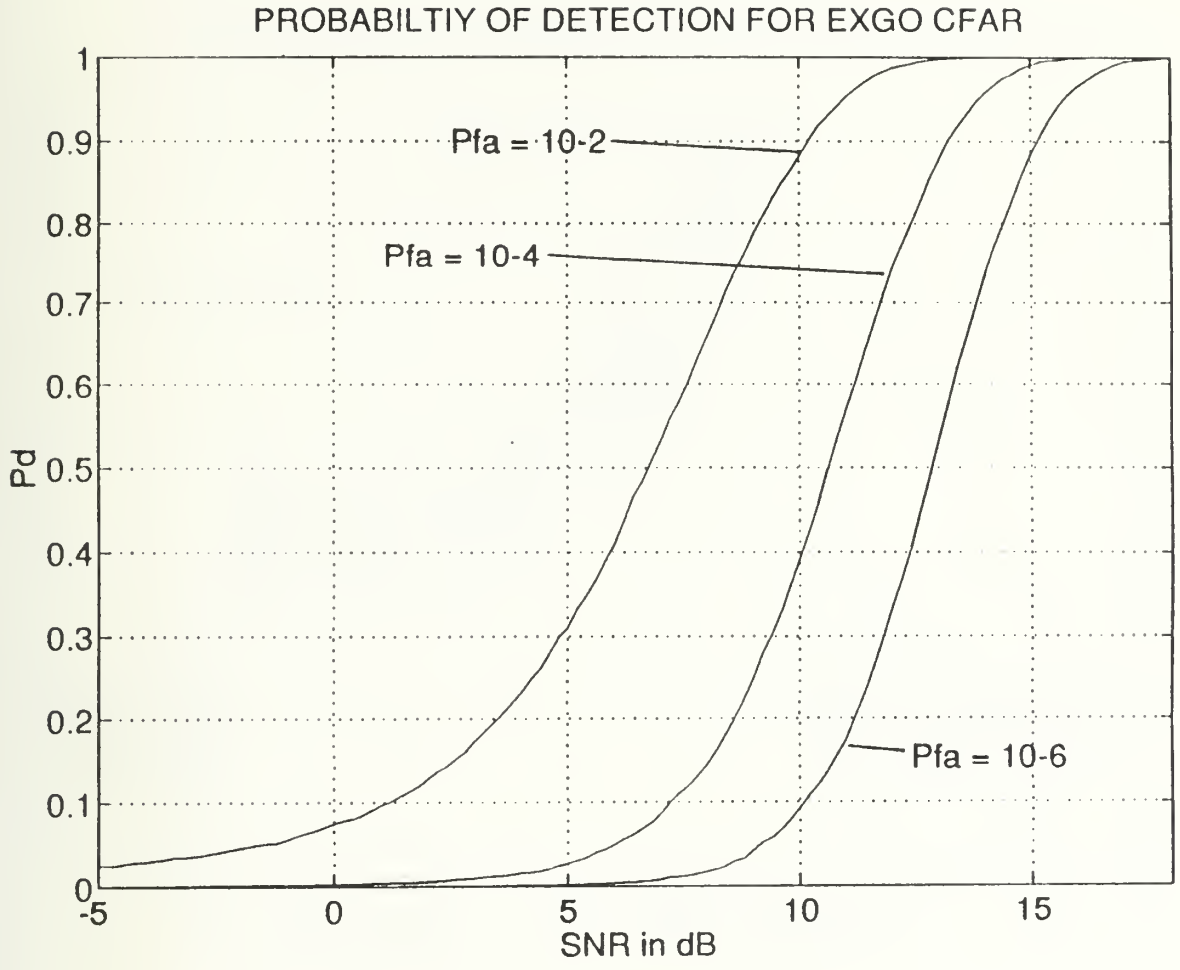

Figure 58. EXGO Probability of Detection Curves

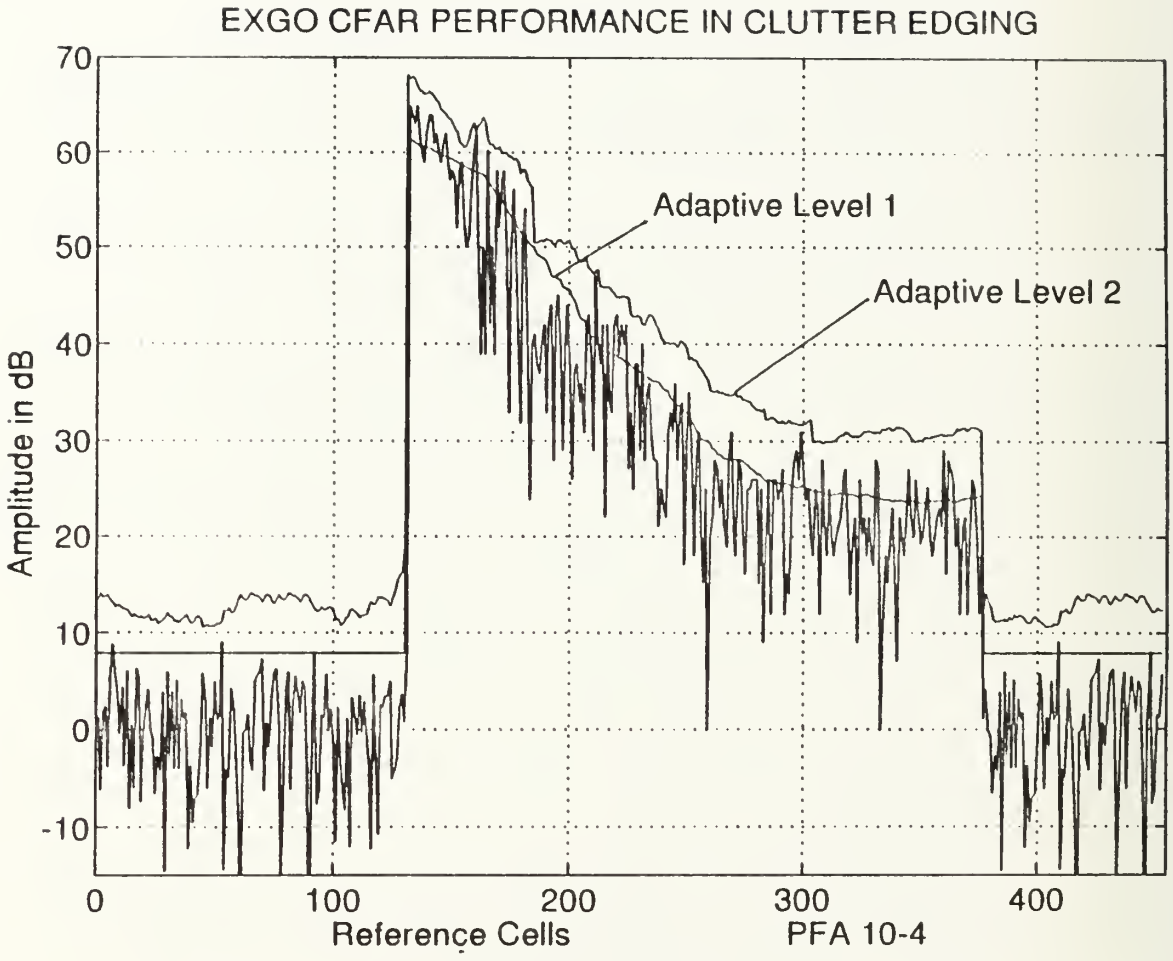

Figure 59. EXGO Performance in Clutter Edges

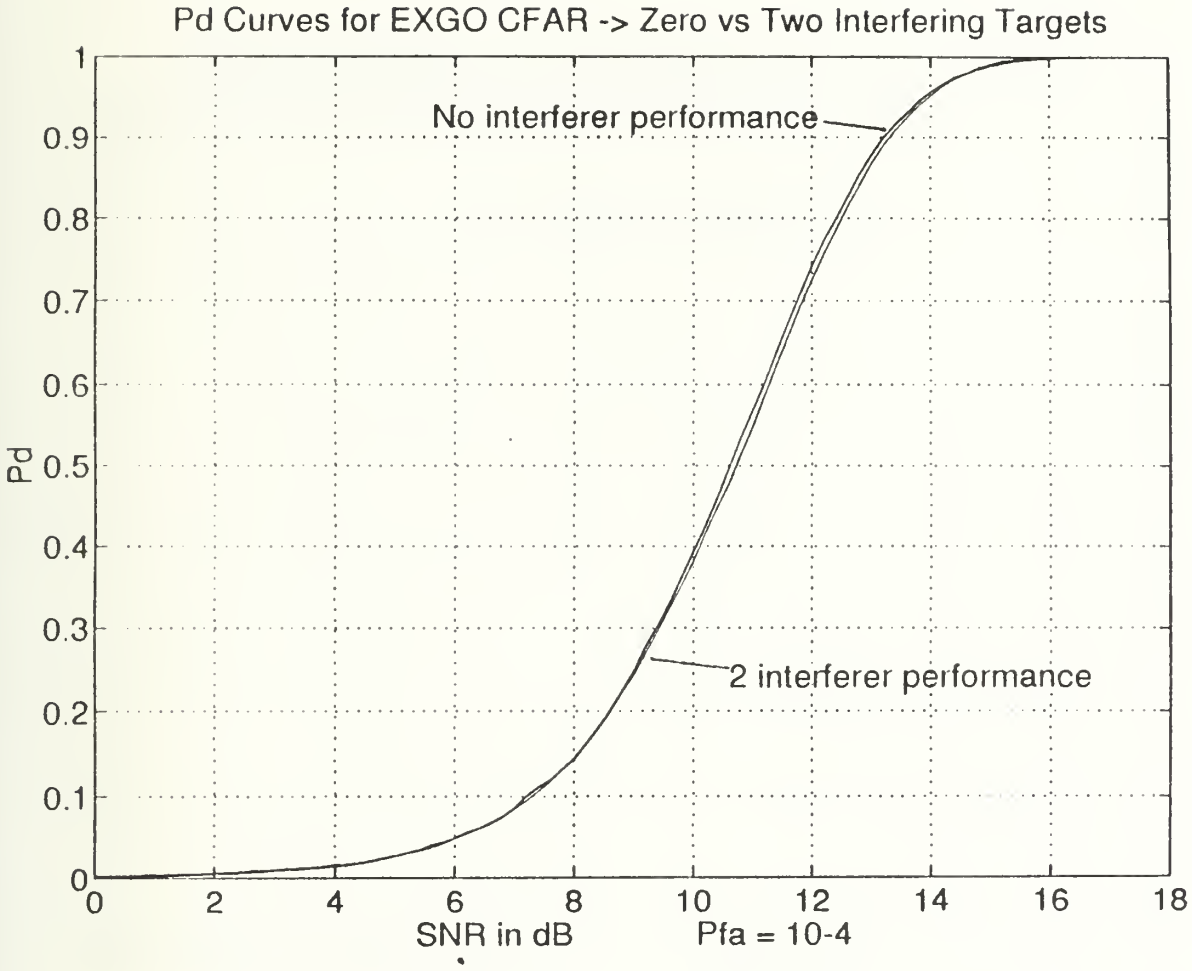

Figure 60. Effect of Two Interferers on EXGO CFAR

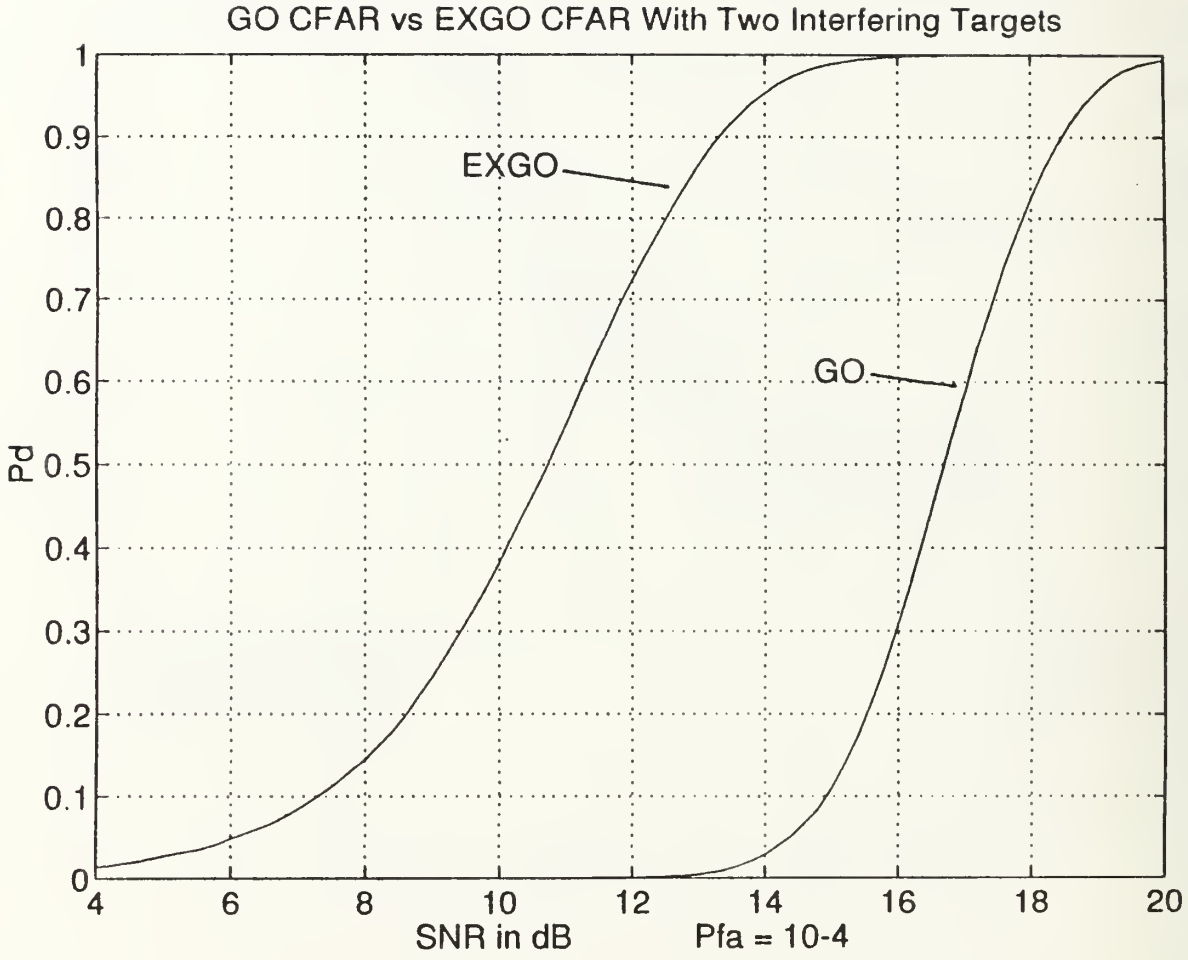

Figure 61. EXGO vs GO with Two Interfering Targets

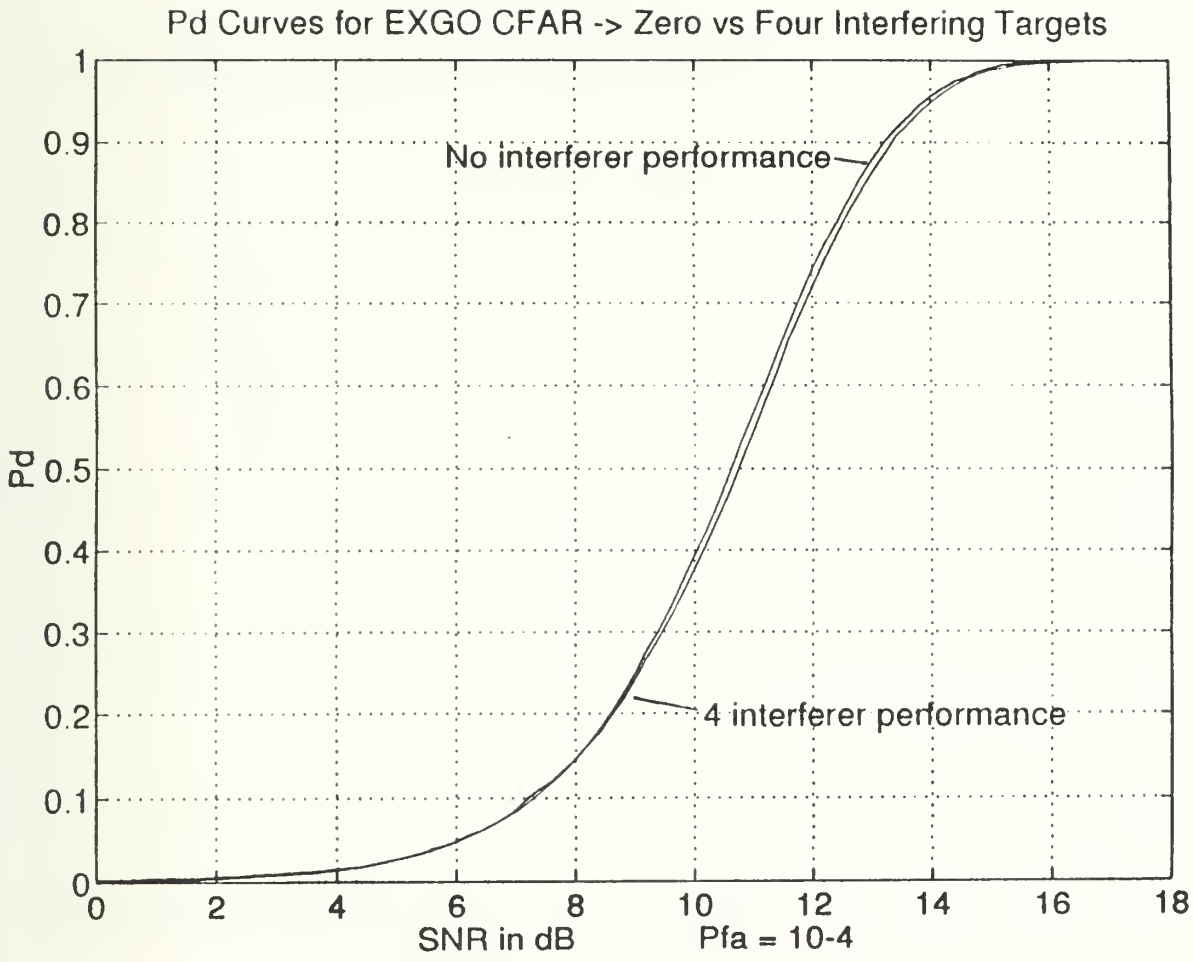

Figure 62. Effect of Four Interferers on EXGO CFAR

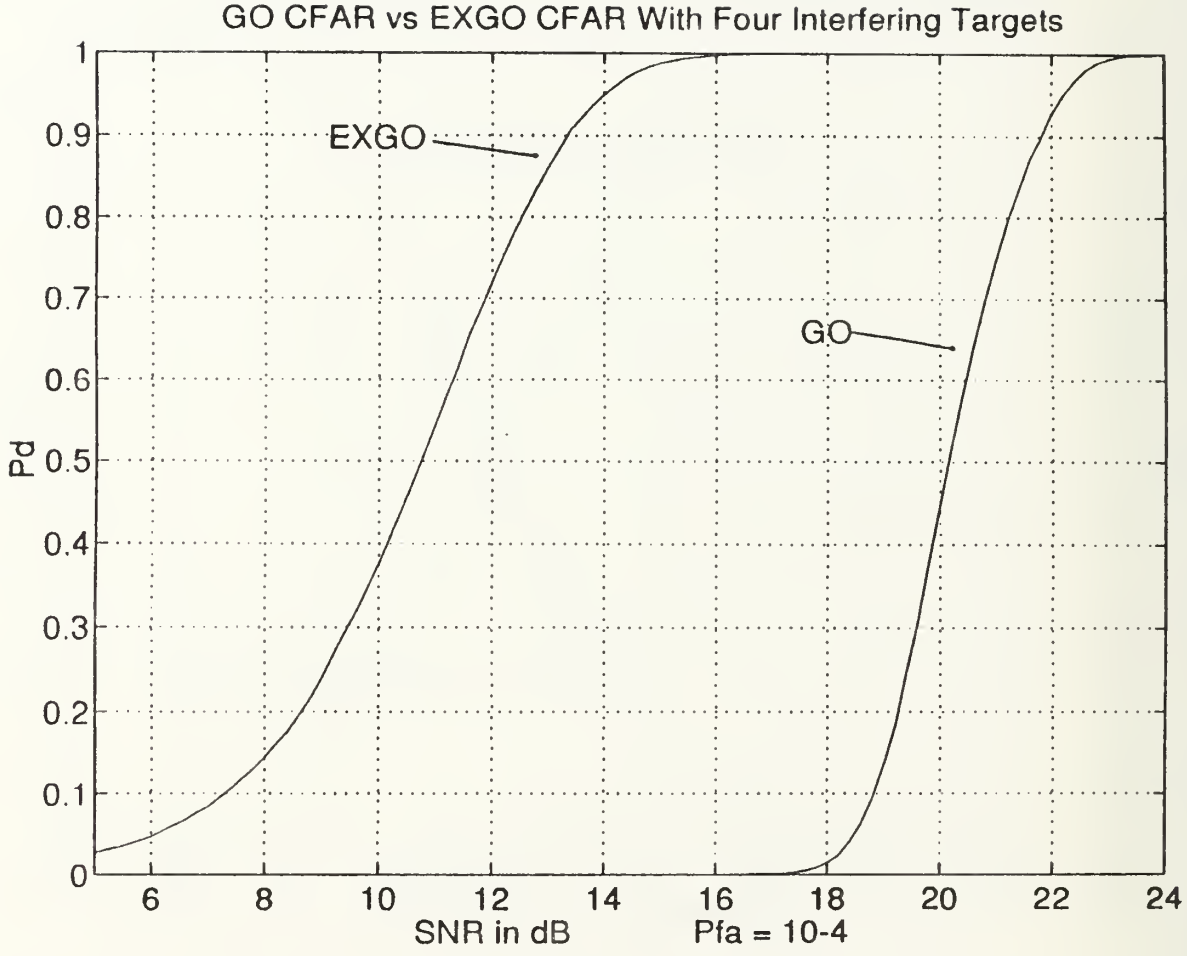

Figure 63. EXGO vs GO with Four Interfering Targets

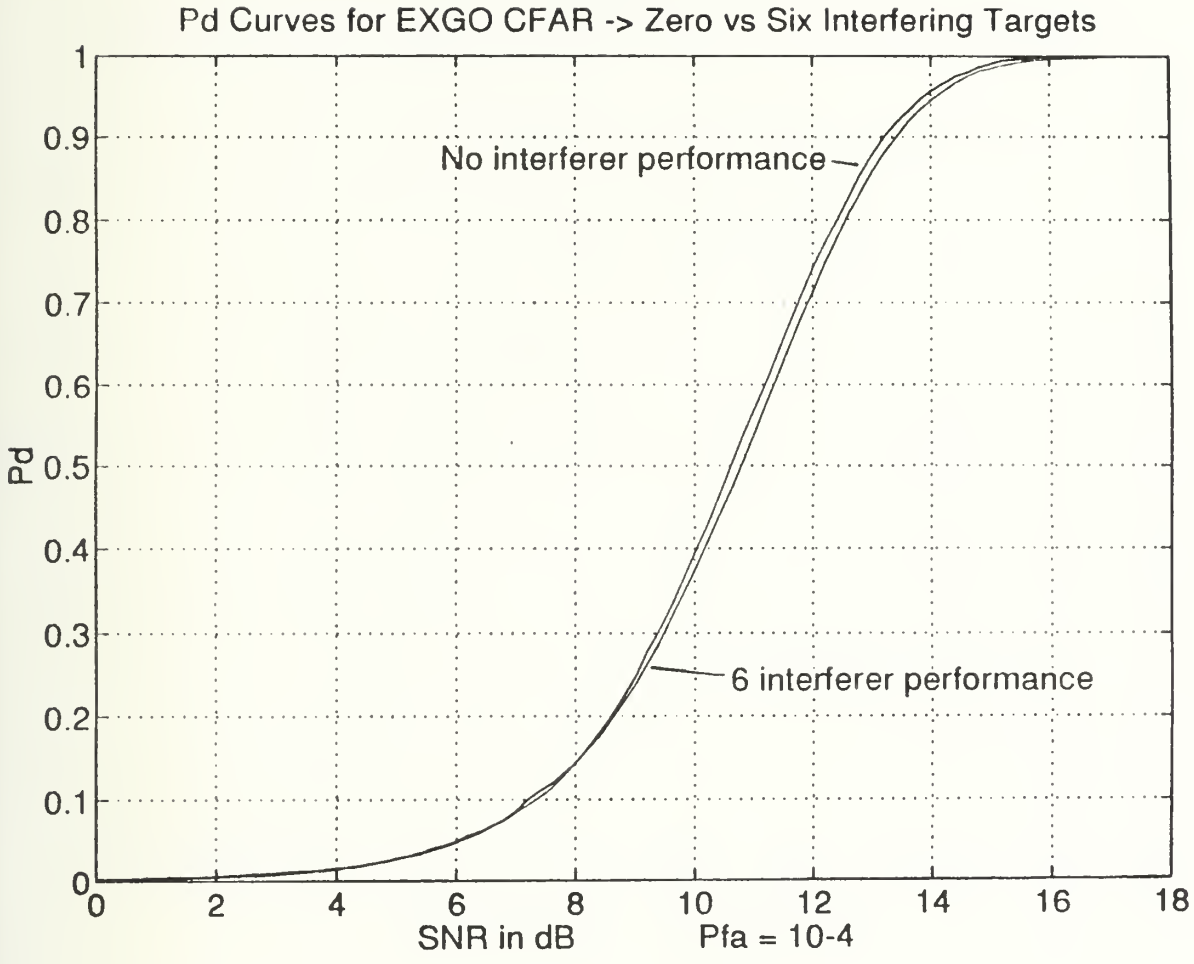

Figure 64. Effect of Six Interferers on EXGO CFAR

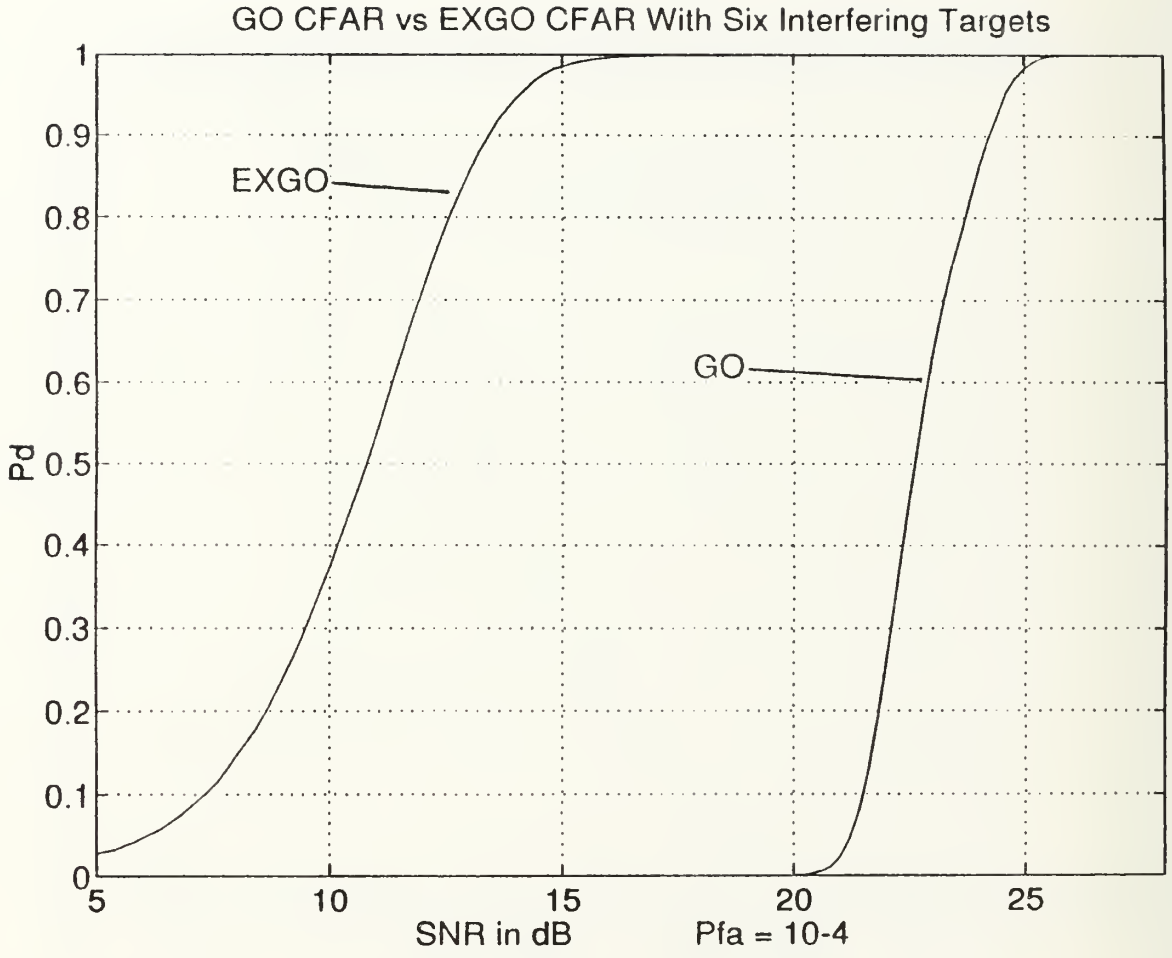

Figure 65. EXGO vs GO with Six Interfering Targets

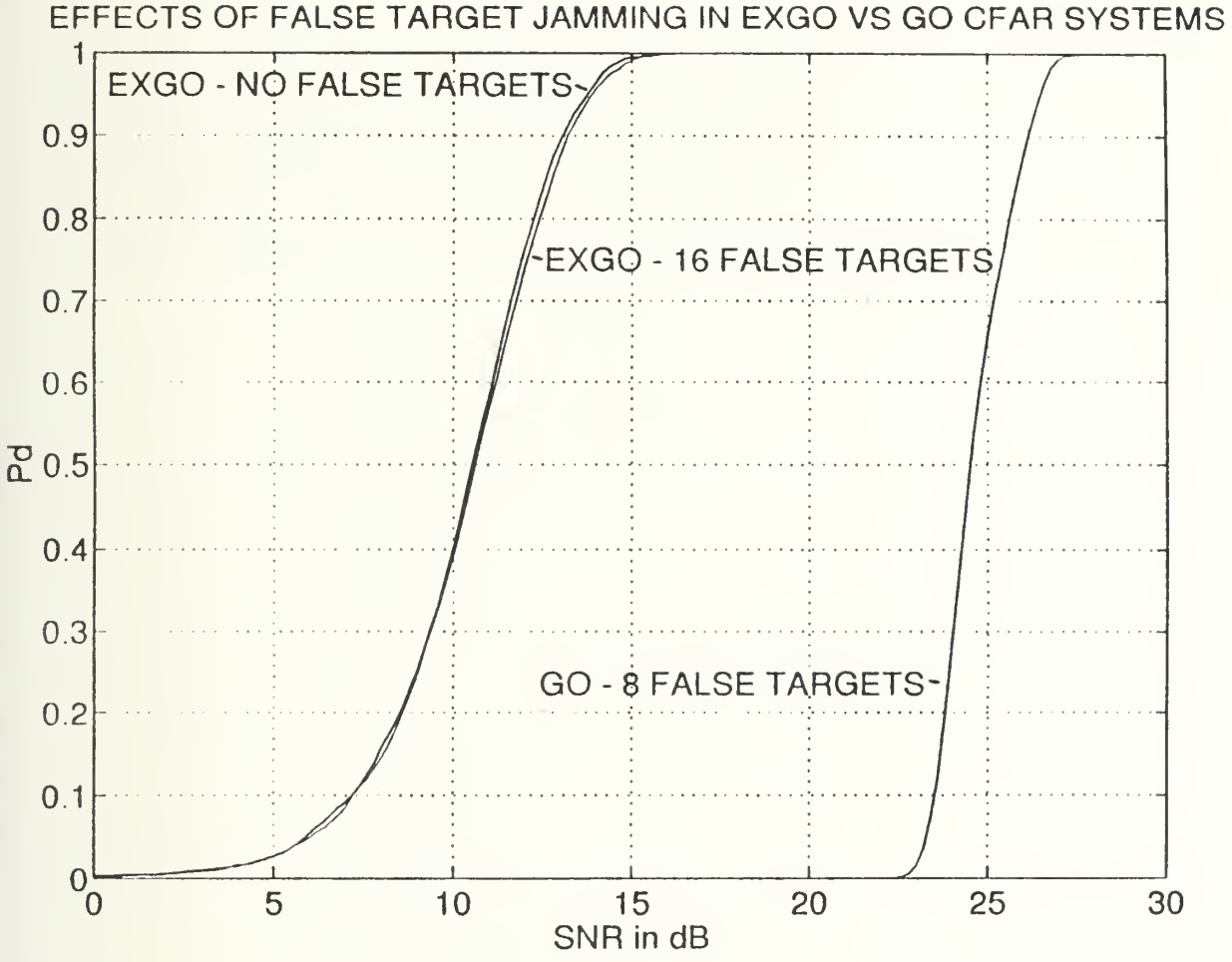

Figure 66. EXGO vs GO in Multiple False Target Jamming

D. SUMMARY

The EXGO CFAR processor shows significant improvements over the conventional GO system. The price paid for these improvements are in the form of a small additional CFAR loss in the homogeneous environment due to excising a small number of legitimate noise samples. Also, additional detector complexity is required as compared to the standard mean level detectors. Although complex, the EXGO system is easily implemented and performs faster than many of the rank ordering system that require cell sorting routines.

The introduction of the extended reference cell concept enables a system to be adaptive to its real time operating situation. The ability to shift between 32 or 64 total reference cells enables the system to conserve its resources in the benign environment and increase its capability in large multiple target/false target jamming situations. As shown, even at relatively high excision rates, The EXGO adaptive performance is superior.

APPENDIX

The four following programs are the GO CFAR and EXGO CFAR probability of detection and probability of false alarm curve generating code. In all programs an Envelope Approximation detector is used.

```
/*******************************************************/
/* THIS PROGRAM IS A MONTE CARLO SIMULATION OF A 'GO' */
/* CFAR ALGORITHM.  THIS PROGRAM PRODUCES THE PROB-   */
/* ABILITY OF FALSE ALARM DATA POINTS TO BE MATLAB    */
/* PLOTTED.                                           */
/*******************************************************/

#include <stdio.h>
#include <math.h>
#include <stdlib.h>
#include <time.h>

/*******************************************************/
#define PI (double)(4.0*atan(1.0))
#define TOTRV 1000000

/*******************************************************/

int z,first,overcount,supercount,randhold[2];
int i,t,n;
double threshold,a,b;
double max,compval,rcdata,window[33],numcells;
double percen,x1,x2,u1,u2,ldgval,ldgnorm,lagval,lagnorm;

/*******************************************************/
main ()

 {

 FILE *writer;

 a=1; b=1;
 compval = 0.0;
 overcount=0;
 numcells=16.0;
 supercount=0;

 if ((writer=fopen("gopfa.dat","w"))==NULL)
  {
   printf("no can do");
   exit(1);
  }

 /*******************************************************/
 /* THIS LOOP ITERATES THE THRESHOLD MULTIPLIER FROM 0  */
 /* THOUGH 5.5.  100 DATA POINTS RESULT.                */
 /*******************************************************/
 for(t=0;t<150;++t)
  {
   first=0; percen=0.0;
   overcount=0; supercount=0;
   max=0.0;

   threshold=((float)t)/10.0;
   srandom(1);

   /*****************************************************/
   /* THIS LOOP ITERATES THROUGHT THE 10 MILLION RANDOM   */
   /* VARIABLES TO GIVE ACCURACIES DOWN TO 10-7.          */
   /*****************************************************/
   while (overcount<TOTRV)
    {
     ldgval=0.0;lagval=0.0;
     for(i=0;i<2;++i)
      {
       randhold[i] = random();
```

```
 }
/*******************************************************/
/* BUILDING THE RANDOM VARIABLES TO BE UNIFORM.        */
/*******************************************************/
u1=((double)randhold[0])/2147483647;
u2=((double)randhold[1])/2147483647;
x1=sqrt((-2)*log(u1))*cos(2*PI*u2);
x2=sqrt((-2)*log(u1))*sin(2*PI*u2);
rcdata = fabs(x1)*a+fabs(x2)*b;

/*******************************************************/
/* INITIAL REFERENCE WINDOW LOAD UP.                   */
/*******************************************************/
if(overcount<33)
 {
  window[32-overcount] = rcdata;
  overcount +=1;
 }
else
 /*******************************************************/
 /* SLIDING THE REF WINDOW AND INPUTTING A NEW R.V.     */
 /*******************************************************/
 {
  for(n=0;n<32;++n)
   {
    window[32-n]=window[31-n];
   }
  window[0]=rcdata;
  overcount+=1;

  /*******************************************************/
  /* SUMMING THE LEADING AND LAGGING REF CELLS THEN      */
  /* NORMALIZING BY THE NUMBER OF CELLS.                 */
  /*******************************************************/
  for(n=0;n<16;++n)
   {
    ldgval+=window[n];
   }
  for(n=17;n<33;++n)
   {
    lagval+=window[n];
   }

  lagnorm=lagval/numcells;
  ldgnorm=ldgval/numcells;

  /*******************************************************/
  /* FINDING THE GREATEST OF VALUE AND USING IT TO DET-  */
  /* ERMINE THE ADAPTIVE THRESHOLD VALUE. THE GO IS MULT-*/
  /* IPLIED WITH THE SCALING FACTOR. IF THIS VALUE IS    */
  /* LESS THAN THE TEST CELL, A TARGET IS DECLARED.      */
  /*******************************************************/
  if(ldgnorm>lagnorm)
   {
    max=ldgnorm;
   }
  else
   {
    max=lagnorm;
   }

  compval=threshold*max;
  if (window[16]>compval)
   {
    supercount+=1;
   }
```

```
      }
     }
    percen=((double)supercount)/(TOTRV-33);
    fprintf(writer,"%f %11.10f\n",threshold,percen);
  }
 fclose(writer);
}
```

```
/*****************************************************************/
/* THIS PROGRAM IS A MONTE CARLO SIMULATION OF A 'GO' CFAR        */
/* ALGORITHM.  THIS PROGRAM PRODUCES THE PROBABILITY OF DETECTION*/
/* DATA POINTS TO BE MATLAB PLOTTED.                              */
/*****************************************************************/
#include <stdio.h>
#include <math.h>

#define NCELL 20000
#define SAMPLE (double)(1.0/200.00)
#define PI (double)(4.0*atan(1.0))

/*******************/
#define TOTRV 10000
#define THRESHOLD 3.65
#define SNRFROM -10.0
#define SNRTO 30.0
/*******************/

int i,j,idelay;
double pp1[NCELL],pp2[NCELL],pp4[NCELL],pp8[NCELL],pp16[NCELL];
double x,ccc,cc0,cc1t,cc1b,dd1,dd2,p1,p2,sum;
double sumvar,summean,summ,noisepwr;

int overcount,randhold[3],n,i,supercount,t;
double snr,amp,numcells,a,b,ldgval,lagval,gonorm;
double var,x1,x2,u1,u2,u3,I[33],Q[33],adaptive,percen;
double phi,s,cut,go,threshprime;
double max1,max2,max3,min1,min2,min3;

main()
 {
 FILE *writer;

 a=1.0; b=1.0; adaptive=0.0; numcells=16.0;
 overcount=0;
 supercount=0; sumvar=0.0;

 threshprime=((numcells-1.0)*THRESHOLD)/(numcells-THRESHOLD);

/*****************************************************************/
 for(i=0;i<NCELL;++i)      /*************************/
  {                        /* PDF for test cell noise*/
  x=(double)i*SAMPLE;      /*************************/
  cc0=-pow(x,2.0)/(2.0*pow(b,2.0));
  cc1t=pow(a,2.0)*pow(x,2.0);
  cc1b=2.0*pow(b,2.0)*(pow(a,2.0)+pow(b,2.0));
  ccc=cc0+(cc1t/cc1b);
  dd1=a*x/(b*sqrt(2.0)*sqrt(pow(a,2.0)+pow(b,2.0)));
  dd2=b*x/(a*sqrt(2.0)*sqrt(pow(a,2.0)+pow(b,2.0)));
  p1=a*b*exp(ccc)*sqrt(PI/2.0)*erf(dd1)/(sqrt(pow(a,2.0)+pow(b,2.0)));
  p2=a*b*exp(ccc)*sqrt(PI/2.0)*erf(dd2)/(sqrt(pow(a,2.0)+pow(b,2.0)));
  pp1[i]=(4.0/(2.0*PI*a*b))*(p1+p2);
  summ+=(pp1[i]*SAMPLE);
  summean+=(pp1[i]*SAMPLE*x);
  sumvar+=(pp1[i]*SAMPLE*x*x);
  }
 noisepwr=sumvar-pow(summean,2.0);
/*****************************************************************/

   if ((writer=fopen("gopd.dat","w"))==NULL)
    {
    printf("bad");
    )
```

```
/*****************************************************************/
/* THIS LOOP ITERATES THROUGH THE SNR RATIOS USED TO CREATE TARGETS*/
/* IN THE CELL UNDER TEST.  WE INCREMENT SNR BY 0.02 dB STEPS TO   */
/* ACHIEVE A SMOOTH PLOT OF SNR vs PROBABILITY OF DETECTION.       */
/*****************************************************************/
   s=SNRFROM;
   while (s<=SNRTO)
   {
   overcount=0;
   percen=0.0;
   supercount=0;
   go=0.0;

   /*****************************************************************/
   /* HERE WE FIND THE VALUE OF SOME TARGETS AMPLITUDE.  AMPLITUDE IS*/
   /* EQUAL TO THE SQUARE ROOT OF TWO TIMES THE SNR TIMES THE EST-    */
   /* IMATE OF THE NOISE POWER.  THIS VALUE IS THEN ADDED TO THE     */
   /* NOISE ALREADY FOUND IN THE CELL UNDER TEST.                    */
   /*****************************************************************/
   noisepwr=1.0;
   snr=pow(10.0,(s/10.0));
   amp=sqrt(2*noisepwr*snr);

   srandom(1);

   /*****************************************************************/
   /* THIS LOOP ITERATES THROUGH ALL THE RANDOM VARIABLES.            */
   /*****************************************************************/
   while(overcount<TOTRV)
    {
    ldgval=0.0;lagval=0.0;
    for(i=0;i<3;++i)
     {
     randhold[i]=random();
     }
     /*****************************************************************/
     /* BUILDING UP THE UNIFORM RANDOM VARIABLES                       */
     /*****************************************************************/
     u1=((double)randhold[0])/2147483647;
     u2=((double)randhold[1])/2147483647;
     u3=((double)randhold[2])/2147483647;
     x1=sqrt((-2)*log(u1))*cos(2*PI*u2);
     x2=sqrt((-2)*log(u1))*sin(2*PI*u2);

     phi=(PI/4)*u3;

     /*****************************************************************/
     /* INITIAL REFERENCE WINDOW LOAD UP AND SLIDING OF THE REF CELLS.  */
     /*****************************************************************/
     if (overcount<33)
      {
      I[32-overcount]=(x1);
      Q[32-overcount]=(x2);
      overcount+=1;
      }
     else
      {
      for(n=0;n<32;++n)
       {
       I[32-n]=I[31-n];
       Q[32-n]=Q[31-n];
       }

      I[0]=(x1);
      Q[0]=(x2);
      overcount+=1;
```

```
/*****************************************************************/
/* USING AN ENVELOPE DETECTOR, THE CELL UNDER TEST VALUE IS FOUND*/
/*****************************************************************/
if(fabs(I[16]+(amp*cos(phi)))>fabs(Q[16]+(amp*sin(phi))))
  {
  max1=fabs(I[16]+(amp*cos(phi)));
  min1=fabs(Q[16]+(amp*sin(phi)));
  }
else
  {
  max1=fabs(Q[16]+(amp*sin(phi)));
  min1=fabs(I[16]+(amp*cos(phi)));
  }

cut=a*max1+b*min1;

/*****************************************************************/
/* SUMMING THE LEADING AND LAGGING CELLS FOR 'GO' DETERMINATION.  */
/*****************************************************************/

for(n=0;n<16;++n)
 {
 if(fabs(I[n])>fabs(Q[n]))
   {
   max2=fabs(I[n]);
   min2=fabs(Q[n]);
   }
 else
   {
   max2=fabs(Q[n]);
   min2=fabs(I[n]);
   }
 ldgval+=a*max2+b*min2;
 }

 for(n=17;n<33;++n)
  {
  if(fabs(I[n])>fabs(Q[n]))
    {
    max3=fabs(I[n]);
    min3=fabs(Q[n]);
    }
  else
   {
   max3=fabs(Q[n]);
   min3=fabs(I[n]);
   }
  lagval+=a*max3+b*min3;
  }

if (ldgval>lagval)
 {
 go=ldgval;
 }
else
 {
 go=lagval;
 }

/*****************************************************************/
/* FINDING THE ADAPTIVE THRESHOLD LEVEL.  IT IS THE PRODUCT OF THE    */
/* NORMALIZE 'GO' AND THE SCALING FACTOR.  THE CELL UNDER TEST IS THEN */
/* COMPARED TO THIS LEVEL TO DETERMINE IF A TARGET IS DETECTED.       */
/*****************************************************************/
gonorm=go/numcells;
```

```
      adaptive=THRESHOLD*gonorm;


      if (cut>=adaptive)
       {
       supercount+=1;
       }
     }
   }
   percen=((double)supercount)/(TOTRV-31);
   fprintf(writer,"%f %11.10f\n",s,percen);
   s=s+.2;
  }
  fclose(writer);
}
```

```
/*************************************************************/
/* THIS PROGRAM IS A MONTE CARLO SIMULATION OF A CFAR ALGORITHM */
/* THE ALGORITHM IS THE AUTHORS OWN AND IS CALLED 'EXGO' WHICH  */
/* IS SHORT FOR EXCISION GREATEST OF.  THIS PROGRAM PRODUCES THE*/
/* PROBABILITY OF FALSE ALARM DATA POINTS TO BE MATLAB PLOTTED  */
/*************************************************************/
#include <stdio.h>
#include <math.h>

#define EXCISELVL 3.0
#define TOTALRV 1000000
#define PI (double)(4.0*atan(1.0))

/*************************************************************/
int overcount,supercount,curcount,ldgcount,lagcount,randhold[2];
int t,i,n,y,cluttcount;

double a,b,x1,x2,u1,u2,go,I[65],Q[65],adaptive,threshmult,lagval;
double ldgval,cut,curest,curestnorm,exciseval,lagnorm,ldgnorm;
double percen,cluttsum,cluttlevel;
/*************************************************************/

main()
  {
  FILE *writer;
  a=1.0; b=1.0;

  if((writer=fopen("far2.dat", "w"))==NULL)
    {
    printf("fu");
    exit(1);
    }

  /*********************************************************************/
  /* THIS LOOP ITERATES THE THRESHOLD MULTIPLIER FROM 0 THROUGH 5.5.*/
  /* 550 DATA POINTS RESULT.                                           */
  /*********************************************************************/
  for(t=0;t<126;++t)  /* Threshold multiplier loop from T = 0 to 5.2 */
    {
    percen=0.0;
    overcount=0;
    curcount=0;
    supercount=0;
    go=0.0;
    y=0;
    curest=0.0;
    exciseval=10.0;

    threshmult=((float)t/25.0);

    srandom(1);
    /*********************************************************************/
    /* THIS LOOP ITERATES THROUGH THE TEN MILLION RANDOM VARIABLES TO */
    /* PRODUCE PFA DATA WITH AN ACCURACY DOWN TO 10-7.                   */
    /*********************************************************************/

    while(overcount<TOTALRV)
       {
       ldgval=0.0;
       lagval=0.0;
       lagcount=0;
       ldgcount=0;

       for(i=0;i<2;++i)
         {
         randhold[i]=random();
```

```
  }

/*************************************************************/
/* BUILDING THE RANDOM VARIABLES TO BE UNIFORM.              */
/*************************************************************/
u1=((double)randhold[0])/2147483647;
u2=((double)randhold[1])/2147483647;
x1=sqrt((-2)*log(u1))*cos(2*PI*u2);
x2=sqrt((-2)*log(u1))*sin(2*PI*u2);

/*************************************************************/
/* INITIAL REFERENCE WINDOW LOAD UP.                         */
/*************************************************************/
if(overcount<65)
  {
  I[64-overcount]=x1;
  Q[64-overcount]=x2;
  overcount+=1;
  }
else
  {
  /***********************************************************/
  /*SLIDING THE REFERENCE WINDOW AND INPUTTING THE NEW RANDOM  */
  /*VARIABLE.  THE IF STATEMENT IS TRUE ONLY THROUGH THE FIRST */
  /*REF WINDOW SLIDE.  THIS STATEMENT ALLOWS FOR THE INITIAL   */
  /*ESTIMATION OF THE CURRENT NOISE.  ONCE INITIALIZED, THE EST-*/
  /*IMATE IS UPDATED WHEN A NEW RANDOM VARIABLE IS INTRODUCED  */
  /*INTO THE REFERENCE CELLS.                                  */
  /***********************************************************/
  for(n=0;n<64;++n)
    {
    I[64-n]=I[63-n];
    Q[64-n]=Q[63-n];
    if(y==0)
      {
      curest+=fabs(I[64-n])+fabs(Q[64-n]);
      curcount+=1;
      }
    }
  y=1;
  I[0]=x1;
  Q[0]=x2;
  overcount+=1;

  /***********************************************************/
  /* UPDATING THE NOISE ESTIMATE WITH THE NEW RANDOM VARIABLE */
  /* ONLY IF IS NOT RECOGNIZED AS AN ADDITIONAL TARGET OR JX. */
  /***********************************************************/
  if(fabs(I[0])+fabs(Q[0])<exciseval)
    {
     curest+=fabs(I[0])+fabs(Q[0]);
     curcount+=1;
    }

 /*********************************************************/
 /* EXCISEVAL IS DETERMINED TO BE THAT ADAPTIVE LEVEL IN  */
 /* WHICH THE REFERENCE CELLS ARE MEASURED AGAINST TO SEE */
 /* IF THEY ARE NOISE VALUES OR POSSIBLE INTERFERING      */
 /* TARGETS.  EXCISE VALUE DETERMINED FROM THE CURRENT    */
 /* ESTIMATE OF THE NORMALIZED NOISE.                     */
 /*********************************************************/
 curestnorm=curest/curcount;
 exciseval=(curestnorm*EXCISELVL);

  /*********************************************************/
  /* HERE THE LEADING AND LAGGING CELLS ARE SUMMED AS LONG */
```

```
/* AS THEY ARE LESS THAN THE EXCISE VALUE -ELSE THEY ARE */
/* IGNORED.                                              */
/*******************************************************/

for(n=16;n<32;++n)
  {
  if(exciseval>=fabs(I[n])+fabs(Q[n]))
    {
    ldgval+=fabs(I[n])+fabs(Q[n]);
    ldgcount+=1;
    }
  }

 for(n=33;n<49;++n)
   {
   if(exciseval>=fabs(I[n])+fabs(Q[n]))
     {
     lagval+=fabs(I[n])+fabs(Q[n]);
     lagcount+=1;
     }
   }

 /*******************************************************/
 /* This code checks for false target generating jamming   */
 /* If more than some percentage of targets are excised    */
 /* it is assummed that FTG jamming is occuring.  In this  */
 /* case we assume that if 25% or > cells are excised than */
 /* we increase our excision threshold and expand our ref  */
 /* cell summation to 32&32 in order to maintain our system*/
 /* performance at high excision rates                     */
 /*******************************************************/
 if(lagcount+ldgcount <= 24)
   {
   lagcount=0;ldgcount=0;
   lagval=0.0;ldgval=0.0;


   if(lagcount+ldgcount <= 16)
     {
     for(n=0;n<64;++n)
       {
       if(exciseval <= fabs(I[n])+fabs(Q[n]))
         {
         cluttcount+=1;
         cluttsum+=fabs(I[n])+fabs(Q[n]);
         }
       }
      cluttlevel=cluttsum/((double)cluttcount);
      exciseval=EXCISELVL*cluttlevel;
      cluttcount=0;
      cluttsum=0.0;
     }
     for(n=0;n<32;++n)
     {
     if(exciseval>=fabs(I[n])+fabs(Q[n]))
      {
      ldgval+=fabs(I[n])+fabs(Q[n]);
      ldgcount+=1;
      }
     }


  for(n=33;n<64;++n)
     {
     if(exciseval>=fabs(I[n])+fabs(Q[n]))
       {
```

```
            lagval+=fabs(I[n])+fabs(Q[n]);
            lagcount+=1;
            }
          }
        }

        /*********************************************************/
        /* THE NORMALIZED VALUES OF EITHER THE 16X16 OR 32X32 ARE*/
        /* DETERMINED. AT THIS POINT THE GREATER OF VALUE WILL   */
        /* BE DETERMINED AND USED TO FIND THE SYSTEM ADAPTIVE    */
        /* THRESHOLD LEVEL.                                      */
        /*********************************************************/
        lagnorm=lagval/((double)lagcount);
        ldgnorm=ldgval/((double)ldgcount);

        if(lagnorm>ldgnorm)
          {
          go=lagnorm;
          }
        else
          {
          go=ldgnorm;
          }

        adaptive=threshmult*go;

        /*********************************************************/
        /* HERE WE FIND THE VALUE OF THE CELL UNDER TEST AND COMPARE IT*/
        /* TO THE ADAPTIVE THRESHOLD LEVEL.  IF THE CUT IS GREATER WE  */
        /* INCREMENT SUPERCOUNT REFLECTING TARGET DETECTION.           */
        /*********************************************************/
        cut=fabs(I[32])+fabs(Q[32]);

        if(cut>adaptive)
          {
          supercount+=1;
          }
       }
      }
      percen=((double)supercount)/(TOTALRV-65);
      fprintf(writer,"%f %11.10f\n",threshmult,percen);

    }
    fclose(writer);
}
```

```
/*************************************************************************/
/*-----------------------------------------------------------------------*/
/*                                                                       */
/*      xxxxxxxxxx      xx           xx          xxxxxxxxx       xxxxxxxxxx */
/*      xx               xx         xx           xx              xx       xx */
/*      xx                 xx       xx           xx              xx       xx */
/*      xx                   xx    xx            xx              xx       xx */
/*      xxxxxxxxx              xxx               xx     xxxx     xx       xx */
/*      xxxxxxxxx               x                xx      xxx     xx       xx */
/*      xx                     xxx               xx       xx     xx       xx */
/*      xx                   xx  xx              xx        x     xx       xx */
/*      xx                 xx      xx            xx        x     xx       xx */
/*      xx               xx          xx          xx        x     xx       xx */
/*      xxxxxxxxx      xx             xx         xxxxxxxxxx      xxxxxxxxxx */
/*                                                                       */
/*-----------------------------------------------------------------------*/
/*************************************************************************/

#include <stdio.h>
#include <math.h>

#define NCELL 20000
#define SAMPLE (double)(1.0/200.00)
#define PI (double)(4.0*atan(1.0))
/********************/
#define TOTRV 5000
#define THRESHOLD  2.42
#define SNRFROM -10.0
#define SNRTO 30.0
#define EXCISELVL 3.0
/********************/

/************************************/
int i,j,idelay,bool,boolcount,cluttcount;
double pp1[NCELL],pp2[NCELL],pp4[NCELL],pp8[NCELL],pp16[NCELL];
double x,ccc,cc0,cclt,cclb,dd1,dd2,p1,p2,sum;
double sumvar,summean,summ,noisepwr,cluttsum,cluttlevel;

int overcount,randhold[3],n,supercount,t,curcount,ldgcount,lagcount,y;
double snr,amp,a,b,ldgval,lagval,gonorm;
double x1,x2,u1,u2,u3,I[65],Q[65],adaptive,percen;
double phi,s,cut,go,curest,curestnorm,ldgnorm,lagnorm,exciseval;
double max1,max2,max3,min1,min2,min3;

/************************************/
main()
 {
 FILE *writer;

 a=1.0; b=1.0;
 overcount=0;
 supercount=0;
 bool=0;
 boolcount=0;


/*********************************************************************/

   if ((writer=fopen("exgo2pda.dat","w"))==NULL)
    {
    printf("bad");
    }
```

```
/*****************************************************************/
/* THIS OUTER LOOP ITERATES THROUGH THE SNR VALUE RANGE SELECTED.  */
/*****************************************************************/
   s=SNRFROM;
   while (s<=SNRTO)
   {
   overcount=0;
   percen=0.0;
   supercount=0;
   go=0.0;
   y=0;
   curcount=0;
   curest=0.0;
   exciseval=10.0;

   noisepwr=1.0;
   snr=pow(10.0,(s/10.0));
   amp=sqrt(2*noisepwr*snr);

   srandom(1);
   /*************************************************************/
   /* THIS INNER LOOP ITERATES THROUGH THE RANDOM VARIABLES   */
   /*************************************************************/
   while(overcount<TOTRV)
    {
    ldgval=0.0;lagval=0.0;
    ldgcount=0;lagcount=0;
    for(i=0;i<3;++i)
     {
     randhold[i]=random();
     }
     u1=((double)randhold[0])/2147483647;
     u2=((double)randhold[1])/2147483647;
     u3=((double)randhold[2])/2147483647;
     x1=sqrt((-2)*log(u1))*cos(2*PI*u2);
     x2=sqrt((-2)*log(u1))*sin(2*PI*u2);

     phi=(PI/4)*u3;

     /*********************************************************/
     /* INITIAL REFERENCE WINDOW LOAD UP AND SLIDING ACTION   */
     /*********************************************************/
     if (overcount<65)
       {
       I[64-overcount]=(x1);
       Q[64-overcount]=(x2);
       overcount+=1;
       }
     else
       {

       for(n=0;n<64;++n)
         {
         I[64-n]=I[63-n];
         Q[64-n]=Q[63-n];
         if(y==0)
           {
           curest+=fabs(I[64-n])+fabs(Q[64-n]);
           curcount+=1;
           }
         }
       y=1;
       I[0]=x1;
       Q[0]=x2;
       overcount+=1;
```

```
/*******************************************************/
/* USING THE NEW RV TO ADJUST THE EXCISE VALUE AVERAGE.*/
/*******************************************************/
if(fabs(I[0])+fabs(Q[0])<exciseval)
  {
  curest+=fabs(I[0])+fabs(Q[0]);
  curcount+=1;
  }

/*******************************************************/
/* NORMALIZING THE RUNNING NOISE ESTIMATE AND THEN     */
/* FINDING THE EXCISE VALUE BASED ON THAT ESTIMATE.    */
/*******************************************************/

curestnorm=curest/curcount;
exciseval=(curestnorm*EXCISELVL);

/*********************************************************/
/* summing the lagging and leading ref cells that do not  */
/* exceed the excision value.  Bool is used to count the  */
/* total number is excisions for the first run.  This data*/
/* will help us decide on a proper EXCISELVL to choose so */
/* that very few data points are excised in a normal noise*/
/* environment                                            */
/*********************************************************/


for(n=16;n<32;++n)
  {
  if(exciseval>=fabs(I[n])+fabs(Q[n]))
    {
    ldgval+=fabs(I[n])+fabs(Q[n]);
    ldgcount+=1;
    }
  else
    {
    if(bool==0)
      {
      boolcount+=1;
      }
    }
  }

for(n=33;n<49;++n)
  {
  if(exciseval>=fabs(I[n])+fabs(Q[n]))
    {
    lagval+=fabs(I[n])+fabs(Q[n]);
    lagcount+=1;
    }
   else
     {
     if(bool==0)
       {
       boolcount+=1;
       }
     }
  }

/*********************************************************/
/* False Target Jamming is checked here.  If greater than    */
/* 25% of the data samples are excise FTG jamming is assumed */
/* We then reset the ldg and lagging sums to zero and recalc-*/
/* ulate based on 32X32 ref cells and a higher excision level*/
/*********************************************************/
```

```
if(lagcount+ldgcount<=24)
  {
  lagcount=0;ldgcount=0;
  ldgval=0.0;lagval=0.0;

  if(lagcount+ldgcount<=16)
    {
    for(n=0;n<64;++n)
       {
       if(exciseval<=fabs(I[n])+fabs(Q[n]))
          {
          cluttcount+=1;
          cluttsum+=fabs(I[n])+fabs(Q[n]);
          }
        )

        cluttlevel=cluttsum/((double)cluttcount);
        exciseval=EXCISELVL*cluttlevel;
        cluttcount=0; cluttsum=0.0;
    }

  for(n=0;n<32;++n)
     {
     if(exciseval>=fabs(I[n])+fabs(Q[n]))
       {
       ldgval+=fabs(I[n])+fabs(Q[n]);
       ldgcount+=1;
       )
     }
   for(n=33;n<65;++n)
     {
     if(exciseval>=fabs(I[n])+fabs(Q[n]))
       {
       lagval+=fabs(I[n])+fabs(Q[n]);
       lagcount+=1;
       }
     }
   )


/*********************************************************/
/* NORMALIZING THE LAG AND LEADING REF WINDOWS THEN      */
/* CHOOSING THE GREATER OF. THIS VALUE IS THEN USED TO */
/* DETERMINE THE ADAPTIVE THRESHOLD LEVEL.               */
/*********************************************************/

lagnorm=lagval/((double)lagcount);
ldgnorm=ldgval/((double)ldgcount);


if(lagnorm>ldgnorm)
  {
  go=lagnorm;
  }
else
  {
  go=ldgnorm;
  }

adaptive=THRESHOLD*go;

/*********************************************************/
/* HERE WE FIND THE VALUE OF THE TEST CELL AND THEN COMP-*/
/* ARE IT TO THE ADAPTIVE THRESHOLD LEVEL FOR DETECTION. */
/*********************************************************/
cut=fabs(I[32]+(amp*cos(phi)))+fabs(Q[32]+(amp*sin(phi)));
```

```
        if(cut>adaptive)
          {
          supercount+=1;
          }

      }
    }
    percen=((double)supercount)/(TOTRV-65);
    fprintf(writer,"%f %11.10f\n",s,percen);
    s=s+.2;
    bool+=1;
  }
  fclose(writer);
  printf("%d",boolcount);
}
```

LIST OF REFERENCES

1. Schleher, D.C., *Automatic Detection and Radar Data Processing* , pp.1-17, Artech House, Dedham, Massachusetts, 1980

2. Levanon, N., *Radar Principles*, pp. 247-266, John Wiley and Sons, New York 1988

3. Anastassopoulos, V., and Lampropoulos, G., "A New and Robust CFAR Detection Algorithm", IEEE Trans. on AES, Vol. AES-28, No. 2, pp. 420-427 , April 1992

4. Farina, A., and Studer, F.A., "A Review of CFAR Detection Techniques in Radar Systems", Microwave Journal, pp. 115-128, September 1986

5. Filip, A.E., "A Baker's Dozen Magnitude Approximations and their Detection Statistics", IEEE Trans on AES, Vol. AES-12, No. 1, pp. 86-89, January, 1976

6. Rickard, R.L., and Dillard, G.M., "Adaptive Detection Algorithms for Multiple Target Situations", IEEE Trans. on AES, Vol. AES-13, No. 4 pp. 608-621, July 1983

7. Taylor, J.W., "Receivers" in *Radar Handbook*,Skolnik, M.I., pp. 3.1-3.54, McGraw Hill, New York, 1990

8. Barkat,M., and Varshney,P., " Decentralized CFAR Signal Detector", IEEE Trans. on AES, Vol. AES-25, No. 2, pp. 141-148, March 1989

9. Eaves, J.L., and Reedy, E. K., *Principles of Modern Radar* , Van Nostrand Reihold Co., New York, 1987

10. Donohue, K. D., and Bilgutay, B.M., "OS Characterization of Local CFAR Detection", IEEE Trans. on AES, CD ROM, #0018-9472/91

11. Finn, H.M., "A CFAR Design for a Window Spanning Two Clutter Fields", IEEE on AES, Vol. AES-22, pp. 155-169, March 1986

12. Shor, M., and Levanon, N., "Performances of Order Statistics CFAR" , IEEE Trans. on AES, Vol. AES-27, No. 2, pp. 214-223, March 1991

13. Long, M.W., "Polarization and Statistical Properties of Clutter", Proc. of 1984 Intl. Symposium on Noise and Clutter Rejection in Radars and Imaging Sensors, Tokyo, pp. 25-32, October 1984

14. Nathanson, F.E., *Radar Design Principles*, McGraw Hill, New York, 1969

15. Weiss, M., "Analysis of some Modified Cell Averaging CFAR Processors in Multiple Target Situations"' IEEE Trans. on AES, Vol. AES-18, No. 1, pp. 102-114, January 1982

16. Rohling, H., "New CFAR-Processor Based on an Ordered Statistic", IEEE International Radar Conference, pp. 271-275, 1985

17. Al-Hussaini, E.K., "Performance of the Greatest-Of and Censored Greatest-Of Detectors in Multiple Target Environments", IEE Proceedings, Vol. AES-135 No. 3, pp 193-198, June 1988

18. Schleher, D.C., *Introduction to Electronic Warfare*, Artech House, Norwood Massachusetts, 1990

19. Lothes, R.N., Szymanski, M.B.,and Wiley, R.G., *Radar Vulnerablity to Jamming*, Artech House, Norwood Massachusetts, 1990

20. Finn, H.M., and Johnson, R.S., "Adaptive Detection Mode with Threshold Control as a Function of Spatially Clutter Level Samples", RCA Review, Vol. 29, pp. 414-464, September 1968

21. Himonas, S.D., and Barkat, M., "Automatic Censored CFAR Detection for Non-Homogeneous Environments, IEEE Trans. on AES, Vol. AES-28, No. 1, pp. 286-304, January 1992

22. Hansen, V.G., "Constant False Alarm Rate Processing in Search Radars", IEE Conference on 'Radar - Present and Future', London, England , pp. 325-332, October 1973

23. Trunk, G.V., "Range Resolution of Targets Using Automatic Detectors", IEEE Trans. on AES, Vol. AES-14, No. 5, pp. 750-755, September 1978

24. Ritcey, J.A., and Hines, J.L., "Performance of Max Family Ordered Statistic CFAR Detectors", IEEE on AES, Vol. AES-27, No. 1, pp. 213-221, January 1991

25. Hansen, V.G., "Detectability Loss Due to 'Greatest Of' Selection in a Cell Averaging CFAR", IEEE Trans. on AES, Vol. AES-16, No. 1, pp. 115- 118, January 1980

26. Gandhi, P.P., and Kassam, S.A., "Analysis of CFAR Processors in Nonhomogeneous Background", IEEE on AES, Vol. AES-24, No. 24, pp. 427-444 , July 1988

27. Rohling, H., "Radar CFAR Thresholding in Clutter and Multiple Target Situations" , IEEE Trans. on AES, Vol. AES-19, No. 4, pp. 608-621, July 1983

28. Levanon, N., "Detection Loss Due to Interfering Targets in Ordered Statistic CFAR", IEEE Trans. on AES, Vol. AES-24, No. 6, pp. 678-681, November 1988

29. Elias-Fuste, A.R., "Analysis of Some Modified Order Statistic CFAR : OSGO and OSSO CFAR", IEEE Trans. on AES, Vol. 26, No. 1, pp. 197-202, January 1990

30. Barkat, M., Himonas, S.D., and Varshney, P.K., "CFAR Detection for Multiple Target Situations", IEE Proceedings, Vol 136, Pt. F, No. 5, pp. 1933-209, October 1985

31. Himonas, S.D., "A Robust Automatic Censored CFAR Detector for a Non- Homogeneous Environment", Proceedings of the 1991 IEEE Radar Conference, pp. 117-120, 1991

32. Khoury, E.N., and Hoyle, J.S., "Clutter Maps Design and Performance", Proceedings of the 1984 National Radar Conference, pp. 1-7, IEEE Press, New York, Pub. No. ch1963-8/184/0000-0001, 1984

33. Thomas, J.B., "Non-Parametric Detectors", Proceedings of the IEEE, Vol. AES-5, No. 5, pp. 623-631, May 1970

34. Trunk, G.V.,"Automatic Detection, Tracking, and Sensor Integration", in *Radar Handbook* , Skolnik, M.I., pp. 8.19-8.21, McGraw Hill, New York, 1990

35. Moore, J.D., and Lawrence, W.B., "Comparison of Two CFAR Methods Used with Square Law Detection of Swerling I Targets", IEEE Int'l Radar Conference, 1980

36. Ozgunes, I., and Gandhi, P.P., and Kassam, S.A., "A Variably Trimmed Mean CFAR Radar Detector, IEEE Trans. on AES, Vol AES-28, No. 4, pp. 1002-1013, October 1982

37. Pace, P.E., and Taylor, L.L., "False Alarm Analysis of the Envelope Detection GO CFAR Processor, IEEE Trans. on AES, Vol. AES-30, 1994

38. Pace, P.E., Bowman, P.J., Taylor, L.L., and Laulusa, G., "Detection Analysis of the Envelope GO CFAR processor", to be submitted IEEE

39. Goldman, H.,and Bar David, I., "Analysis and application of the excision CFAR detector, IEE Proc., Vol. 135, Pt. F, No. 6, pp. 563-575, December, 1988

INITIAL DISTRIBUTION LIST

		No. Copies
1.	Defense Technical Information Center Cameron Station Alexandria, VA 22304-6145	2
2.	Library, Code 52 Naval Postgraduate School Monterey, CA 93943-5002	2
3.	Dr. M.I. Skolnik Superintendent Radar Division (Code 5300) Naval Research Laboratory Washington, DC 20375-5000	1
4.	Dr. P.E. Pace Code Ec/Pc Naval Postgraduate School Monterey, CA. 93940	2
5.	Mr. G. Laulusa Research Engineering Hughes Missile Systems Company MZ-4-49 P.O. Box 2507 Pomona, CA 91769	1
6.	Mr. L.L. Taylor Research Engineering Hughes Missile Systems Company MZ-4-49 P.O. Box 2507 Pomona, CA 91769	1
7.	Mr. L.T. Bowman 1222 Sandy Plains Ln. Houston, TX 77062	1
8.	Mr. L.B. Smith Phalanx Program Manager Ship Defense Systems Hughes Missile Systems Co. MZ-50-88 P.O. Box 2507 Pomona, CA 91769	1

9. Mr. F. Levien 1
Code Ec/Lv
Naval Postgraduate School
Monterey, CA 93940

10. LCDR D. Farley 1
Code Ec/Fr
Naval Postgraduate School
Monterey, CA 93940

11. Director,Space and Electronic Combat Division (N64) 1
Space and Electronic Warfare Directorate
Chief of Naval Operations
Washington DC 20350-2000

12. Curricular Officer 1
Code 3A
Naval Postgraduate School
Monterey, CA 93940